

Electronic Thesis and Dissertation Repository

2-6-2015 12:00 AM

ATRX loss-of-function in mouse neuroprogenitor cells as a model of early events in gliomagenesis

Hannah E. Goldberg
The University of Western Ontario

Supervisor
Dr. Nathalie Berube
The University of Western Ontario

Graduate Program in Developmental Biology
A thesis submitted in partial fulfillment of the requirements for the degree in Master of Science
© Hannah E. Goldberg 2015

Follow this and additional works at: <https://ir.lib.uwo.ca/etd>



Part of the [Cancer Biology Commons](#)

Recommended Citation

Goldberg, Hannah E., "ATRX loss-of-function in mouse neuroprogenitor cells as a model of early events in gliomagenesis" (2015). *Electronic Thesis and Dissertation Repository*. 2693.
<https://ir.lib.uwo.ca/etd/2693>

This Dissertation/Thesis is brought to you for free and open access by Scholarship@Western. It has been accepted for inclusion in Electronic Thesis and Dissertation Repository by an authorized administrator of Scholarship@Western. For more information, please contact wlsadmin@uwo.ca.

**ATRX LOSS-OF-FUNCTION IN MOUSE NEUROPROGENITOR CELLS AS A
MODEL OF EARLY EVENTS IN GLIOMAGENESIS**

(Thesis format: Monograph)

by

Hannah Elisabeth Goldberg

Graduate Program in Biochemistry

A thesis submitted in partial fulfillment
of the requirements for the degree of
Master of Science

The School of Graduate and Postdoctoral Studies
The University of Western Ontario
London, Ontario, Canada

© Hannah E. Goldberg 2015

Abstract

ATRX is a chromatin remodeling protein important for neural development, and ATRX inactivation leads to genomic instability, mitotic defects and TP53-mediated apoptosis. In the last few years, *ATRX* mutations were identified in a large proportion of paediatric and adult gliomas that often coincide with mutations in the tumor suppressor *TP53*. The present work shows that combinatorial loss of ATRX and TP53 function *in vitro* leads to excessive genomic instability albeit improving cell viability, identifying potential early events in gliomagenesis. Furthermore, several gene transcripts associated with glioma development and known oncogenic pathways were significantly upregulated in the *Atrx*-null neonatal mouse forebrain. Finally, a mouse model of *Atrx* and *Tp53* deficiency in the mouse CNS was generated, providing a tool for future investigations.

Keywords: ATRX, *Alpha thalassaemia mental retardation X-linked*, cancer, glioma, gliomagenesis, neuroprogenitor cell, NPC, TP53

Acknowledgements

I would like to express my sincere thank you to all those who have supported and encouraged me throughout the duration of my academic career. First of all, thank you to my family, especially my parents Doris and Carl Goldberg and my brother Daniel Goldberg, for always encouraging me to be my best and supporting all of my endeavours. Your love and support has helped me grow into the person I am today, and has definitely aided in my success throughout my academic life. A special thank you to my close friends who have had to put up with long nights and weekends at the lab, and making plans around my laboratory experiments. You always pushed me to succeed and continuously encouraged me even in the face of experimental failure. And finally, a huge thank you to my wonderful boyfriend, Alex, who always kept my spirits up when things went wrong and who gave me a lot of guidance with my western blots!

A big thank you to all of the Bérubé lab members who always maintained a positive and supportive work environment, and helped me succeed even when I was most doubtful. I would especially like to thank my supervisor, Dr. Nathalie Bérubé, for being so passionate about her work, and for always encouraging me to work and think as a scientist. Finally, I would like to thank my advisory committee, Dr. Ann Chambers and Dr. Gabriel DiMattia, for their helpful advice and insightful suggestions throughout the duration of my thesis project.

Table of Contents

ABSTRACT.....	ii
ACKNOWLEDGEMENTS.....	iii
TABLE OF CONTENTS.....	iv
LIST OF TABLES.....	vii
LIST OF FIGURES.....	viii
LIST OF ABBREVIATIONS.....	ix

CHAPTER 1 – Introduction

1.1 Glioma.....	1
1.1.1 Histology and Pathology of Glioma	1
1.1.2 Key Players in Glioma Pathogenesis.....	2
1.1.3 <i>TP53</i> Mutations in Glioma.....	3
1.1.4 <i>IDH1/2</i> Involvement in Glioma Initiation and Progression.....	5
1.1.5 First Links for <i>ATRX</i> Mutation in Gliomagenesis.....	6
1.2 Alpha Thalassaemia Mental Retardation X-linked.....	7
1.2.1 <i>ATRX</i> and Neuronal Development.....	10
1.2.2 Cellular Functions of <i>ATRX</i>	11
1.2.3 <i>ATRX</i> and Histone Variants.....	13
1.3 <i>ATRX</i> in Cancer.....	15
1.3.1 Early Findings for <i>ATRX</i> Loss in Tumorigenesis.....	15
1.3.2 <i>ATRX</i> Loss in Neuroendocrine Tumors.....	16
1.3.3 <i>ATRX</i> Mutations Across the Glioma Spectrum.....	19
1.3.4 Association of <i>ATRX</i> Mutations and <i>ALT</i>	25
1.4 Hypothesis and Summary of Findings.....	27

CHAPTER 2 – Materials and Methods

2.1	Animal Husbandry and Genotyping.....	28
2.2	Quantitative Real Time PCR.....	34
2.3	<i>In Situ</i> Hybridization.....	34
2.4	Western Blot Analysis.....	35
2.5	Immunofluorescence.....	36
2.6	Haematoxylin and Eosin Staining.....	39
2.7	Neuroprogenitor Cell Culture.....	39
2.8	Adenovirus- <i>Cre Recombinase</i> Infection of Neuroprogenitor Cells.....	39
2.9	Trypan Blue Dye Exclusion Assay.....	40
2.10	Database Mining.....	40

CHAPTER 3 – Results: *In Vitro* Modelling of Gliomagenesis

3.1	Establishment of ATRX and TP53 Loss Sequentially <i>In Vitro</i>	41
3.2	Phenotypic Characterization of Sequential ATRX and TP53 Loss in Mouse Neuroprogenitor Cells.....	44
3.3	Establishment of ATRX and TP53 Loss Simultaneously <i>In Vitro</i>	48
3.4	Phenotypic Characterization of Simultaneous ATRX and TP53 Loss in Mouse Neuroprogenitor Cells.....	49
3.5	Summary of Results.....	53

CHAPTER 4 – Results: *In Vivo* Modelling of Gliomagenesis

4.1	Database Mining to Investigate Known <i>ATRX</i> Loss-of-Function Mutations.....	58
4.2	Using <i>In Vivo</i> Model Systems for Insights into Gliomagenesis.....	61
4.2.1	Transcriptional Profiling of <i>Atrx</i> -null Neonatal Mouse Forebrain.....	65
4.2.2	<i>In Vivo</i> Model of <i>Atrx</i> and <i>Tp53</i> Inactivation.....	67

CHAPTER 5 – Discussion and Conclusions

5.1	Summary of Thesis Findings.....	77
5.2	<i>In Vitro</i> NPC Culture Systems as a Model of Glioma Development.....	79

5.2.1	Sequential Loss of ATRX and TP53 Function in Mouse NPCs.....	80
5.2.2	Simultaneous Loss of ATRX and TP53 Function in Mouse NPCs.....	82
5.2.3	Future Directions for <i>In Vitro</i> Model Systems of Glioma.....	84
5.3	<i>In Vivo</i> Analysis of ATRX Deletion in the Mouse Brain.....	85
5.3.1	Dysfunction of <i>ATRX</i> in Glioma Patients.....	85
5.3.2	<i>Atrx</i> Loss is Associated with Alterations in Cancer-Related Signalling Pathways.....	86
5.4	<i>In Vivo</i> Modelling of Combined <i>Atrx</i> and <i>Tp53</i> Loss.....	88
5.4.1	Future Directions for <i>In Vivo</i> Modelling of Combined <i>Atrx/Tp53</i> Loss.....	90
5.5	Conclusions.....	91
	CHAPTER 6 – References.....	94
	APPENDIX A.....	112
	CURRICULUM VITAE.....	115

List of Tables

- Table 1.1 List of *ATRX* mutations in cancer literature.
- Table 2.1 List of genotypes used in this thesis.
- Table 2.2 List of oligonucleotides used in genotyping, qRT-PCR and ISH.
- Table 4.1 GO term analysis of the P0.5 microarray.
- Table 4.2 Outline of internal abnormalities in *Atrx* and *Tp53* heterozygous mice.

List of Figures

- Figure 1.1 Overview of the *ATRX* gene and protein.
- Figure 1.2 Outline of *ATRX* mutations in panNETs and gliomas.
- Figure 2.1 Regions of the mouse forebrain used for experimental analyses.
- Figure 3.1 Immunoblots from DMSO- and cPFT α -treated NPCs *in vitro*.
- Figure 3.2 DNA damage foci in DMSO- and cPFT α -treated NPCs in culture.
- Figure 3.3 Cellular viability for DMSO- and cPFT α -treated NPCs *in vitro*.
- Figure 3.4 GFP fluorescence validation for ad-*GFP* and ad-*CreGFP* infected NPCs.
- Figure 3.5 Immunoblots from ad-*GFP* and ad-*CreGFP* infected NPCs *in vitro*.
- Figure 3.6 DNA damage foci in ad-*GFP* and ad-*CreGFP* infected NPCs.
- Figure 3.7 Cellular viability in ad-*GFP* and ad-*CreGFP* infected NPCs in culture.
- Figure 4.1 Database mining from The Cancer Genome Atlas (TCGA).
- Figure 4.2 *ATRX* mutation analysis from the COSMIC database.
- Figure 4.3 Database mining from the Catalogue of Somatic Mutations in Cancer (COSMIC).
- Figure 4.4 qRT-PCR validation of the *Atrx*-null P0.5 microarray.
- Figure 4.5 Validation via ISH (mRNA) and western blot (protein) for increased *ErbB3* expression.
- Figure 4.6 Weight measurement and survival curve of *Atrx/TP53* heterozygous mice.
- Figure 5.1 Visual summary of the conclusions from this thesis.

List of Abbreviations

1p/19q	Co-deletion of chromosomes 1p and 19q
2-HG	2-hydroxyglutarate
α -KG	α -ketoglutarate
AC3	Activated cleaved caspase 3
ADD	ATRX-DNMT3-DNMT3L
Ahnak	AHNAK nucleoprotein; desmoyokin
AKT	Protein kinase B
ALT	Alternative lengthening of telomeres
AML	Acute myeloid leukemia
APH	Aphidicolin
ATR-X	α -thalassaemia mental retardation, X-linked syndrome
ATRX	α -thalassaemia mental retardation X-linked
ATRXt	α -thalassaemia mental retardation X-linked truncated
C-terminal	Carboxy-terminal
ChIP	Chromatin immunoprecipitation
CIN	Chromosomal instability
CNS	Central nervous system
cPFT α	Cyclic Pifithrin-alpha
CSC	Cancer stem cell
Cxcl2	Chemokine (C-X-C motif) ligand 2
DAXX	Death domain associated protein 6
DIG	Dioxygenin
DIV	Days <i>in vitro</i>
DMSO	Dimethyl Sulfoxide
DNA	Deoxyribonucleic acid
DNMT	DNA methyltransferase
DSB	Double-stranded break
E8.5	Embryonic day 8.5
E9.5	Embryonic day 9.5
E11.5	Embryonic day 11.5
E13.5	Embryonic day 13.5
ECL	Enhanced chemiluminescence
EGFR	Epidermal growth factor receptor
ErbB3	v-erb-b2 avian erythroblastic leukemia viral oncogene homolog 3
ESC	Embryonic stem cell
FISH	Fluorescence <i>in situ</i> hybridization
Flt3	FMS-like tyrosine kinase 3
FoxC1	Forkhead box C1
FoxC2	Forkhead box C2
FoxG1	Forkhead box G1

Fzd7	Frizzled 7
G4	G-quadruplex
GABRA1	Gamma-aminobutyric acid (GABA) A receptor, alpha 1
GBM	Glioblastoma multiforme
GIC	Glioblastoma initiating cell
Glast3	Glial high affinity glutamate transporter 3
Gsn	Gelsolin
H2A	Histone 2A
γ H2A.X	gamma-Histone 2A family, member X
H3	Histone 3
H3.1	Histone 3 variant 1
H3.2	Histone 3 variant 2
H3.3	Histone 3 variant 3
HEK293	Human embryonic kidney cell line
HeLa	Henrietta Lacks (cervical cancer cells)
HGG	High-grade glioma
HP1 α	Heterochromatin-associated protein 1 α
HU	Hydroxyurea
IDH	Isocitrate dehydrogenase
Igfbp1	Insulin-like growth factor binding protein 2
iPSC	Induced pluripotent stem cell
kb	Kilobase
kDa	Kilodalton
LGG	Low-grade glioma
Lox	Lysyl oxidase
MAPK	Mitogen activated protein kinase
Mdk	Midkine
mESC	Mouse embryonic stem cell
MeCP2	Methyl CpG binding protein 2
MEF	Mouse embryonic fibroblast
MEN1	Multiple endocrine neoplasia type 1
Mmp2	Matrix metalloproteinase 2
Mmp14	Matrix metalloproteinase 14
MNK	Menke's disease gene
N-terminal	Amino-terminal
NADPH	Nicotinamide adenine dinucleotide phosphate
NEFL	Neurofilament light chain
NEC	Neuroendocrine carcinoma
NET	Neuroendocrine tumour
NF1	Neurofibromin 1
NLS	Nuclear localization signal
NSC	Neural stem cell

NPC	Neuroprogenitor cell
OCT	Optimal cutting temperature
P0.5	Postnatal day 0.5 (birth)
P7	Postnatal day 7
p16 ^{INK4A}	Cyclin-dependent kinase inhibitor 2A, multiple tumor suppressor protein 1
p27	Cyclin-dependent kinase inhibitor 1B
p107	Retinoblastoma-like protein 1
panNET	Pancreatic neuroendocrine tumour
PGK1	Phosphoglycerate kinase-1
PDGFA	Platelet-derived growth factor α
PHD	Plant homeodomain
PI	Propidium iodide
PI3K	Phosphoinositide-3-kinase
PML	Promyelocytic leukemia
pRB	Retinoblastoma protein
PTEN	Phosphatase and tensin homolog deleted from chromosome 10
RNA	Ribonucleic acid
RunX3	Runt related transcription factor 3
S100A11	S100 calcium binding protein A11
shRNA	Short hairpin ribonucleic acid
siRNA	Short interfering ribonucleic acid
SLC12A5	Solute carrier family 12, member 5
SLC1A3	Solute carrier family 1, member 3
SNF	Sucrose non-fermenting
SWI	Yeast mating type switching
SYT1	Synaptotagmin 1
T-SCE	Telomeric sister chromatid exchange
TERT	Telomerase reverse transcriptase
Tp53	Tumour suppressor protein 53
WHO	World Health Organization
Wnt5a	Wingless-type MMTV integration site family, member 5a
Wnt7b	Wingless-type MMTV integration site family, member 7b
XIST	X-inactivation specific transcript

CHAPTER 1 – Introduction

1.1 Glioma

Gliomas are the most common primary brain malignancies and constitute a wide and heterogeneous population of tumours (Furnari 2007). Despite being defined across various malignancy states – from low-grade, benign tumours to highly aggressive and invasive glioblastoma multiforme (GBM) tumours – gliomas are extremely challenging to treat in the clinic because of their infiltrative nature and high tendency for recurrence (Wen 2008). Recent work has identified numerous genetic and epigenetic alterations that define various subtypes of glioma (Verhaak 2010). However, the underlying mechanisms of glioma initiation and progression have yet to be fully elucidated, and this may be achieved through the development of novel *in vitro* and *in vivo* model systems.

1.1.1 Histology and Pathology of Glioma

Classically, gliomas can be categorized based on their histology as astrocytomas, oligodendrogliomas, or mixed-lineage oligoastrocytomas, and subsequently graded on the World Health Organization (WHO) scale based on their degree of malignancy (Marumoto 2012). The majority of high grade glial tumours are termed glioblastomas and display several features of malignancy, including vascularization, necrosis, and pleomorphism. Glioblastomas can be further subdivided into primary and secondary GBMs based on their clinical presentation; however, histologically these two tumour subtypes are indistinguishable. Primary GBMs typically arise *de novo* in older patients, while secondary GBMs are most commonly seen in younger patients (below age 45) and develop from lower grade tumours about 5-10 years following diagnosis (Marumoto 2012).

Contrastingly, low-grade gliomas (LGGs) are classified as grade I or II on the WHO grading scale and constitute 30-50% of all central nervous system (CNS) solid tumours in children (Stieber 2001; Louis 2007). Again, LGGs can be histologically categorized into

pilocytic or low-grade astrocytomas, oligodendrogliomas, or oligoastrocytomas; however, these tumour types have prolonged survival and reduced recurrence rates compared to their high-grade counterparts. Low-grade gliomas are also considerably heterogeneous in nature and often undergo anaplastic dysplasia (Louis 2007).

1.1.2 Key Players in Glioma Pathogenesis

Genetically, both primary and secondary GBMs commonly show alterations in *tumour suppressor protein 53 (TP53)*, *phosphatase and tensin homolog deleted from chromosome 10 (PTEN)*, and *epidermal growth factor receptor (EGFR)*, including loss or mutation of either *TP53* or *PTEN* and/or amplification or overexpression of *EGFR* (Marumoto 2012). Additionally, both primary and secondary GBMs commonly show abnormal activation of growth factor signalling, leading to aberrant signalling through the mitogen activated protein kinase (MAPK) and phosphoinositide-3-kinase (PI3K)-AKT pathways, as well as cell cycle checkpoint dysregulation, including *retinoblastoma protein (pRB)* and/or *p16^{INK4A}* inactivation (Marumoto 2012).

Until recently, high-grade gliomas (HGGs) – including glioblastoma multiforme and anaplastic astrocytomas – were distinguished solely by their histological properties. However, recent evidence indicates that these histological subtypes may represent several sub-classes of HGG that can be further defined based on their molecular and genetic profiles. From this, four subtypes of primary GBMs have emerged based on tumour gene expression/mutation profiles. These subtypes have been termed ‘proneural’, ‘neural’, ‘classical’, and ‘mesenchymal’, and are distinguished by their unique pattern of genetic changes (Phillips 2006; Verhaak 2010). While two major features in proneural GBM subtype tumours are alterations in the expression of *Platelet Derived Growth Factor Alpha (PDGFA)* as well as point mutations in *Isocitrate Dehydrogenase 1 (IDH1)*, the neural subtype demonstrates expression of neuron markers like *NEFL*, *GABRA1*, *SYT1*, and *SLC12A5* (Verhaak 2010). Alternatively, classical GBM tumours typically show amplification of chromosome 7 along with loss of chromosome 10 and overexpression of

EGFR (Verhaak 2010). Finally, mesenchymal tumours generally show loss of *NF1* and/or *PTEN*, both of which impact signalling through the AKT pathway (Verhaak 2010).

The underlying genetic mechanisms surrounding LGG pathogenesis have not been extensively studied; however, mutation of the *Isocitrate Dehydrogenase 1 or 2 (IDH1/2)* genes appears to be a common pathogenic initiating event (Sanson 2009; Hartmann 2009; Ducray 2009) associated with massive changes to the epigenomic landscape (Turcan 2012). Additionally, coordinated loss of chromosomes 1p and 19q (1p/19q co-deletion) appears to converge with mutations in *IDH1/2* and delineates a prognostically favourable outcome within oligodendrogliomas and some oligoastrocytomas (Cairncross 1998). Tumours harbouring intact 1p/19q but mutated *IDH1/2* commonly overlap with mutations in *TP53* and display a much more diverse genomic landscape (Thon 2012).

1.1.3 TP53 Mutations in Glioma

Alterations in *TP53* were one of the first recurrent mutations discovered within gliomas, and have now become the most common genetic abnormalities observed across the glioma tumour spectrum. *TP53* is a transcription factor that regulates a large number of genes involved in cell cycle control, DNA damage response, metabolism, cellular senescence, autophagy and apoptosis (Guimaraes 2002), along with its other non-transcriptional roles in the regulation of autophagy and apoptosis (Green 2009). The *TP53* protein can be activated by a number of internal and external stimuli, including DNA damage, aberrant growth factor signalling, oncogene activation, and hypoxia (Vousden 2009). Failure to activate *TP53* in response to tumorigenic stimuli, like DNA damage or oncogene activation, will prevent the initiation of downstream DNA repair, cellular senescence and apoptotic pathways which may allow cells to become oncogenic.

The *TP53* protein is also pivotal in the regulation of stem cell self-renewal, potency, and differentiation. In fact, inhibition of the *TP53* protein in induced pluripotent stem cells (iPSCs) caused a 100-fold increase in proliferative capacity (Krizhanovsky 2009) and a concomitant increase in genetic instability at levels similar to that seen in cancer stem cells

(CSCs; Marión 2009). A variety of mouse models harbouring complete loss of *Tp53*, or loss of specific codons/exons of *Tp53*, show increased susceptibility to spontaneous tumour formation and decreased overall survival (Pohl 1988; Donehower 1992; Jacks 1994). Deletion of *TP53* in conjunction with loss of other tumour suppressor genes or overexpression of oncogenes further promotes tumour development, progression, as well as aggressiveness and metastatic potential, specifically in high-grade adult astrocytoma (Chow 2011). However, in glioma patients, it is uncertain how the loss of TP53 affects prognostic outcome, as *TP53* mutations do not correlate with patient survival or time-to-recurrence (Houillier 2006; Weller 2009).

Inhibitors of TP53 have been developed and are beginning to be widely used to examine the cytotoxic effects of TP53 inhibition both *in vitro* and *in vivo*. One such inhibitor, called Pifithrin- α (PFT α) was originally discovered in a broad screen of approximately 10,000 compounds to inhibit cell death induced by γ -irradiation (Komarov 1999). Although the complete mechanism of TP53 inhibition has not been explored, studies showed that PFT α treatment was associated with reduced nuclear, but not cytoplasmic, levels of TP53 (Komarov 1999). This indicates that PFT α acts to modulate the nuclear import and/or export of TP53, thereby preventing TP53 from binding to its transcriptional targets. PFT α was later shown to prevent apoptosis in mouse embryonic fibroblasts (MEFs) transformed with *Ela+ras*, a cell line that undergoes rapid TP53-mediated apoptosis in response to treatment with various genotoxic stressors, including doxorubicin, etoposide, UV light, and γ -irradiation (Komarov 1999). Additionally, PFT α prevented the appearance of apoptotic cells in doxorubicin-treated human umbilical vein endothelial cells (HUVECs) along with blocking promoter induction and protein up-regulation of CD95 in response to doxorubicin treatment (Lorenzo 2002). Following several years of development, new isoforms of PFT α have been developed. The cyclic form of PFT α (cPFT α) is a more stable analog of PFT α with similar biological activities and reduced cytotoxicity, and studies have shown that cPFT α sensitizes wildtype TP53 tumour cells to antimicrotubule agent-induced apoptosis (Zuco 2008). Thus, these drugs have been described throughout the literature as being effective and specific inhibitors of the transcriptional activation activities of TP53 and their use has enabled the discovery of novel TP53 functions in carcinogenesis.

1.1.4 IDH1/2 Involvement in Glioma Initiation and Progression

Mutations in the *Isocitrate Dehydrogenase 1 and 2 (IDH1/2)* genes were first identified in 2008 from the analysis of over 20,000 genes in 22 GBM samples (Parsons 2008). Since then, *IDH1* mutations have become an extremely prominent player in gliomagenesis, as other studies identified *IDH1* alterations in up to 80% of grade 2 and 3 gliomas as well as secondary GBMs (Hartmann 2009; Sanson 2009; Yan 2009; Watanabe 2009; Kanamori 2013). Mutations in *IDH2* are also found within the glioma spectrum; however, they arise at a much lower frequency and are mutually exclusive from *IDH1* modifications (Hartmann 2009; Yan 2009).

To date, mutations in *IDH1* or *IDH2* can be narrowed down to a single amino acid residue (R132 in *IDH1*; R172 in *IDH2*). The R132 residue in *IDH1*, as well as the analogous R172 residue in *IDH2*, lies in the active site of the enzyme and is critical for isocitrate binding (Xu 2004). Mutation at this residue abolishes the ability of *IDH* to perform its catalytic activities, resulting in reduced levels of α -ketoglutarate (α -KG) and nicotinamide adenine dinucleotide phosphate (NADPH; Xu 2004). Exactly how *IDH* mutation leads to oncogenic transformation remains unclear; however, recent evidence suggests that mutated *IDH* is able to bind and convert α -KG into (R)-2-hydroxyglutarate (2-HG; Dang 2009). Whether reduced activity of *IDH* or elevated 2-HG levels leads to tumorigenesis is unknown, but evidence suggests that the mutated *IDH* genes act as oncogenes, while 2-HG acts as an oncometabolite. Regardless of the mechanism, it is known that introduction of mutated *IDH* into normal cells leads to increased cellular proliferation, reduced differentiation, and increased colony formation (Koivunen 2012).

Though mutations in *IDH* appear to be an early event in oncogenic transformation, further mutations in other tumour suppressors (like *TP53*) or genomic instability events (like 1p/19q co-deletion) are necessary for cells to fully gain their oncogenic potential. Within astrocytic tumours, co-mutation of *IDH1* and *TP53* is common, with up to 80% of secondary GBMs and anaplastic astrocytomas harbouring both mutations (Yan 2009). On the other hand, oligodendrogliomas that harbour 1p/19q co-deletion typically show

mutations in *IDH1* but not *TP53* (Kanamori 2013; Watanabe 2009; Yan 2009). Finally, although commonly seen alongside mutations that are associated with LGGs and secondary GBMs, mutations in *IDH* rarely overlap with alterations common to primary GBMs (like mutation of *EGFR*; Watanabe 2009), which is indicative of a role for *IDH* mutation as an early event in gliomagenesis, but not as a driver of primary GBM.

1.1.5 *ATRX*: a new player in Gliomagenesis

Mutations in *alpha thalassaemia mental retardation X-linked (ATRX)* were first identified in gliomas through an association with the alternative lengthening of telomeres (ALT) phenotype (Heaphy 2011) – a telomerase independent mechanism whereby cells can lengthen their telomeres. *ATRX* mutations were detected in various tumours of the central nervous system (CNS), including pediatric GBM (14.3%), adult GBM (7.7%), and medulloblastoma (1.5%) (Heaphy 2011). Other studies used whole exome sequencing of pediatric GBMs and identified mutations in *ATRX* in 33.3% of cases, and these mutations significantly overlapped with alterations in *TP53* (Schwartzentruber 2012). Immunostaining of patient tissue microarrays for *ATRX* in 124 samples identified 35% lacking detectable *ATRX* staining, indicative of impaired *ATRX* transcription/translation resulting in low or no *ATRX* protein expression and function (Schwartzentruber 2012). Thus, these two studies first identified a role for *ATRX* perturbation in pediatric glioblastoma multiforme.

Since then, research has delved into the field of both adult and pediatric glioma, and *ATRX* mutations have been identified across the glioma landscape (Jiao 2012; Liu 2012; Kannan 2012; Wiestler 2013). Alterations in *ATRX* were identified by Sanger sequencing in 67% of WHO grade II astrocytomas, 73% of WHO grade III astrocytomas, 57% of secondary GBMs, and 68% of mixed oligoastrocytomas (Jiao 2012), and these tumours almost always showed co-mutation of *TP53* and/or *IDH1* (Jiao 2012; Liu 2012). Mutations in *ATRX* were rare, however, in primary GBMs (4%) (Jiao Y et al 2012). Within LGGs, *ATRX* mutations were discovered in three out of four WHO grade II gliomas that harboured *IDH* mutations, and this correlated with mutation in *TP53* and intact 1p/19q (Kannan 2012). Investigation

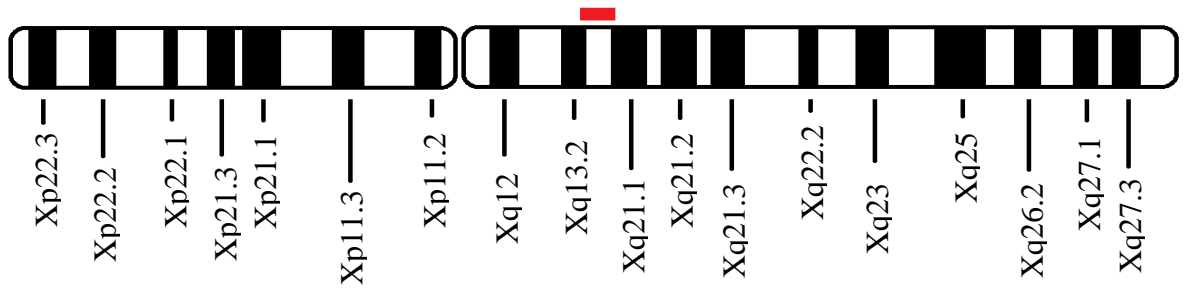
of another 28 WHO grade II and III gliomas identified *ATRX* mutations in 43% of samples, and these mutations again significantly correlated with alteration of *IDH* and *TP53* (Kannan 2012). Collectively, these studies identify *ATRX* as a potential biomarker for glioma subtype classification when investigated in combination with *IDH*, *TP53*, and 1p/19q mutation status.

1.2 Alpha Thalassaemia Mental Retardation X-Linked

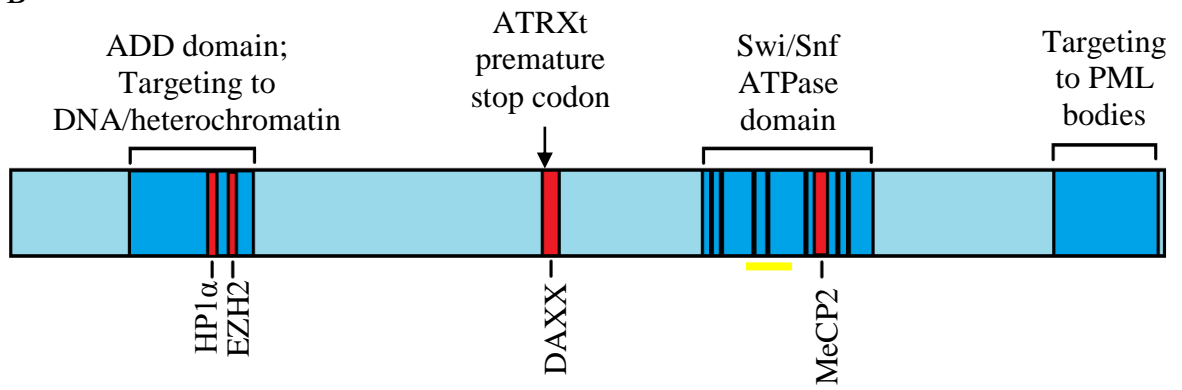
The *ATRX* gene lies on the long arm of the X-chromosome (Xq13.3; Fig. 1.1) and spans approximately 300kb of genomic sequence (Picketts 1996). In humans, the *ATRX* gene has been mapped between the gene for Menkes disease (*MNK*) and the X-chromosome region DXS56 (Stayton 1994); whereas in mice, the *Atrx* homolog maps between the *Phosphoglycerate kinase-1* (*Pgk1*) and *X-inactivation specific transcript* (*Xist*) genes (Gecz 1994). This gene gives rise to the large ATRX protein (approximately 280kDa), which contains an N-terminal ADD (ATRX-DNMT3-DNMT3L) domain as well as a C-terminal SWI/SNF2-like motif (Fig. 1.1; Picketts 1996). The ADD domain of ATRX shows homology to the DNMT (DNA methyltransferase) family of proteins (Picketts 1996; Argentaro 2007) and consists of three regions, including a GATA-like zinc finger, an imperfect PHD-like zinc finger, and a C-terminal helix that packs together using hydrophobic interactions (Argentaro 2007). In this way, the ADD domain of ATRX can bind directly to the tail of histone 3 (H3) using two binding pockets: one that reads unmethylated lysine 4 (H3K4me0) and one that reads di- or trimethylated lysine 9 (H3K9me2 or H3K9me3) (Iwase 2011; Eustermann 2011). This combinatorial readout, which is further enhanced by HP1 α binding, allows for ATRX recruitment to heterochromatin (Eustermann 2011). At the other end of ATRX, the SWI/SNF2-like domain contains an ATPase/helicase motif, and this region is necessary for the nucleosome remodelling and translocase activity of ATRX (Picketts 1996). ATRX also harbours many binding sites for various protein-protein interactions (Fig 1.1), including DAXX (death domain associated protein 6; Tang 2004; Xue 2003), HP1 α (heterochromatin-associated protein 1 alpha; McDowell 1999), and MeCP2 (methyl CpG binding protein 2; Nan 2007). An additional, truncated isoform of *ATRX* (called *ATRXt*) was discovered when

Figure 1.1 Overview of the *ATR*X gene and protein. (A) Outline of the human X chromosome and location of the *ATR*X gene, indicated in red. (B) Schematic of the *ATR*X protein including its conserved protein domains (coloured in dark blue) and protein interaction sites (coloured in red). The yellow line indicates the placement of the *neo* cassette in our *Atrx* floxed mice. (C) *Cre/loxP* targeting of the *Atrx* mouse gene. The top line indicates the wildtype *Atrx* allele (*Atrx*^{WT}). The middle line shows the insertion of *loxP* target sites flanking exon 18 along with a *neo* marker (*Atrx*^{flax}). The bottom line demonstrates the recombination of *Atrx* upon *Cre recombinase* activation in which exon 18 and the *neo* cassette have been removed (*Atrx*^{Δ18Δneo}).

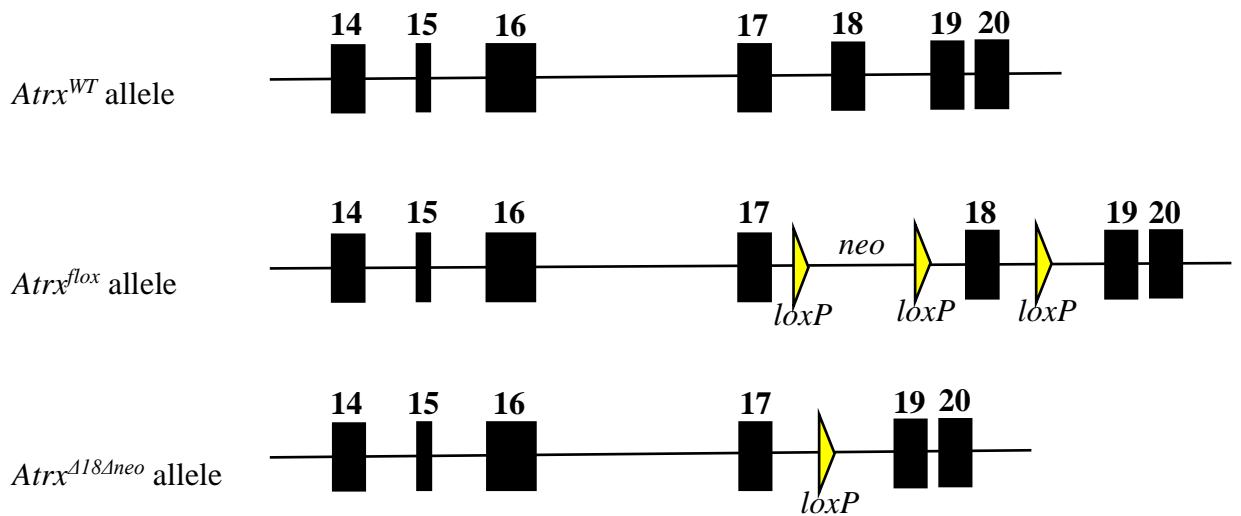
A



B



C



immunoblots using ATRX N-terminal antibodies consistently detected a shorter protein product of about 180kDa (Bérubé 2000; McDowell 1999). This short isoform results from an alternative splicing event that leads to the creation of a premature stop codon within intron 11 (Fig 1.1; Garrick 2004). Due to the truncation, the resulting short polypeptide still contains the ADD domain but lacks the Swi/Snf C-terminal domain, PML targeting region, and the interaction sites for DAXX and MeCP2 (Fig 1.1). As expected, ATRXt can localize to regions of the nucleus dictated by the ADD domain, like pericentromeric heterochromatin, but is no longer found in PML bodies (Garrick 2004). Biologically, the function of ATRXt still remains elusive; however, it is predicted that ATRXt may interact with the full-length ATRX protein (Garrick 2004) and could modulate the activity of ATRX at heterochromatin.

1.2.1 ATRX and Neuronal Development

ATRX is expressed in the proliferating neuroprogenitor cells of the brain and retina during development. *ATRX* exhibits a typical punctate staining pattern that overlaps with heterochromatic foci (Bérubé 2005), and upon differentiation, *ATRX* protein levels increase within the nucleus (Bérubé 2005; Ritchie 2008). Studies over the past decade or so have determined that incorrect expression or activity of *ATRX* is clearly detrimental to development in both humans and mice. Mutations in *ATRX* in humans results in ATR-X syndrome (alpha thalassaemia mental retardation, X-linked; OMIM: #30032), characterized by mild to severe mental retardation, distinct facial dysmorphisms, urogenital abnormalities, loss of white matter, and α -thalassaemia (Weatherall 1981; Gibbons 2006). The majority of disease mutations map within the ADD and Swi/Snf domains of *ATRX*, resulting in reduced protein expression levels (hypomorphic) rather than a complete loss-of-function, which is presumed to be lethal (Gibbons 1995; Picketts 1996).

Study of *ATRX* gain- and loss-of-function in mice provided insights into the role of *ATRX* during development. Examination of *ATRX* overexpression led to a wide array of developmental abnormalities, including embryonic lethality and disorganization of the proliferative neuroepithelium (Bérubé 2002). The few surviving *ATRX* transgenic pups

exhibited craniofacial abnormalities and spontaneous seizures (Bérubé 2002). On the other hand, loss of ATRX in mouse embryonic stem cells (mESCs) resulted in reduced cellular proliferation and survival (Garrick 2006). Complete ATRX loss in the mouse via early inactivation at the morula stage prevented the formation of a normal trophectoderm and resulted in embryonic lethality around E9.5 (Garrick 2006).

To better investigate the loss of ATRX specifically in the developing mouse brain, the *Cre/loxP* system was utilized to ensure precise spatial and temporal ablation of ATRX function (Bérubé 2005). This system incorporates *loxP* sites flanking exon 18 of *Atrx* along with *Cre*-mediated recombination and silencing of *Atrx* using a specific *Cre*-driver line (Fig 1.1). For example, when the *Cre recombinase* gene is placed under the control of the *Forkhead box G1 (FoxG1)* promoter, *Cre recombinase* expression is confined to the mouse forebrain beginning at E8.5 (Hebert 2000). As a result of ATRX loss in the developing telencephalon, a significant increase in apoptosis was observed along with a profound size reduction of the frontal cortex, hippocampus, and a loss of the dentate gyrus structure (Bérubé 2005). At birth, ATRX-null male mice are also much smaller in length and weight than their littermate-matched control male counterparts (Bérubé 2005). This result indicates the importance of ATRX for the survival of neurons during corticogenesis, as a loss of ATRX in proliferating cells was succeeded by an increase in TP53 activation along with downstream TP53 target genes (Seah 2008). Combined loss of ATRX with TP53 in mice demonstrated a rescue of cell death embryonically; however, overall brain and body size at birth were not rescued (Seah 2008), indicating that TP53 activation is responsible for some but not all of the ATRX-null phenotypes observed.

1.2.2 Cellular Functions of ATRX

The finding of an N-terminal nuclear localization signal (NLS) within the ATRX protein led to the discovery that ATRX is associated with pericentromeric heterochromatin during all stages of the cell cycle (Bérubé 2000; McDowell 1999). This soon led to the finding that ATRX is phosphorylated mainly on serine residues and in a cell cycle-dependent manner (Bérubé 2000). In fact, depletion of ATRX in human HeLa cells (cervical cancer cell line)

using both stable shRNA constructs and transient small interfering RNA (siRNA) led to nuclear blebbing, chromosomal bridging, and poorly resolved chromatin during interphase (Ritchie 2008). Additionally, ATRX-depleted HeLa cells exhibited prolonged prometaphase to metaphase transitions during mitosis, leading to an overall lengthening of the time required to complete mitosis compared to ATRX wildtype HeLa cells (Ritchie 2008). This was accompanied by abnormal sister chromatid congression to the metaphase plate, reduced sister chromatid cohesion at metaphase, and chromosome decondensation (Ritchie 2008). These results were further validated *in vivo* where DAPI staining revealed pyknotic nuclei, micronuclei, and misaligned chromosomes within the hippocampal hem, the hippocampal primordium, and the dorsal cortical neuroepithelium in embryonic brain sections (Ritchie 2008). Furthermore, ATRX is required for proper meiotic spindle organization and chromosome alignment during metaphase II in mouse oocytes (De La Fuente 2004; Ritchie 2014). Thus, ATRX is necessary for the maintenance, organization, and architecture of the chromosomes at the metaphase plate in both meiosis and mitosis.

During S-phase, ATRX has been shown to localize to G-rich tandem repetitive DNA like G-quadruplexes, satellite repeats, and telomeres, and ATRX depletion results in delays in S-phase and replication stress (Wong 2010; Huh 2012; Leung 2013; Watson 2013). In myoblasts, ATRX depletion led to alterations in cell cycle checkpoint proteins (p107, cyclin E, cyclin A, and p27), along with TP53 accumulation (Huh 2012). ATRX loss in mESCs, mouse embryonic fibroblasts (MEFs) and somatic cell lines was also associated with sensitivity to hydroxyurea (HU) and aphidicolin (APH) genotoxic treatments, but not to γ -irradiation (Clynes 2014; Watson 2013; Leung 2013), indicating that ATRX-null cells demonstrate a specific sensitivity to drugs that induce replication fork stalling. Replication stress was observed in conjunction with significant increases in genomic instability and DNA damage (Clynes 2014; Leung 2013; Watson 2013), along with ATRX localization to DNA double-stranded break (DSB) sites (Leung 2013) and increased fork stalling during replication (Leung 2013; Watson 2013; Clynes 2014).

Significant increases in DNA damage were also observed in the ATRX-null embryonic telencephalon and in the neonatal hippocampus (P0.5), which remains proliferative at this timepoint (Watson 2013). However, by postnatal day 7 (P7), DNA damage was no longer

present in both control and ATRX-null brains (Watson 2013), suggesting that endogenous DNA damage from ATRX loss occurs primarily in replicating cells. Interestingly, the cells in the embryonic telencephalon that harboured γ H2A.X foci also showed staining for cleaved caspase 3 (AC3), a canonical marker for apoptosis activation (Watson 2013), indicating that cell death is likely a downstream consequence of DNA damage accumulation. Assessment of DNA DSBs in ATRX/TP53 compound mutant mice demonstrated a further increase in γ H2A.X immunostaining embryonically (Watson 2013), along with a rescue of cell death in the hippocampal hem and basal telencephalon at E13.5 (Seah 2008). This result demonstrates that ATRX loss is associated with increased genomic instability that leads to TP53 stabilization and activation of its downstream apoptotic pathways. Thus, ATRX is necessary for proper mitotic and meiotic integrity, as well as for maintaining chromatin stability and architecture, particularly during S-phase.

1.2.3 ATRX and Histone Variants

In addition to its ability to target heterochromatin by directly binding to histone tails, ATRX also influences the histone composition of chromatin. Firstly, recent research identified a link between ATRX and a histone variant known as macroH2A (Ratnakumar 2012). MacroH2A is typically associated with transcriptionally inert DNA, and is frequently found within heterochromatin (Zhang 2005). ATRX was found to interact with macroH2A in a chromatin-free cellular fraction, and loss of ATRX resulted in altered levels of macroH2A (Ratnakumar 2012). Targeted knockdown of ATRX in HEK293 cells (human embryonic kidney cells) led to a global increase in macroH2A levels in chromatin, but not total cellular levels, indicating a role for ATRX as a negative regulator of macroH2A incorporation into chromatin (Ratnakumar 2012). Chromatin immunoprecipitation (ChIP) analysis identified increased levels of macroH2A at the telomeres upon loss of ATRX, as well as an accumulation at the α -globin gene cluster (Ratnakumar 2012). While still unclear, ATRX-mediated prevention of macroH2A deposition at telomeres may act to ensure telomeric integrity.

In addition to its role with macroH2A, ATRX also works with its binding partner DAXX to mediate histone 3.3 (H3.3) deposition into pericentric, telomeric and ribosomal repeat chromatin (Drané 2010; Goldberg 2010). H3.3 is a replication-independent histone variant predominantly associated with active and open chromatin (Loyola 2006), while phosphorylation of H3.3 at serine 31 (H3.3S31P) is enriched in heterochromatin and acts as a mitosis-specific marker (Hake 2005). During H3.3 deposition, DAXX acts as a highly specific histone chaperone that can discriminate between H3 isoforms H3.1, H3.2, and H3.3 (Drané 2010). ATRX can subsequently bind with DAXX/H3.3 and target this complex to repetitive sequences to enhance H3.3 deposition (Drané 2010; Lewis 2010). Remodeling assays also identified the ability of the ATRX-DAXX complex to successfully mobilize H3.3-containing nucleosomes along DNA templates (Lewis 2010).

At the telomeres, ATRX has been shown to colocalize with H3.3 in mES cells, and ATRX knockdown led to a significant increase in telomere induced dysfunction foci (TIF; a marker for DNA damage at the telomeres identified by γ H2A.X staining) as well as an extreme reduction of HP1 α localization (Wong 2010). ATRX-null ESCs exhibit an extreme loss of H3.3 at the telomeres but maintain the ability of DAXX to associate with H3.3, indicating that ATRX is not necessary for the interaction between DAXX and H3.3 but may be necessary for H3.3 localization to telomeres (Lewis 2010). In contrast, DAXX-null ES cells showed no interaction between ATRX and H3.3 and showed no change in H3.3 incorporation at telomeres, indicating that DAXX mediates the H3.3-ATRX interaction but is not required for specific H3.3 deposition at telomeres (Lewis 2010).

Further studies in ATRX-null myoblasts identified a significant increase in DNA damage at the telomeres as well as increased levels of telomere bridging, duplications and merging (Huh 2012). This result is further supported by ATRX-null primary neuroprogenitor cells (NPCs) which showed a significant increase in γ H2A.X staining at the telomeres along with increased telomere-centromere/telomere-telomere fusions (Watson 2013). Loss of telomeric integrity is commonly associated with replicative disruption at the telomeres (Sampathi 2011), and G-rich DNA sequences, like telomeres, have been recently shown to form G-quadruplex (G4) structures which are difficult to replicate (Wu 2010). ATRX has been demonstrated to bind to G-quadruplexes, and may potentially help to resolve these

secondary DNA structures during cellular replication (Watson 2013; Levy 2014). Thus, it appears that ATRX is required for telomere stability and integrity, and this could be due to its roles in facilitating replication fork bypass within these G-rich regions.

1.3 ATRX and Cancer

Mutations in chromatin remodeling proteins are not common alterations in the pathology of cancer; nevertheless, *ATRX* mutations have recently become a hot topic in the field of cancer biology. After cataloguing the outcomes of ATRX loss within the cell, however, it is clear to see how the loss of ATRX function could allow for the transformation of cells towards tumorigenesis. Not only does ATRX loss correlate with replication stress (Clynes 2014; Watson 2013) and mitotic defects (Ritchie 2008; Ritchie 2014), ATRX-null cells also show significant increases in DNA damage both across the genome (Clynes 2014; Watson 2013) as well as specifically at the telomeres (Huh 2012; Wong 2013; Watson 2013). Finally, ATRX loss also leads to an increase in TP53-mediated cell death following the accumulation of DNA damage (Watson 2013; Conte 2012). These phenotypes are well known hallmarks of tumorigenesis, and combinatorial alterations in *ATRX* and other tumor suppressors or oncogenes, like *TP53* and *IDH1/2*, may reveal an underlying genetic mechanism for some subtypes of glioma and neuroendocrine tumours.

1.3.1 Early Findings for ATRX Loss in Tumorigenesis

Gene expression profiling of *de novo* childhood acute myeloid leukemia (AML) patients first identified ATRX loss of expression as a predictor of patient outcome (Lacayo 2004). Mutations in *Fms-like tyrosine kinase 3 (FLT3)* are a known prognosticator of poor outcome in AML patients, but further diagnostic markers were needed to distinguish between patients who were at high-risk for treatment failure versus those who were not. Among those patients who harboured *FLT3* mutations, high expression of *Runt related transcription factor 3 (RUNX3)* and low expression of *ATRX* correlated with worse outcome and were more likely to resist treatment (Lacayo 2004). On the contrary, patients

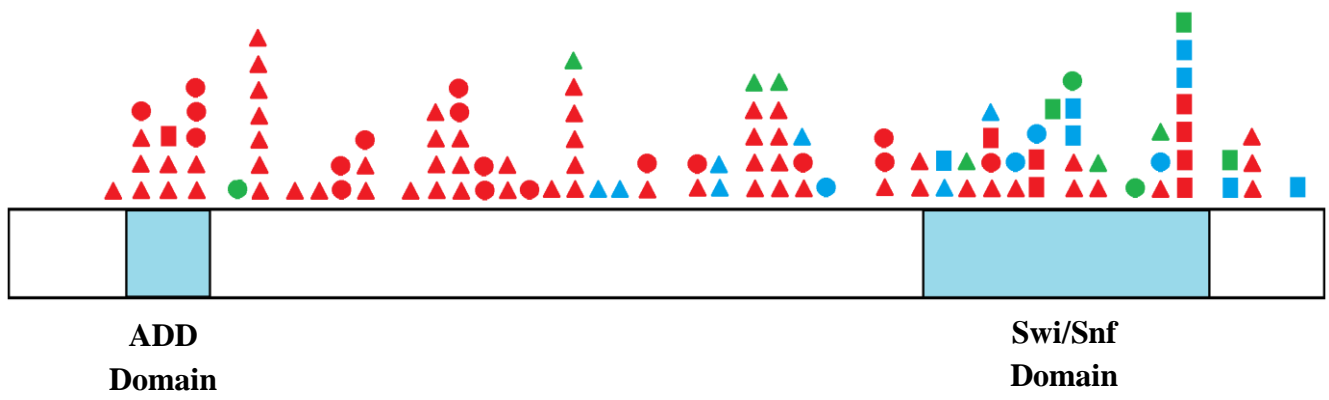
with higher *ATRX* expression demonstrated a more favourable outcome (Lacayo 2004). Thus, this was the first study to identify *ATRX* expression levels as a predictor of patient prognosis during tumorigenesis.

1.3.2 *ATRX* Loss in Neuroendocrine Tumours

Several years after the finding of *ATRX* mutations in AML patients, alterations in *ATRX* were discovered again in a significant population of pancreatic neuroendocrine tumours (panNETs; Jiao 2011). PanNETs are the second most common pancreatic malignancy with a ten-year survival rate of only 40% (Fendrich 2009). Currently, surgical resection of these tumours is the front-line of treatment, but many patients present with unresectable tumours or extensive metastatic disease which is not responsive to current medical therapies (Fendrich 2009). Whole-exome sequencing was used to identify commonly mutated genes within a subset of panNETs, and 17.6% harboured mutations in *ATRX*, 25% had alterations in *DAXX*, and 3% showed *TP53* mutations (Jiao 2011). They concluded that mutations in the *DAXX/ATRX* pathway are the second most common alteration after mutations in *Multiple endocrine neoplasia type 1 (MEN1)*, and *ATRX* mutations were most commonly insertion/deletions leading to frameshifts within the resulting polypeptide (Fig 1.2; Jiao 2011). Additionally, *DAXX* and *ATRX* alterations were mutually exclusive, and both correlated with an earlier age of diagnosis as well as better overall patient survival (Jiao 2011). In fact, 100% of patients with metastatic disease and mutations in *DAXX/ATRX* and *MEN1* survived at least 10 years, versus over 60% of patients without these mutations succumbing to their tumours within five years of diagnosis (Jiao 2011). This may indicate that *ATRX/DAXX* mutations could define a molecular subgroup of panNETs and may serve to aid prognosis and prioritize patients for treatment.

Subsequent studies of panNETs identified further alterations in *ATRX* and *DAXX* expression. Firstly, immunohistochemical analysis of well-differentiated neuroendocrine carcinomas (NECs), also considered panNETs, demonstrated a loss of *ATRX* nuclear staining in 36.4% of tumours and a loss of *DAXX* staining in 9.1% (Yachida 2012). Again,

Figure 1.2 Overview of mutations identified within the *ATRX* gene in various glioma/panNET patient studies. Triangles represent frameshift mutations, circles denote nonsense mutations, and squares signify missense mutations. Symbols coloured in red were mutations described in Jiao 2012 (glioma), symbols in blue were mutations described in Schwartzenruber 2012 (pediatric GBM), and symbols in green denote mutations described in Jiao 2011 (panNETs).



loss of *ATRX* and *DAXX* immunostaining was mutually exclusive in these tumours; however, immunostaining for both *ATRX* and *DAXX* was intact in the small- and large-cell NECs investigated, which are not considered to be panNETs (Yachida 2012). These findings identify panNETs as genetically distinct entities from other pancreatic neoplasms, and that *ATRX* and/or *DAXX* mutation status may aid in the distinction between pancreatic tumour subtypes. More recently, a large panNET sample collection (243 patient samples across a variety of hospitals) identified a loss of *DAXX* in 15% and a loss of *ATRX* in 28% of samples, with only two samples harbouring a loss of both proteins (Marinoni 2014). Loss of *ATRX/DAXX* was also shown to correlate with chromosomal instability (CIN), which is a characteristic of malignant panNETs (Marinoni 2014). Prognostically, in contrast to the findings by Jiao (2011), Marinoni (2014) correlated *ATRX/DAXX* loss as a predictor of inferior outcome, and did not find a correlation with age of diagnosis. It is evident that loss of *ATRX/DAXX* defines a biologically specific subgroup of panNETs, but it is unclear whether *ATRX/DAXX* mutations are prognostically useful to predict patient outcome.

Finally, a study by Chen (2013B) examined neuroendocrine tumours originating from various organ systems, including gastric, duodenal, rectal, pancreatic, and pulmonary tissues. Immunostaining for *ATRX* and *DAXX* showed loss of these proteins in at least one sample within neuroendocrine tumours (NETs) from all organs examined (Chen 2013B). For example, loss of nuclear labelling of either *ATRX* or *DAXX* was found in 16.1% of lung NETs, 7.3% of stomach NETs, 10.9% of duodenum NETs, 51% of panNETs, and 14.6% of rectal NETs; however, no samples showed loss of staining for both proteins (Chen 2013B). Therefore, loss of *ATRX* and/or *DAXX* may not only be relevant to pancreatic lesions, but can also be found within neuroendocrine tumours across many organ systems.

1.3.3 *ATRX* Mutations Across the Glioma Spectrum

Mutations in *ATRX* are highly prominent across the glioma tumour landscape (Table 1.1). First associations linked mutations in *ATRX* to pediatric glioblastoma multiforme, where 14.3% of samples harboured alterations in the *ATRX* gene along with 0% showing mutation in *DAXX* (Heaphy 2011). This study also examined the U2-OS osteosarcoma cell line and

Table 1.1 List of *ATRX* mutations identified in cancers within the literature.

Tumor Type, Grade	Mutation	Mutation Type	Reference
Diffuse Astrocytoma, II	p.E1702*	Nonsense	Cryan, J.B., <i>et al.</i> 2014
Diffuse Astrocytoma, II	p.K971fs	Frameshift	
Diffuse Astrocytoma, II	p.R808*	Nonsense	
Diffuse Astrocytoma, II	p.F2113fs	Frameshift	
Anaplastic Astrocytoma, III	p.R781*	Nonsense	
Anaplastic Astrocytoma, III	p.R2197C	Missense	
Anaplastic Astrocytoma, III	p.E2265A	Missense	
Anaplastic Astrocytoma, III	p.E2277A	Missense	
Anaplastic Astrocytoma, III	p.L1602*	Nonsense	
Anaplastic Astrocytoma, III	p.D789V	Missense	
Anaplastic Astrocytoma, III	p.S118fs	Frameshift	
Anaplastic Astrocytoma, III	p.R418*	Nonsense	
Anaplastic Astrocytoma, III	p.S1387*	Nonsense	
Anaplastic Astrocytoma, III	p.R808*	Nonsense	
Anaplastic Astrocytoma, III	p.K1332fs	Frameshift	
Oligoastrocytoma, II	p.R1426*	Nonsense	
Oligoastrocytoma, II	p.K1332fs	Frameshift	
Oligoastrocytoma, II	p.R418*	Nonsense	
Oligoastrocytoma, II	p.K2283splice	Splice Variant	
Oligoastrocytoma, III	p.R781*	Nonsense	
Oligoastrocytoma, III	p.G1937E	Missense	
Oligoastrocytoma, III	p.Y2083C	Missense	
Oligoastrocytoma, III	p.R1426*	Nonsense	
Oligoastrocytoma, III	p.E935*	Nonsense	
Oligoastrocytoma, III	p.E884D	Missense	
Oligodendroglioma, II	p.D1051E	Missense	
Oligodendroglioma, III	p.G2075R	Missense	
High Grade Glioma	p.F2113fs	Frameshift	Huether, R., <i>et al.</i> 2014
High Grade Glioma	p.D1791H	Missense	
High Grade Glioma	p.T1610R	Missense	
High Grade Glioma	p.D2144G	Missense	

High Grade Glioma	p.R188*	Nonsense	
Neuroblastoma	p.L407F	Missense	
Neuroblastoma	p.A1690D	Missense	
Neuroblastoma	p.E555*	Nonsense	
Neuroblastoma	p.R2188Q	Missense	
Neuroblastoma	p.E426fs	Frameshift	
Adrenocortical Carcinoma	p.R2164S	Missense	
Adrenocortical Carcinoma	p.Q811*	Nonsense	
Adrenocortical Carcinoma	p.E2253*	Nonsense	
Osteosarcoma	p.Y266*	Nonsense	
Osteosarcoma	p.D1383fs	Frameshift	
Osteosarcoma	p.R1803C	Missense	
Osteosarcoma	p.S213*	Nonsense	Chen, X., <i>et al.</i> 2014
Osteosarcoma	p.Y266*	Nonsense	
Osteosarcoma	p.D1383fs	Frameshift	
Osteosarcoma	p.L1755V	Missense	
Osteosarcoma	p.R1803C	Missense	
Cutaneous Melanoma	p.E453K	Missense	Qadeer, Z.A., <i>et al.</i> 2014
Cutaneous Melanoma	p.R444Q	Missense	
Cutaneous Melanoma	p.H756Y	Missense	
Cutaneous Melanoma	p.S334F	Missense	
Cutaneous Melanoma	p.D1263E	Missense	
Cutaneous Melanoma	p.A1790fs	Frameshift	
Cutaneous Melanoma	p.D1487N	Missense	
Cutaneous Melanoma	p.E2050K	Missense	
Cutaneous Melanoma	p.S342F	Missense	
Cutaneous Melanoma	p.K1936R	Missense	
Cutaneous Melanoma	p.S925F	Missense	
Cutaneous Melanoma	p.M1005I	Missense	
Cutaneous Melanoma	p.R2150I	Missense	
Cutaneous Melanoma	p.E2351*	Nonsense	
Cutaneous Melanoma	p.L639F	Missense	
Cutaneous Melanoma	p.E641K	Missense	
Cutaneous Melanoma	p.E2333K	Missense	
Cutaneous Melanoma	p.E1258*	Nonsense	
Cutaneous Melanoma	p.R2153C	Missense	
Cutaneous Melanoma	p.S576L	Missense	

Cutaneous Melanoma	p.L2069F	Missense	
Cutaneous Melanoma	p.P657K	Missense	
Cutaneous Melanoma	p.P97S	Missense	
Anaplastic Astrocytoma	p.S871*	Nonsense	Aihara, K., <i>et al.</i> 2014
Glioblastoma, IV	p.K923*	Nonsense	
Pilocytic Astrocytoma	p.E991K	Missense	Zhang, J., <i>et al.</i> 2013
PanNET	p.E990*	Nonsense	Pugh, T.J., <i>et al.</i> 2013
PanNET	p.L1645*	Nonsense	
PanNET	p.S2017P	Missense	
PanNET	p.R2188Q	Missense	
PanNET	p.R2197C	Missense	
PanNET	p.F2113fs	Frameshift	
Oligoastrocytoma, II	p.R1426*	Nonsense	Kannan, K., <i>et al.</i> 2012
Oligoastrocytoma, II	p.R907*	Nonsense	
Oligoastrocytoma, II	p.E1010fs	Frameshift	
Astrocytoma, II	p.L639fs	Frameshift	
Astrocytoma, II	p.K1001fs	Frameshift	
Astrocytoma, II	p.E991fs	Frameshift	
Astrocytoma, III	p.K1018fs	Frameshift	
Astrocytoma, III	p.R1302fs	Frameshift	
Astrocytoma, III	p.R221K	Missense	
Glioblastoma, IV	p.Y187*	Nonsense	Jiao, Y., <i>et al.</i> 2012
Glioblastoma, IV	p.R1504*	Nonsense	
Glioblastoma, IV	p.R1803H	Missense	
Glioblastoma, IV	p.R2153C	Missense	
Glioblastoma, IV	p.W263*	Nonsense	
Oligodendroglioma, II	p.R221M	Missense	
Oligodendroglioma, II	p.R1514*	Nonsense	
Astrocytoma, II	p.Q292*	Nonsense	
Astrocytoma, II	p.E533*	Nonsense	
Astrocytoma, II	p.R808*	Nonsense	
Astrocytoma, III	p.R781*	Nonsense	
Astrocytoma, III	p.S788*	Nonsense	
Astrocytoma, III	p.R808*	Nonsense	
Astrocytoma, III	p.V2189L	Missense	
Astrocytoma, III	p.R937*	Nonsense	
Astrocytoma, III	p.Y1115*	Nonsense	

Astrocytoma, III	p.S125*	Nonsense	
Astrocytoma, III	p.T1747K	Missense	
Astrocytoma, III	p.A1804P	Missense	
Astrocytoma, III	p.L253*	Nonsense	
Oligoastrocytoma, II	p.G551*	Nonsense	
Oligoastrocytoma, III	p.E2172G	Missense	
Oligoastrocytoma, III	p.R1426*	Nonsense	
Oligoastrocytoma, III	p.R1739*	Nonsense	
Neuroblastoma	p.L407F	Missense	Cheung, N.K., <i>et al.</i> 2012
Neuroblastoma	p.K425fs	Frameshift	
Neuroblastoma	p.E555*	Nonsense	
Neuroblastoma	p.A1690D	Missense	
Neuroblastoma	p.R2188Q	Missense	
Glioblastoma, IV	p.E1757*	Nonsense	Schwartzentruber, J., <i>et al.</i> 2012
Glioblastoma, IV	p.K1057fs	Frameshift	
Glioblastoma, IV	p.R1739*	Nonsense	
Glioblastoma, IV	p.M1800T	Missense	
Glioblastoma, IV	p.C1122fs	Frameshift	
Glioblastoma, IV	p.S1394fs	Frameshift	
Glioblastoma, IV	p.E1757*	Nonsense	
Glioblastoma, IV	p.H2254R	Missense	
Glioblastoma, IV	p.R2111*	Nonsense	
Glioblastoma, IV	p.G1589V	Missense	
Glioblastoma, IV	p.R1426*	Nonsense	
Glioblastoma, IV	p.K1584fs	Frameshift	
Glioblastoma, IV	p.N2443D	Missense	
Glioblastoma, IV	p.R1302fs	Frameshift	
Glioblastoma, IV	p.D2136N	Missense	
Glioblastoma, IV	p.W263*	Nonsense	Heaphy, C., <i>et al.</i> 2011
Glioblastoma, IV	p.R2153C	Missense	
Glioblastoma, IV	p.R1803H	Missense	

identified a homozygous deletion of exons 2 to 19 within *ATRX* (Heaphy 2011). Schwartzentruber (2012) surveyed four pediatric GBMs that harboured mutations in the histone variant H3.3. Two recurrent mutations were found, G34R and K27M, both of which lie near the tail of the protein that undergoes important post-translational modifications involved with transcriptional repression or activation. Interestingly, all four of these samples also harboured mutations in *ATRX* that may indicate an underlying dysfunction in the *ATRX/DAXX/H3.3* histone deposition pathway. Whole-exome sequencing analysis was performed in 42 additional pediatric GBMs and identified *ATRX/DAXX/H3.3* mutations in 50% of samples (15/42 *H3.3*; 14/42 *ATRX*; 2/42 *DAXX*) (Schwartzentruber 2012). The majority of *ATRX* mutations were insertions/deletions leading to frameshifts, followed by nonsense and missense mutations, and these mutations localized either within the C-terminal SWI/SNF2 domain of *ATRX* or led to a truncation of the protein upstream of this domain (Fig 1.2; Schwartzentruber 2012). Notably, mutations in *ATRX* and *H3.3* overlapped significantly with mutations in *TP53*, and eight samples had mutations in all three genes (Schwartzentruber 2012). These data indicate a central role for the *ATRX/DAXX/H3.3* axis in normal cellular morphology, and perturbation of this axis may underlie the pathology of a subset of pediatric GBM.

Research was soon extended into adult glioma samples, including WHO grade II and III astrocytomas and oligodendrogliomas, WHO grade III and IV anaplastic astrocytomas, oligoastrocytomas, and WHO grade IV primary and secondary GBMs. For example, mutations in *ATRX* were identified in 93 out of 363 (26%) gliomas samples ranging across all age groups and tumour grades (Jiao 2012). Specifically, *ATRX* alterations were found in 67% of grade II astrocytomas, 73% grade III astrocytomas, 57% secondary GBMs, 68% oligoastrocytomas, and 20% pediatric GBMs (Jiao 2012). The majority of *ATRX* mutations in pediatric GBMs clustered again in the C-terminal SWI/SNF2 domain, while adult gliomas displayed an even distribution across the *ATRX* gene; however, both adult and pediatric gliomas showed a bias towards frameshift and nonsense mutations (Fig. 1.2; Jiao 2012). Another study identified *ATRX* mutations by Sanger sequencing in 47.8% of adult glioma samples distributed across age and subtype, with again the majority of mutations being insertions/deletions leading to frameshift mutations in the *ATRX* polypeptide (Liu 2012). Further immunohistochemical staining for *ATRX* in another 96 samples showed a

loss of nuclear ATRX staining in 32% of adult glioma samples, while ATRX staining remained intact in 34 pilocytic astrocytomas (Liu 2012). Finally, a study that examined low-grade gliomas identified *ATRX* mutations in 12/32 samples ranging across grade II and III astrocytomas and oligoastrocytomas (Kannan 2013). Thus, it is clear that *ATRX* mutations represent a recurring abnormality not only in pediatric GBM, but also in adult gliomas across the tumour spectrum.

Worthy of note is the frequent overlap of *ATRX* mutations with mutations in other genes, like *TP53* and *IDH1/2*. One study identified 100% of grade II astrocytomas, grade III astrocytomas, and grade IV secondary GBMs that harboured *ATRX* mutations also showed alteration of *IDH*, and 94% showed alteration of *TP53* (Jiao 2012). Conversely, *ATRX* mutations were mutually exclusive from mutations in *Homolog of Drosophila capicua (CIC)* as well as 1p/19q co-deletion (Jiao 2012). Furthermore, out of 51 samples with *ATRX* mutations, 47 samples had concurrent mutations in *IDH1/2*, and within this population of *IDH*-mutated tumours, *ATRX* mutations were associated with tumours that also harboured alterations in *TP53* (Liu 2012). Lastly, Kannan (2013) identified 25% of adult glioma samples distributed across age and subtype that harboured all three mutations (*IDH1*, *ATRX*, and *TP53*). Taken together, these findings reveal a strong overlap between *ATRX* mutations and alteration of *IDH* and/or *TP53*, signifying that loss of *ATRX* alone is unlikely to direct tumorigenesis and requires additional alteration of known tumour suppressors/oncogenes to drive carcinogenesis.

1.3.4 Association of *ATRX* Mutations and Alternate Lengthening of Telomeres (ALT)

Cells undergoing tumorigenic transformation have the difficult job of acquiring immortality and this requires counteracting the gradual telomeric attrition that accompanies semi-conservative DNA replication. To do this, most carcinogenic cells will reactivate the telomerase enzyme, which is a ribonucleoprotein that can add TTAGGG nucleotides to the ends of chromosomes mainly through the activity of its catalytic subunit TERT (telomerase reverse transcriptase) (Morin 1989; Harley 2008; Günes 2013). Approximately 10-15% of

tumours, however, do not reactivate telomerase and instead use a mechanism called alternative lengthening of telomeres to maintain the length of their telomeres using homologous recombination mechanisms (Bryan 1995; Conomos 2012). Cells that have activated the ALT pathway exhibit numerous characteristics that are distinct from cells that express the telomerase subunit TERT. Differences include telomere length heterogeneity (Bryan 1995), abundant extrachromosomal linear and circular DNA (Ogino 1998), high frequency of telomeric sister chromatid exchange (T-SCE) events (Bechter 2004), and the presence of a specific subclass of PML bodies that contain telomeric DNA, shelterin proteins, and homologous recombination factors (Yeager 1999). Little is known about the molecular details of the ALT pathway, and even less about how the ALT pathway is initially activated in cells. Nevertheless, we do know that ALT is commonly associated with high amounts of genomic instability, especially at the telomeres (Lovejoy 2012), along with remodeling of the telomere architecture (Conomos 2012), and occurs in a particularly high fraction of certain tumour types like sarcomas, panNETs and brain tumours.

As we know from loss-of-function studies, ATRX plays a major role in maintaining telomere stability and structure, particularly during S-phase (Watson 2013; Lovejoy 2012). Loss of ATRX leads to a significant increase in telomeric DNA damage and telomeric abnormalities, like bridging and fusions (Watson 2013; Lovejoy 2012). Given this potential role for ATRX in modulating telomeric chromatin, it is perhaps not surprising that ATRX mutation in glioma samples was highly correlated with the activation of the ALT pathway (Heaphy 2011; Schwartzentruber 2012; Jiao 2012; Kannan 2013). Furthermore, evaluation of mutations in either the *ATRX* gene or the *TERT* promoter revealed a mutual exclusivity of these two events, supporting the strong link between ATRX loss and the activation of ALT (Killela 2013). Tumours harbouring a loss of ATRX commonly show heterogeneous, ultrabright telomere FISH (fluorescence *in situ* hybridization) foci (Heaphy 2011; Schwartzentruber 2012; Kannan 2013), which is an established marker of ALT activation. As well, many human ALT cancer cell lines show a loss of ATRX function, though loss of ATRX alone in normal cell lines was not sufficient to induce ALT activation (Lovejoy 2012). Thus, ATRX is required for the maintenance of the ALT phenotype, while activation of the ALT pathway likely requires additional genetic or epigenetic changes.

1.4 Hypothesis and Summary of Findings

ATR_X loss of function induces cellular phenotypes that are associated with tumorigenic conversion, yet it also leads to an increase in TP53-mediated cell death. Therefore, the aim of this study was to determine whether the deletion of both ATR_X and TP53 can prevent apoptosis but still induce genomic instability in neuroprogenitor cells. I hypothesize that *Atrx* deletion in conjunction with the loss of TP53 function both *in vitro* and *in vivo* will lead to cellular phenotypes conducive to tumor development. This hypothesis was addressed using several mouse models that are described in subsection 2.1.

Chapter 3 describes two *in vitro* systems that were developed to model the initiation and progression of glioma in patients harbouring mutations in *Atrx* and *Tp53*. These systems consist of cultured mouse neuroprogenitor cells and take advantage of the *Cre/loxP* system to recombine and silence either the *Atrx* gene alone, in combination with a TP53 inhibitor, or to silence both the *Atrx* and *Tp53* genes simultaneously. The development and validation of these systems is described in subsections 3.1 and 3.3, while the phenotypic characterization of sequential or simultaneous loss of ATR_X and TP53 function in cultured neuroprogenitor cells is described in subsections 3.2 and 3.4, respectively.

Subsection 4.1 assesses available online patient data in correlation with ATR_X expression levels or copy number variation at the ATR_X locus. Genetic alteration analysis upon the loss of *Atrx* alone in the differentiated cells of the neonatal frontal cortex is examined in subsection 4.2.1. Finally, subsection 4.2.2 describes an *in vivo* model system following *Atrx* and *Tp53* heterozygosity in the murine central nervous system to determine whether combined *Atrx* and *Tp53* loss *in vivo* would affect the survival of the mice because of oncogenic phenotypes in the CNS.

CHAPTER 2 – Materials and Methods

2.1 Animal Husbandry and Genotyping

Several mouse lines were used throughout the following studies and these are summarized in Table 2.1. Conditional deletion of *Atrx* in the mouse forebrain was achieved by crossing *Atrx^{loxP}* female mice (129Sv background) with heterozygous *FoxG1-Cre recombinase* knock-in males (129Sv/FVBN mixed background). *Atrx^{loxP}* mice contain *loxP* sites flanking intron 18 of *Atrx* (see Fig. 1.1). The *FoxG1-Cre recombinase* gene directs recombination and silencing of *Atrx* specifically in the mouse forebrain beginning at embryonic day 8.5 (E8.5; Hebert 2000). Control male animals harbour the *FoxG1-Cre recombinase* gene, but lack the *Atrx^{loxP}* allele (*Atrx^{wt/y} Cre⁺*), while experimental male animals have both the *Atrx^{loxP}* allele along with the *FoxG1-Cre recombinase* knock-in gene (*Atrx^{loxP/y} Cre⁺*) (Table 2.1). *Atrx^{loxP}* mice were kindly provided by D. Higgs (Weatherall Institute of Molecular Medicine, John Radcliffe Hospital, Oxford, United Kingdom) and the *FoxG1-Cre recombinase* mice were provided by R. Slack (Ottawa Hospital Research Institute, Ottawa, Ontario) from a line originally obtained from S. McConnell (Stanford University, Stanford, California, USA).

A second approach was taken to achieve conditional deletion of *Atrx* using the *Nestin-Cre recombinase* transgenic driver line (Tronche 1999). The *Nestin* promoter drives the expression of *Cre recombinase* across the entire mouse central nervous system (CNS) beginning at E11.5. Thus, combination of *Nestin-Cre recombinase* with the *Atrx^{loxP}* mice results in recombination and silencing of *Atrx* throughout the mouse CNS starting at embryonic day 11.5. Control female animals carry one copy of the floxed *Atrx* allele and one wildtype *Atrx* allele, and do not carry the *Nestin-Cre recombinase* gene (*Atrx^{loxP/wt} Nes-Cre⁻*). Experimental females still carry one *Atrx* floxed allele and also harbour the *Nestin-Cre recombinase* gene (*Atrx^{loxP/wt} Nes-Cre⁺*).

To achieve *Atrx* and *Tp53* heterozygosity in the mouse CNS, mice harbouring a *Tp53*-null allele (*Tp53^{-/-}*; Jacks 1994) (Jackson Laboratories) were mated with the *Atrx^{loxP/wt}*

Table 2.1 Summary of mouse genotypes used within this thesis.

Genotype	Description	Short Form
<i>Atrx</i> ^{wt/y} <i>FoxG1-Cre</i> ⁺	<i>Cre recombinase</i> positive male control	<i>Cre</i> ⁺ control
<i>Atrx</i> ^{loxP/y} <i>FoxG1-Cre</i> ⁺	<i>Atrx</i> -null male experimental	<i>Atrx</i> -null
<i>Atrx</i> ^{wt/y} <i>Tp53</i> ^{wt/wt}	Wildtype male control	Wildtype
<i>Atrx</i> ^{loxP/y} <i>Tp53</i> ^{wt/wt}	<i>Atrx</i> floxed, <i>Tp53</i> wildtype male control	<i>Atrx</i> floxed
<i>Atrx</i> ^{wt/y} <i>Tp53</i> ^{loxP/loxP}	<i>Atrx</i> wildtype, <i>Tp53</i> floxed male control	<i>Tp53</i> floxed
<i>Atrx</i> ^{loxP/y} <i>Tp53</i> ^{loxP/loxP}	<i>Atrx</i> floxed, <i>Tp53</i> floxed male experimental	Double floxed
<i>Atrx</i> ^{loxP/wt} <i>Nestin-Cre</i> ⁻ <i>Tp53</i> ^{+/+}	<i>Cre recombinase</i> negative wildtype female control	Wildtype
<i>Atrx</i> ^{loxP/wt} <i>Nestin-Cre</i> ⁺ <i>Tp53</i> ^{+/+}	<i>Atrx</i> heterozygous, <i>Tp53</i> wildtype female control	<i>Atrx</i> het
<i>Atrx</i> ^{loxP/wt} <i>Nestin-Cre</i> ⁻ <i>Tp53</i> ^{+/-}	<i>Atrx</i> wildtype, <i>Tp53</i> heterozygous female control	<i>Tp53</i> het
<i>Atrx</i> ^{loxP/wt} <i>Nestin-Cre</i> ⁺ <i>Tp53</i> ^{+/-}	<i>Atrx</i> heterozygous, <i>Tp53</i> heterozygous female	Double het

Nes-Cre⁺ mice to create *Atrx*^{loxP/wt} *Nes-Cre*⁺ *Tp53*^{+/-} experimental mice. These mice are heterozygous for *Atrx* and are mosaic for ATRX expression within the entire CNS. Additionally, these mice carry a loss of one *Tp53* allele throughout the entire body. Control animals were also created from these crosses, including fully wildtype mice (*Atrx*^{loxP/wt} *Nes-Cre*⁻ *Tp53*^{+/+}), mice heterozygous for only *Atrx* (*Atrx*^{loxP/wt} *Nes-Cre*⁺ *Tp53*^{+/+}) and mice heterozygous for only *Tp53* (*Atrx*^{loxP/wt} *Nes-Cre*⁻ *Tp53*^{+/-}) (Table 2.1).

To achieve conditional and inducible deletion of both *Atrx* and *Tp53* *in vitro*, we had to first generate *Atrx*^{loxP/loxP} *Tp53*^{loxP/loxP} double floxed mice. *Tp53*^{loxP/loxP} mice (Jackson Laboratories, Bar Harbour, Maine, USA) carry two *Tp53* alleles with *loxP* sites flanking exons 2 to 10 of the gene (Marino 2000). *Tp53*^{loxP/loxP} mice were crossed with the previously described *Atrx*^{loxP/loxP} mice to eventually generate *Atrx*^{loxP/loxP} *Tp53*^{loxP/loxP} double floxed mice. These mice were used for *in vitro* studies, and thus mating of *Atrx*^{loxP/wt} *Tp53*^{loxP/wt} females with *Atrx*^{loxP/y} *Tp53*^{loxP/wt} males could generate *Atrx*^{loxP/loxP} *Tp53*^{loxP/loxP} double floxed embryos, along with the necessary controls: *Atrx*^{loxP/loxP} *Tp53*^{wt/wt} (*Atrx* floxed), *Atrx*^{wt/wt} *Tp53*^{loxP/loxP} (*Tp53* floxed), and *Atrx*^{wt/wt} *Tp53*^{wt/wt} (wildtype) embryos (Table 2.1).

For embryonic studies, midday of the day of vaginal plug discovery was considered E0.5. At scheduled gestational time points, typically E13.5, pregnant dams were euthanized by CO₂ suffocation. For postnatal studies, midday of the day of birth was considered P0.5. Animals younger than P10 were euthanized by cervical dislocation, and older animals were euthanized by CO₂ suffocation. All animal studies were conducted in compliance with the regulations of The Animals for Research Act of the province of Ontario, the guidelines of the Canadian Council for Animal Care and the policies and procedures approved by the University of Western Ontario Council on Animal Care (Appendix A).

For genotyping, tail or ear notch samples from mice were digested and genomic DNA was extracted using DirectPCR and proteinase K (Thermo Scientific). DNA from these samples was then genotyped by PCR using primer sets for *Atrx* (17F, 18R and *neoR*), *Tp53* (*Tp53*floxF and *Tp53*floxR; AM3, AM4 and *neo*^F), *Cre* (*Cre*3b and *Cre*5b), and *Sry* (*Sry*F and *Sry*R), as listed in Table 2.2.

Table 2.2 List of oligonucleotides used in genotyping, qRT-PCR and *in situ* hybridization.

Primers used for genotyping of animals

17F:	5` - AGAACCGTTAGTGCAGGTTCA - 3`
18R:	5` - TGAACCTGGGGACTTCTTTG - 3`
<i>neo</i> ^R :	5` - CCACCATGATATTCGGCAAG - 3`
Cre3b:	5` - TGACCAGAGTCATCCTTAGCG - 3`
Cre5b:	5` - AATGCTTCTGTCCGTTTGCC - 3`
SryF:	5` - GCAGGTGGAAAAGCCTTACA - 3`
SryR:	5` - AAGCTTTGCTGGTTTTTGGGA - 3`
Tp53floxF:	5` - GGTTAAACCCAGCTTGACCA - 3`
Tp53floXR:	5` - GGAGGCAGAGACAGTTGGAG - 3`
AM3:	5` - ATAGGTCGGCGGTTTCAT - 3`
AM4:	5` - CCCGAGTATCTGGAAGACAG - 3`
<i>neo</i> ^F :	5` - GATCGGCCATTGAACAAGAT - 3`

Primers used to amplify cDNA for RT-PCR

Atrx F:	5` - AGAACCGTTAGTGCAGGTTCA - 3`
Atrx R:	5` - TGAACCTGGGGACTTCTTTG - 3`
Gapdh F:	5` - GACAAGCTTCCCGTTCTCAG - 3`
Gapdh R:	5` - GAGTCAACGGATTTGGTCGT - 3`
β actin F:	5` - CTGTCGAGTCGCGTCCACCC - 3`
β actin R:	5` - ACATGCCGGAGCCGTTGTCG - 3`
Cxcl12 F:	5` - GTCCTCTTGCTGTCCAGCTC - 3`
Cxcl12 R:	5` - AGATGCTTGACGTTGGCTCT - 3`
Mmp2 F:	5` - ACCAGAACACCATCGAGACC - 3`
Mmp2 R:	5` - AAAGCATCATCCACGGTTTC - 3`
Mmp14 F:	5` - CCCAAGGCAGCAACTTCAG - 3`

Mmp14 R: 5` - ATCAGCCTTGCCTGTCACCT - 3`
Igfbp2 F: 5` - CACATCCCCAACTGTGACAA - 3`
Igfbp2 R: 5` - GCTGGGGTTTACTGCACACT - 3`
Gsn F: 5` - TGCTGCCATCTTTACTGTGC - 3`
Gsn R: 5` - AAAGTGTCCCAGGACACAGG - 3`
Lox F: 5` - TAGGGCGGATGTCAGAGACT - 3`
Lox R: 5` - CCTTCAGCCACTCTCCTCTG - 3`
Mdk F: 5` - CCTGCAACTGGAAGAAGGAA - 3`
Mdk R: 5` - GAGGTGCAGGGCTTAGTCAC - 3`
ErbB3 F: 5` - TACTGGTGGCCATGAATGAA - 3`
ErbB3 R: 5` - CTCAATGTAAACGCCCCCTA - 3`
FoxC1 F: 5` - AGTTCATCATGGACCGATTC - 3`
FoxC1 R: 5` - TCCTTCACTGCGTCCTTCTT - 3`
FoxC2 F: 5` - ATGTTGAGAATGGCAGCTT - 3`
FoxC2 R: 5` - GGGCACATCCTTCTTCTTGA - 3`
S100A11 F: 5` - GCATTGAGTCCCTGATTGCT - 3`
S100A11 R: 5` - ATCTAGCTGCCCGTCACAGT - 3`
Ahnak F: 5` - TGAGCAGAGTCCTGCAAAGA - 3`
Ahnak R: 5` - ACTGGGTCACCTCACCAGAC - 3`
Wnt5a F: 5` - GGTGCCATGTCTTCCAAGTT - 3`
Wnt5a R: 5` - CTTCGCACCTTCTCCAATGT - 3`
Wnt7b F: 5` - GCGTCCTCTACGTGAAGCTC - 3`
Wnt7b R: 5` - GGAGTTCTTGCCCGAAGAC - 3`
Fzd7 F: 5` - GCTTCCTAGGTGAGCGTGAC - 3`
Fzd7 R: 5` - CAACCCGACAGGAAGATGAT - 3`
Akt F: 5` - GGCAGGAAGAAGAGACGATG - 3`
Akt R: 5` - CCTGTGGCCTTCTCTTTCAC - 3`
Erk1 F: 5` - TCCTTTTGAGCACCAGACCT - 3`
Erk1 R: 5` - AGCAGATGTGGTCATTGCTG - 3`
Erk2 F: 5` - ACACGCAGCTGCAGTACATC - 3`
Erk2 R: 5` - AACATTCTCATGGCGGAATC - 3`

Primers used to create DIG-labelled anti-sense RNA probes for ISH

ErbB3 SP6 F: 5` - CGATTTAGGTGACACTATAGAATA-
GAAGTGTGAGGTGGTCATGGGTAAC - 3`

ErbB3 T7 R: 5` - GTAATACGACTCACTATAGGG-
CACGAACCCATCGATATTGCTAGAG - 3`

2.2 Quantitative Real Time PCR (qRT-PCR)

Control and experimental mouse forebrains were dissected at birth (P0.5), tissue was homogenized, and RNA was extracted using the RNeasy[®] Mini or Micro Kit (Qiagen). Extracted RNA was subsequently reverse transcribed into cDNA using the following conditions: RNA (1ug), DEPC-H₂O and random primers were heated for ten minutes at 65°C, and then incubated on ice for two minutes. Following this, 5X first strand buffer, 100mM DTT, 25nM dNTPs, Superscript Reverse Transcriptase, RNA guard and more DEPC-H₂O are added to the reaction mixture and then incubated first for ten minutes at 30°C and then for forty-five minutes at 42°C. Resulting cDNA was quantified and stored at -20°C. Control reactions omitting reverse transcriptase enzyme were prepared in parallel.

cDNA prepared from extracted RNA was used for qRT-PCR using the primers listed in Table 2.2. Amplification of cDNA was done by mixing cDNA with primers, H₂O and iQ[™] SYBR[®] Green mastermix (BioRad) and placing the reaction mixture under the following conditions: 30-35 cycles of 95°C for 10 seconds, 55°C for 20 seconds, 72°C for 30 seconds, and a final melting curve generated in increments of 1°C per plate read. Experiments were performed on a Chromo-4 thermocycler, and gene expression levels were analyzed with Opticon Monitor 3 and GeneX (BioRad) software. Gene expression analysis was repeated in duplicate for each primer set, and all primer data were corrected against *β-actin* or *Gapdh* expression levels as an internal control. To confirm correct gene amplification, 20μL of qRT-PCR product was size-sorted on a 1.5% agarose gel by electrophoresis.

2.3 *In Situ* Hybridization

DIG-labelled (dioxigenin; Roche Diagnostics) anti-sense RNA probes were made using gel extracted cDNA (1ug), T3 5x buffer, RNase Guard (Qiagen), 10X DIG-UTP, T7 RNA polymerase (Affymetrix) and DEPC-H₂O. The resulting DIG-labelled RNA probes, diluted in hybridization buffer, were mixed and heated at 70°C for 10 minutes, and subsequently overlaid onto 8μm brain cryosections and incubated overnight at 65°C. Following the overnight incubation, hybridized cryosections were then washed several times in wash

buffer and 1x MABT. Slides were then blocked in sheep serum plus blocking solution for 1 hour, and then incubated in anti-DIG antibody diluted in blocking solution overnight at room temperature. Following anti-DIG incubation, slides were then washed several times in 1x MABT and prestaining buffer, and subsequently incubated in staining buffer – including 315 μ L of NBT and 245 μ L of BCIP (Roche Diagnostics) – for 4 to 24 hours in the dark. Once the correct staining end point was achieved, slides were then washed in various concentrations of ethanol and xylene, and coverslips were placed over stained sections using Permount mounting medium (Fischer Scientific). Stained and coverslipped sections were visualized with a Leica CTR 6500 microscope, and images were manipulated using Volocity[®] software (PerkinElmer Inc., Massachusetts, USA).

2.4 Western Blot Analysis

Fresh tissue or cells in culture were mixed with ice cold RIPA buffer (3mL per gram of tissue, or 50 μ L per well of a 4-well plate of cultured cells) and homogenized. Cells in RIPA buffer were then incubated on ice for 30 minutes, transferred to a cold 1.5 mL Eppendorf tube, and then spun in a cold centrifuge at 13000 RPM for 20 minutes. The supernatant was then transferred to a new, cold 1.5mL Eppendorf tube, and the cell pellet was discarded. Protein concentration was measured using a Bradford assay (BioRad), and protein extracts were stored at -80°C.

Polyacrylamide gels, including a separating gel (6, 10, 12, or 15%) and a stacking gel (4%), were made, and protein samples were thawed and denatured at 90°C for 10 minutes. 25 μ L of samples in 1x loading buffer were loaded into the gel, along with 8 μ L of protein ladder (BioRad), and gels were run at 90V for 30 minutes followed by 125-130V for 2 hours in 1X running buffer. Following protein separation, gels were transferred to nitrocellulose membranes (BioTrace[™], Pall Life Sciences) at 75V for 2 hours in 1X transfer buffer.

Transferred nitrocellulose membranes were then blocked with 5%-milk-TBST or 5% BSA for 1 hour, and incubated with the primary antibody diluted in either 5%-milk-TBST or 5% BSA overnight at 4°C. Following primary antibody incubation, membranes were washed in 1X TBST and incubated with the secondary antibody diluted in 5%-milk-TBST or 5%

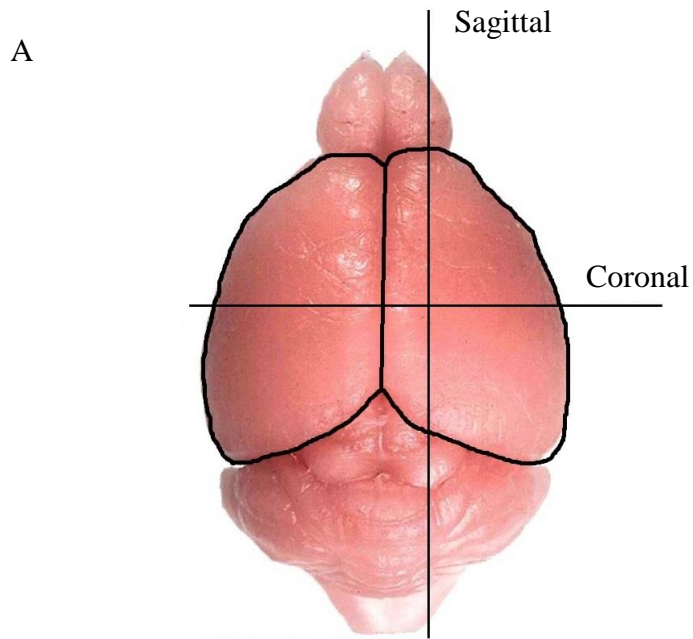
BSA for 1 hour at room temperature. Membranes were then washed, incubated in ECL (enhanced chemiluminescence) for approximately 1 minute, and subsequently imaged onto film using a Konica Minolta SRX-101A developer.

2.5 Immunofluorescence

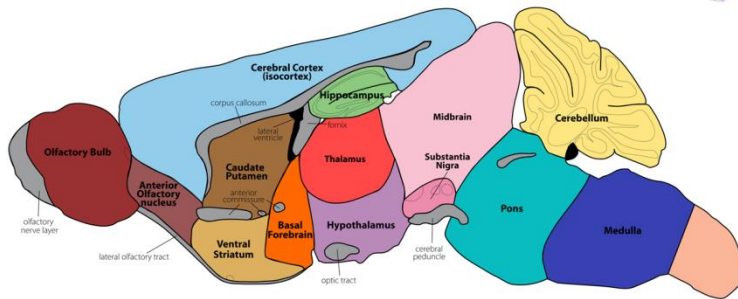
Brains dissected at birth (P0.5) were embedded in OCT (optimal cutting temperature) medium, snap frozen in liquid nitrogen, and stored at -80°C. Brains were subsequently cryosectioned coronally at a thickness of 8µM. Coronal cryosections (Fig. 2.1) were thawed at room temperature for one hour and subsequently rehydrated in 1X PBS for five minutes. Antigen retrieval was performed, if necessary, by placing slides in warm sodium citrate and heated at a low level for ten minutes. Still in sodium citrate, slides were then left to cool for 20 minutes and subsequently washed two times in 1X PBS and two times in 1X PBS+0.3% TritonX-100 to permeabilize the cell membranes. Following permeabilization, slides were incubated with primary antibody diluted in 1X PBS+0.3% TX-100 and 1% BSA overnight at 4°C. Primary antibody was then washed off with 1X PBS plus 0.3% TritonX-100 and slides were incubated in secondary antibody diluted in 1X PBS+0.3% TritonX-100 and 1% BSA for 1 hour at room temperature in the dark. Following secondary antibody incubation, slides were washed with 1X PBS+0.3% TritonX-100, counterstained with DAPI, and subsequently mounted and visualized with a Leica CTR 6500 microscope.

Cells in culture were washed with 1X PBS and fixed in ice cold 4% PFA for ten minutes. Following fixation, cells were washed two times in 1X PBS and then two times in 1X PBS+0.3% TritonX-100 to permeabilize cell membranes. Cells were then incubated in primary antibody diluted in 1X PBS+0.3% TritonX-100 for 1 hour at room temperature. Primary antibody was washed off with 1X PBS+0.3% TritonX-100, and cells were subsequently incubated in secondary antibody diluted in 1X PBS+0.3% TritonX-100 for 45 minutes at room temperature in the dark. Following secondary antibody incubation, cells were washed, counterstained with DAPI, and visualized using a Leica CTR 6500 microscope. Image analysis was performed using Volocity[®] and ImageJ Software[®] (National Institutes of Health, Maryland, USA).

Figure 2.1 Regions of the mouse brain used for experimental analyses. (A) Image of the mouse brain with the cortical lobes outlined, along with axes indicating coronal and sagittal section orientations. (B) Sagittal view of the adult brain at one year of age. Images were adapted from the Allen Brain Atlas website, available online at www.brain-map.org.



B



2.6 Haematoxylin and Eosin Staining

Sagittal cryosections (8 μ M; Fig. 2.1) were rehydrated in 70% ethanol for 2 minutes and subsequently stained with CAT Haematoxylin and Eosin Y (H&E; BioCare Medical) for 2 minutes each. Next, slides were dehydrated in increasing ethanol concentrations followed by xylene washes. Coverslips were then placed onto stained sections using Permount, and H&E stained and coverslipped cryosections were then viewed and imaged using a Leica CTR 6500 microscope.

2.7 Neuroprogenitor Cell (NPC) Culture

Pregnant dams were anesthetized and euthanized at embryonic day 13.5 (E13.5) and mouse embryonic frontal cortices were dissected. At this timepoint, the embryonic cortex is undergoing a major wave of neurogenesis followed by a period of neuronal differentiation which terminally differentiates the neuroprogenitors of the brains into cortical neurons (Slack 1998). Cortical dissection at E13.5 was followed by trituration and plating of cortical cells onto poly-L-lysine coated 4-well plates. Neuroprogenitor cells were cultured *in vitro* in proliferation media – 1% N2 Supplement, 1% penstrep, and 1% glutamax in Neurobasal media (Gibco[®], Life Technologies Inc.) – for two days. After two days *in vitro* (DIV), proliferation media was removed and cells were differentiated through the addition of 2% B-27 Supplement, 1% penstrep, 1% glutamax, and 0.1% bFGF in Neurobasal media (Gibco[®], Life Technologies Inc.) for a further 4 to 8 DIV. In some cases, either 20 μ M DMSO or 20 μ M cPFT α (Sigma) diluted in DMSO was added upon cellular differentiation. Drugs were administered every 24 hours, and media was changed every 48 hours.

2.8 Adenovirus-Cre Recombinase Infection of Neuroprogenitor Cells

Pregnant dams were anesthetized and euthanized 13.5 days following plug detection (E13.5), and embryos were removed. Embryonic cortices were dissected, triturated, and neuroprogenitor cells were cultured *in vitro* in proliferation media for two days. After two DIV, cells were infected with an adenovirus expressing either only the *Green Fluorescent*

Protein (GFP) (ad-GFP) or expressing the Cre Recombinase gene linked to GFP (ad-CreGFP) for 1.5 to 2 hours at 37°C.

Following adenovirus infection, cells were differentiated through the addition of differentiation media for a further 4 to 8 DIV. Differentiation media was changed every 48 hours, and cells were viewed and imaged using a Leica CTR 6500 microscope to look for correct GFP expression, indicating adenoviral infection.

2.9 Trypan Blue Dye Exclusion Assay

Neuroprogenitor cells in culture were trypsinized for 25 to 30 minutes at 37°C in 1X trypsin (Gibco) diluted in 1X PBS. Cells were lifted off the plate through mechanical perturbation, and cell suspensions were placed into 1.5mL Eppendorf tubes and spun in a cold centrifuge at 1400 RPM for 10 minutes. Cell pellets were then resuspended in 1X PBS and mixed at a 1:1 ratio with Trypan Blue (Sigma). The number of blue versus white cells was then counted using a haemocytometer, and percent viability was calculated as follows: % viability = (# white cells) / (# white + blue cells).

2.10 Database Mining

Data was collected from The Cancer Genome Atlas (TCGA; <http://cancergenome.nih.gov/>; n=483) and Catalogue of Somatic Mutations in Cancer (COSMIC; <http://cancer.sanger.ac.uk/>; n=24) databases for tumour samples across the glioma spectrum. Expression levels and copy number variation (CNV) for *ATRX* was examined and compared to the expression of other tumour suppressor genes, like *TP53*, or oncogenes, like *IDH*. *ATRX* expression and CNV was also compared to survival time and age of diagnosis of patients, as well as to tumor grade. Statistical analysis was performed using GraphPad Prism[®] software (GraphPad Software, Inc., California, USA).

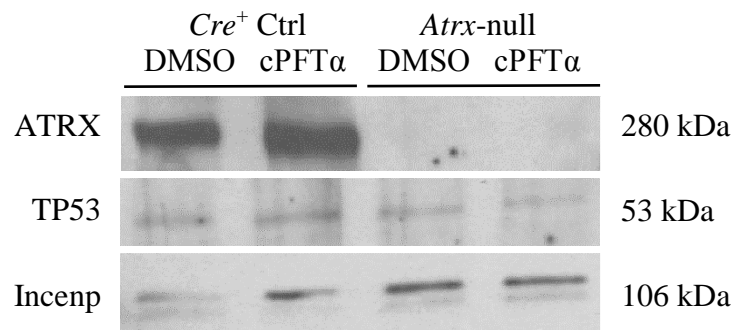
CHAPTER 3 – *In Vitro* Modelling of Gliomagenesis

3.1 Sequential inactivation of *Atrx* and *Tp53* in cultured NPCs

Previous studies identified a significant overlap between mutations in *ATR*X and *TP*53 in glioblastoma multiforme patients (Schwartzentruber 2012; Liu 2012; Kannan 2013). We know from work in our lab that the loss of *Atrx* in primary mouse NPCs is detrimental to cellular viability, genomic stability, and telomeric maintenance (Bérubé 2005; Watson 2013). Furthermore, combined loss of *Atrx* and *Tp53* *in vivo* is associated with a further increase in genomic instability, along with a rescue in cell death in cortical neurons at an embryonic timepoint (Seah 2008). Thus, combinatorial loss of *Atrx* and *Tp53* promotes NPC survival *in vivo*, and I propose that loss of both ATRX and TP53 protein expression may lead to the onset of tumorigenic phenotypes. To test this *in vitro*, we set up a cell culture system with sequential loss of ATRX and TP53 function in primary NPCs.

To examine the effects of ATRX and TP53 deficiency in mouse NPCs grown *in vitro*, primary cultures were established from *Atrx*-null (*Atrx*^{f/y} *FoxG1-Cre*⁺) and control (*Atrx*^{wt/y} *FoxG1-Cre*⁺) embryonic cortices. After two days *in vitro* (DIV), the cells were differentiated and treated with either 20µM cyclic Pifithrin-α (cPFTα), a reversible inhibitor of the transcriptional activation activities of TP53 (Zuco 2008), or with DMSO alone as a control, for four DIV. To confirm the genotyping results, I performed western blot analysis of protein extracts obtained from cultured *Atrx*-null and *Cre*⁺ control NPCs treated with either DMSO or with 20µM cPFTα (Fig. 3.1). Control cells, despite carrying the *FoxG1-Cre recombinase* gene, do not harbour the floxed *Atrx* allele, and thus express wildtype levels of ATRX protein. This result was validated for control cells treated with either DMSO alone or 20µM cPFTα diluted in DMSO (Fig. 3.1). NPCs obtained from *Atrx*-null (*Atrx*^{f/y} *FoxG1-Cre*⁺) embryos show a loss of the ATRX protein, indicating excellent dissection specificity. Again, this result was seen in *Atrx*-null cells treated both with DMSO or cPFTα (Fig. 3.1). As expected, levels of TP53 protein expression remained constant across both the control and *Atrx*-null cultured NPCs treated with either DMSO or cPFTα (Fig. 3.1). These results validate the ability of *FoxG1-Cre recombinase* in deleting the

Figure 3.1. Immunoblot validation of ATRX and TP53 protein expression levels in DMSO- and cPFT α -treated neuroprogenitor cells in culture. Control and *Atrx*-null neuroprogenitor cells were grown *in vitro* and treated with either DMSO alone or with 20 μ M cPFT α . Protein extracts were taken from cells in culture after six DIV, and the expression levels of ATRX and TP53 were assessed.



floxed *Atrx* allele in our cell model while not affecting expression levels of TP53. As well, these results indicate the sensitivity and specificity of the *Cre/loxP* system in recombining and silencing specific gene targets in cultured mouse NPCs.

3.2 Characterization of sequential *Atrx* and *Tp53* inactivation in mouse NPCs

Loss of ATRX in NPCs is associated with genomic insult, indicated by an increased number of cells with γ H2A.X foci, some of which overlap with telomeres (Watson 2013). We further demonstrated that this genomic instability is exacerbated upon the combinatorial loss of *Atrx* and *Tp53* *in vivo* (Watson 2013). I therefore wanted to establish whether this occurs *in vitro*. Control NPCs grown for six DIV and treated with either DMSO or cPFT α exhibit a basal level of genomic instability indicated by low levels of immunostaining for the histone variant γ H2A.X, which marks sites of DNA damage, measured on the sixth DIV. *Atrx*-null mouse NPCs treated with DMSO alone show amplified DNA damage qualitatively (Fig. 3.2), as demonstrated by an increase in γ H2A.X foci. As well, the relative number of γ H2A.X stained pixels in the images were quantified using ImageJ Software[®], and an increase in the relative mean gray value compared to control NPCs was seen (Fig. 3.2). Administration of 20 μ M cPFT α to *Atrx*-null NPCs in culture lead to a further, albeit slight, quantitative increase in γ H2A.X immunostaining (Fig. 3.2), suggestive of an increased number of surviving cells despite enhanced DNA damage upon the loss of both ATRX and TP53 function in mouse NPCs *in vitro*.

I next examined the effect of sequential ATRX and TP53 inactivation on NPC survival *in vitro*, using the trypan blue dye exclusion assay. NPCs were grown in culture for 2 DIV followed by differentiation and treatment with either DMSO alone or cPFT α every 24 hours for another 4 DIV. Cellular viability was then measured at 6 DIV. *Atrx*-null mouse NPCs treated with DMSO alone had reduced cellular viability compared to *Cre*⁺ control cells treated with DMSO (Fig. 3.3). However, *Atrx*-null mouse NPCs treated with 20 μ M cPFT α showed restored cellular viability comparable to *Cre*⁺ control cells treated either with DMSO or cPFT α (Fig. 3.3). These results demonstrate that the loss of ATRX alone in mouse NPCs *in vitro* is associated with reduced cellular viability, and that loss of ATRX

Figure 3.2. Immunofluorescence assessment of DNA damage foci in DMSO- or cPFT α -treated neuroprogenitor cells. Control (*Atrx*^{wt/y} *FoxG1-Cre*⁺) and *Atrx*-null (*Atrx*^{f/y} *FoxG1-Cre*⁺) neuroprogenitor cells were grown *in vitro* for 6 days and treated with either DMSO or 20 μ M cPFT α . (A) Cells were fixed and immunostained for γ H2A.X (green), a histone variant that marks double stranded DNA breaks. Cell nuclei were counterstained with DAPI (blue), and images were taken at 10X magnification. Scale bar = 200 μ m. (B) Quantification of γ H2A.X staining density relative to total DAPI staining intensity. n=3, p<0.05.

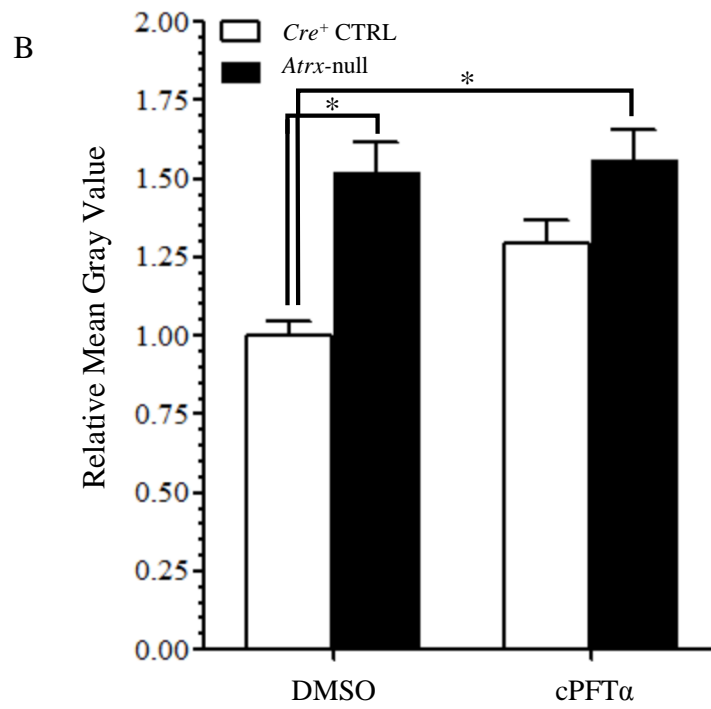
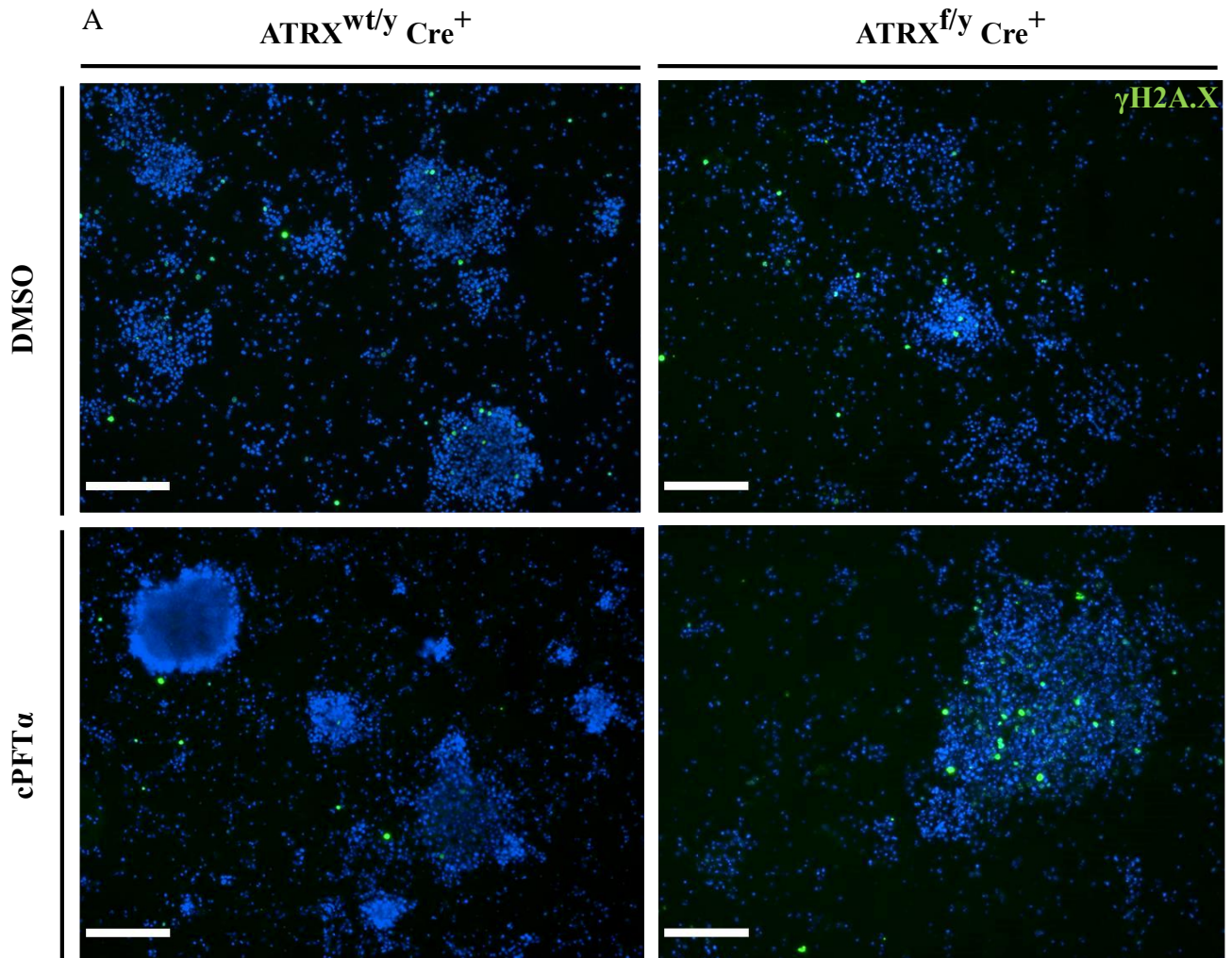
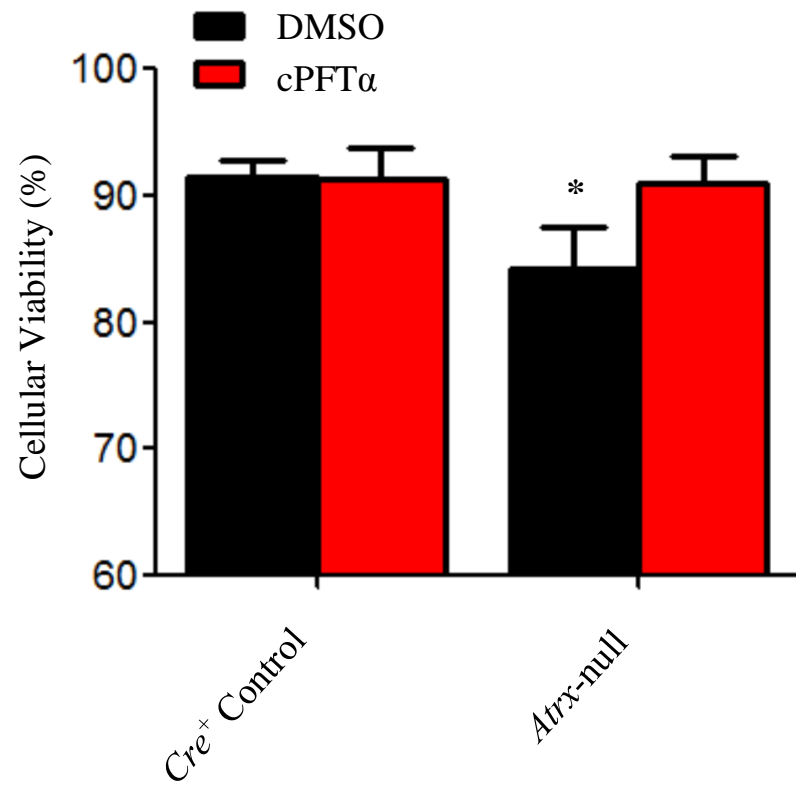


Figure 3.3. Cellular viability in DMSO- and cPFT α -treated neuroprogenitor cells *in vitro*. Control and *Atrx*-null neuroprogenitor cells were grown in culture for 6 days and treated with either DMSO alone or 20 μ M cPFT α . Cellular viability was measured after six DIV using a trypan blue dye exclusion assay. n=4, *p<0.05.



followed by TP53 inhibition enables these cells to survive despite high levels of genomic instability.

Thus, loss of ATRX alone in mouse NPCs causes an accumulation of DNA damage and reduces cellular viability compared to control cells grown in the same conditions. However, genetic loss of *Atrx*, paired with inhibition of TP53 through administration of cyclic-PFT α , is associated with restored levels of cellular viability, explaining the accumulation of NPCs exhibiting excess DNA damage. These results indicate that inhibition of the transcriptional activation activities of TP53, in combination with genetic inactivation of *Atrx*, induces genomic instability and promotes cellular survival *in vitro*.

3.3 Simultaneous deletion of *Atrx* and *Tp53* in cultured NPCs

A second *in vitro* system was developed following the generation of *Atrx* and *Tp53* double floxed mice in order to provide a more complete and sustained inactivation of both genes. This second system uses the *Cre/loxP* system and adenoviral infection to simultaneously delete *Atrx* and *Tp53* in cultured NPCs *in vitro*. *Atrx*^{f/y} *Tp53*^{ff} (double floxed) NPCs are hemizygous for the *Atrx* floxed allele and homozygous for the *Tp53* floxed allele. *Atrx*-floxed (*Atrx*^{f/y} *Tp53*^{wt/wt}), *Tp53*-floxed (*Atrx*^{wt/y} *Tp53*^{ff}), and wildtype (*Atrx*^{wt/y} *Tp53*^{wt/wt}) NPCs were also grown *in vitro* and used as controls. After two DIV, cultured NPCs were differentiated and infected with an adenovirus carrying *Cre recombinase* linked to the *Green fluorescent protein* gene (ad-*CreGFP*), which will recombine and delete sequences flanked by *loxP* sites. Infected cells will also fluoresce green because of the expression of GFP. Through this approach, NPCs lacking ATRX and TP53 proteins (double-null) were created, along with cells harbouring a loss of only ATRX (ATR-null) or only TP53 (TP53-null). Wildtype cells infected with ad-*CreGFP* were used to control for effects of *Cre recombinase* expression. Additionally, an adenovirus carrying only the *GFP* gene and lacking the *Cre recombinase* gene (ad-*GFP*) was used on cultured NPCs to control for any effects of adenovirus infection.

Green fluorescence was observed in NPCs of all genotypes infected with either ad-*GFP* or ad-*CreGFP*, indicating that adenovirus infection was successful. Examination of cellular appearance indicated that adenovirus infection did not affect cell morphology after four DIV (Fig. 3.4). As NPCs differentiate *in vitro*, they begin to develop characteristics of neurons: long finger-like processes reaching out in all directions, large cell bodies, groups of cells growing in clumps, and cell colonies growing flat (horizontally) along the plate (Leach 2011). The wildtype, *Atrx*-floxed, *Tp53*-floxed, and double floxed cells treated with ad-*GFP* demonstrated these characteristics, indicating that adenovirus infection does not affect cellular morphology at a qualitative level. Additionally, wildtype NPCs infected with ad-*CreGFP* also showed these neuronal characteristics, indicating that *Cre recombinase* expression does not affect cellular morphology (Fig. 3.4). Thus, adenovirus infection of NPCs was successful and was not associated with gross cellular morphological alterations.

I next performed western blot analyses to verify deletion of ATRX and TP53 in the appropriate cells. Immunoblot analysis was performed on cellular extracts obtained from wildtype (*Atrx*^{wt/y} *Tp53*^{wt/wt}), *Atrx*-floxed (*Atrx*^{f/y} *Tp53*^{wt/wt}), and double floxed (*Atrx*^{f/y} *Tp53*^{f/f}) cells in culture infected with either ad-*GFP* or ad-*CreGFP*. ATRX and TP53 proteins were present in all genotypes treated with ad-*GFP*, demonstrating that adenovirus infection alone does not lead to alterations in ATRX or TP53 protein levels (Fig. 3.5). Wildtype (*Atrx*^{wt/y} *Tp53*^{wt/wt}) NPCs treated with ad-*CreGFP* also show normal ATRX and TP53 protein levels. Upon ad-*CreGFP* infection, *Atrx*-floxed (*Atrx*^{f/y} *Tp53*^{wt/wt}) NPCs show a reduction of ATRX alone, while double floxed (*Atrx*^{f/y} *Tp53*^{f/f}) NPCs show a reduction of both ATRX and TP53 protein expression (Fig. 3.5). These results validate efficient *Cre*-mediated recombination of the *Atrx* and *Tp53* floxed alleles. The substantial decrease in protein levels upon ad-*CreGFP* infection relative to ad-*GFP* infection indicates a high infection and recombination efficiency in NPCs using this approach.

3.4 Characterization of simultaneous ATRX and TP53 loss in mouse NPCs

Following successful validation of adenovirus infection in mouse NPCs, immunofluorescence staining was performed for the histone variant γ H2A.X to assess

Figure 3.4. Green fluorescence validation of adenovirus infection in ad-*GFP* and ad-*CreGFP* infected neuroprogenitor cells. Wildtype ($Atrx^{wt/y} Tp53^{wt/wt}$; A, A'), *Atrx*-floxed ($Atrx^{f/y} Tp53^{wt/wt}$; B, B'), *Tp53*-floxed ($Atrx^{wt/y} Tp53^{f/f}$; C, C'), and double floxed ($Atrx^{f/y} Tp53^{f/f}$; D, D') neuroprogenitor cells were grown in culture for two DIV and subsequently differentiated and infected with either ad-*GFP* (A, B, C, D) or ad-*CreGFP* (A', B', C', D'). GFP expression (green) was assessed after four DIV to examine adenovirus infection efficiency. Scale bar=200 μ m.

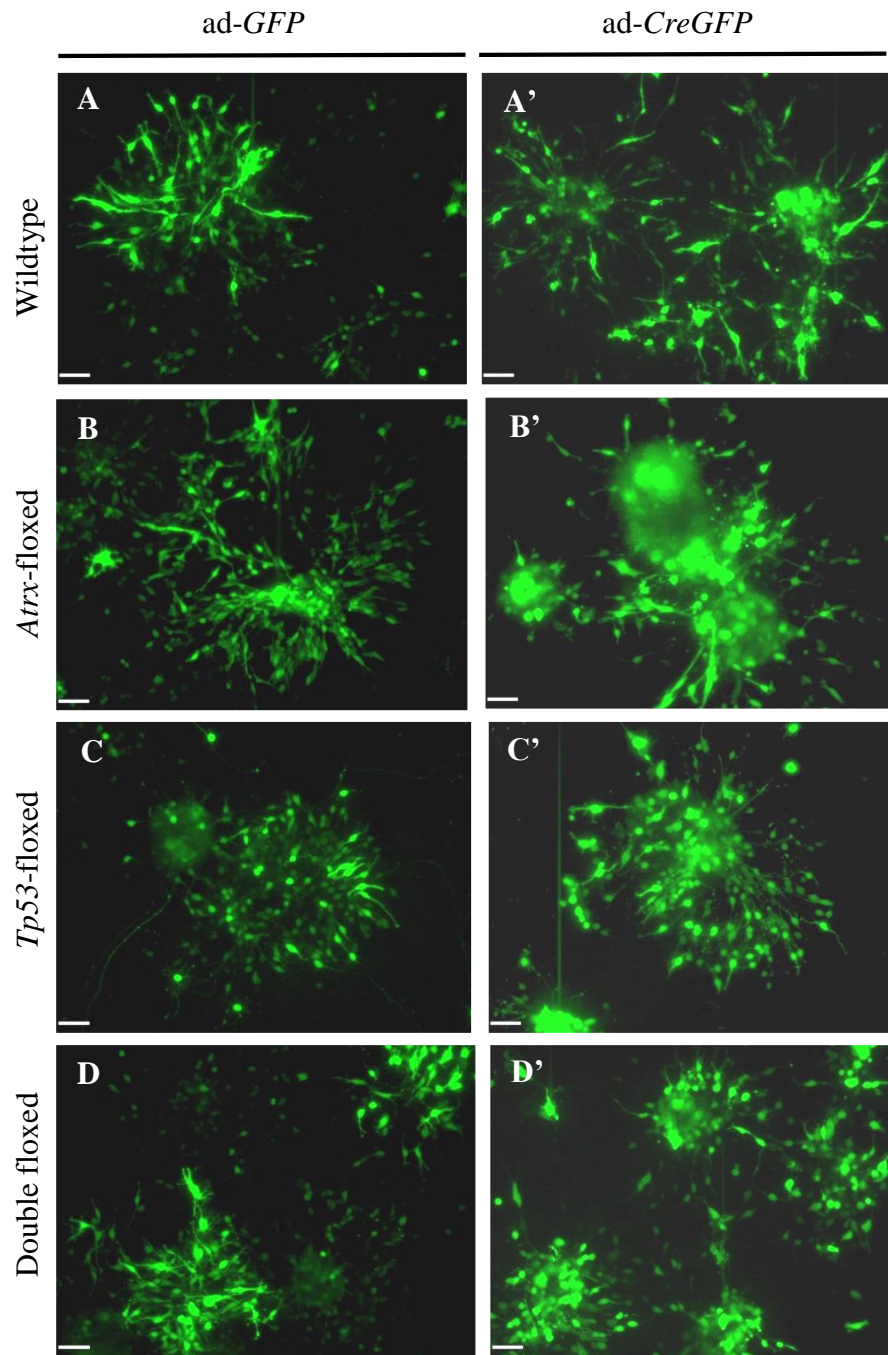
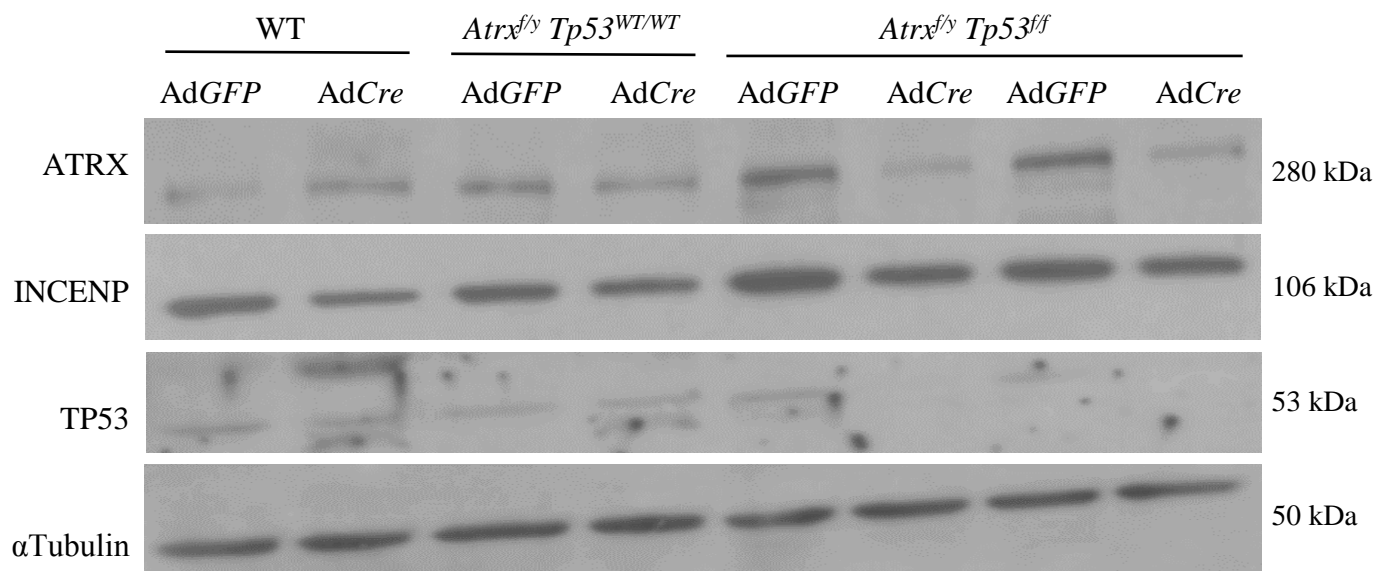


Figure 3.5. Immunoblot validation of *Cre recombinase* activity in infected neuroprogenitor cells. Wildtype ($Atrx^{wt/y} Tp53^{wt/wt}$), *Atrx*-floxed ($Atrx^{f/y} Tp53^{wt/wt}$), and double floxed ($Atrx^{f/y} Tp53^{f/f}$) neuroprogenitor cells were grown *in vitro* for two days and subsequently infected with either ad-*GFP* or ad-*CreGFP*. After six DIV, protein extracts were taken from cells in culture, and ATRX and TP53 protein levels were assessed via immunoblotting techniques. INCENP and α -tubulin were assessed as loading controls.



genomic instability upon the simultaneous loss of ATRX and TP53 in NPCs *in vitro*. Ad-*GFP* infected double floxed NPCs in culture are comparable to wildtype cells, as they do not show loss of ATRX or TP53 protein expression and appear morphologically similar to controls. Staining for γ H2A.X in these cells was minimal, indicative of very little DNA damage occurring in these double floxed cells treated with ad-*GFP* (Fig. 3.6). However, double floxed NPCs treated with ad-*CreGFP* and immunostained for γ H2A.X show an increase in the number of cells with DNA damage foci, indicative of the induction of excessive genomic instability in these cells upon loss of ATRX and TP53 expression (Fig. 3.6). Similar to the results seen in the previous *in vitro* system outlined in section 3.1, the simultaneous loss of ATRX and TP53 in NPCs grown in culture leads to a much more robust and significant increase in genomic insult.

Cellular viability was measured in wildtype (*Atrx*^{wt/y} *Tp53*^{wt/wt}), *Atrx*-floxed (*Atrx*^{f/y} *Tp53*^{wt/wt}), and double floxed (*Atrx*^{f/y} *Tp53*^{f/f}) NPCs infected with either ad-*GFP* or ad-*CreGFP* using the trypan blue dye exclusion assay. All genotypes infected with ad-*GFP* alone showed high levels of cellular viability (Fig. 3.7), demonstrating that adenovirus infection does not have disruptive effects on cell survival. Additionally, wildtype cells treated with ad-*CreGFP* showed no reduction in cellular viability, indicating that *Cre recombinase* expression in NPCs does not have negative effects on cellular survival relative to ad-*GFP* infected controls (Fig. 3.7). However, *Atrx*-floxed NPCs treated with ad-*CreGFP* show reduced cellular viability, consistent with previous results showing decreased cellular survival in *Atrx*-null NPCs. Simultaneous loss of ATRX and TP53 via ad-*CreGFP* infection of double floxed NPCs results in restored cellular viability, comparable to ad-*GFP* infected and wildtype controls (Fig. 3.7). These results indicate that the additional loss of TP53 allows ATRX-null NPCs to survive despite the massive induction of genomic instability in these cells.

3.5 Summary of Results

To summarize, research is identifying large cohorts of glioma patients harbouring mutations in both *ATRX* and *TP53*. We know that ATRX loss alone does not induce

Figure 3.6. Immunofluorescence assessment of DNA damage in ad-GFP and ad-CreGFP infected neuroprogenitor cells *in vitro*. Double floxed (*Atrx^{fl/y} Tp53^{fl/fl}*) neuroprogenitor cells were grown in culture for two days and subsequently infected with either ad-GFP or ad-CreGFP. After six DIV, cells were fixed and immunostained for γ H2A.X (red) to assess DNA damage. GFP expression (green) indicates cells that have been successfully infected with the adenovirus. Scale bar=200 μ m.

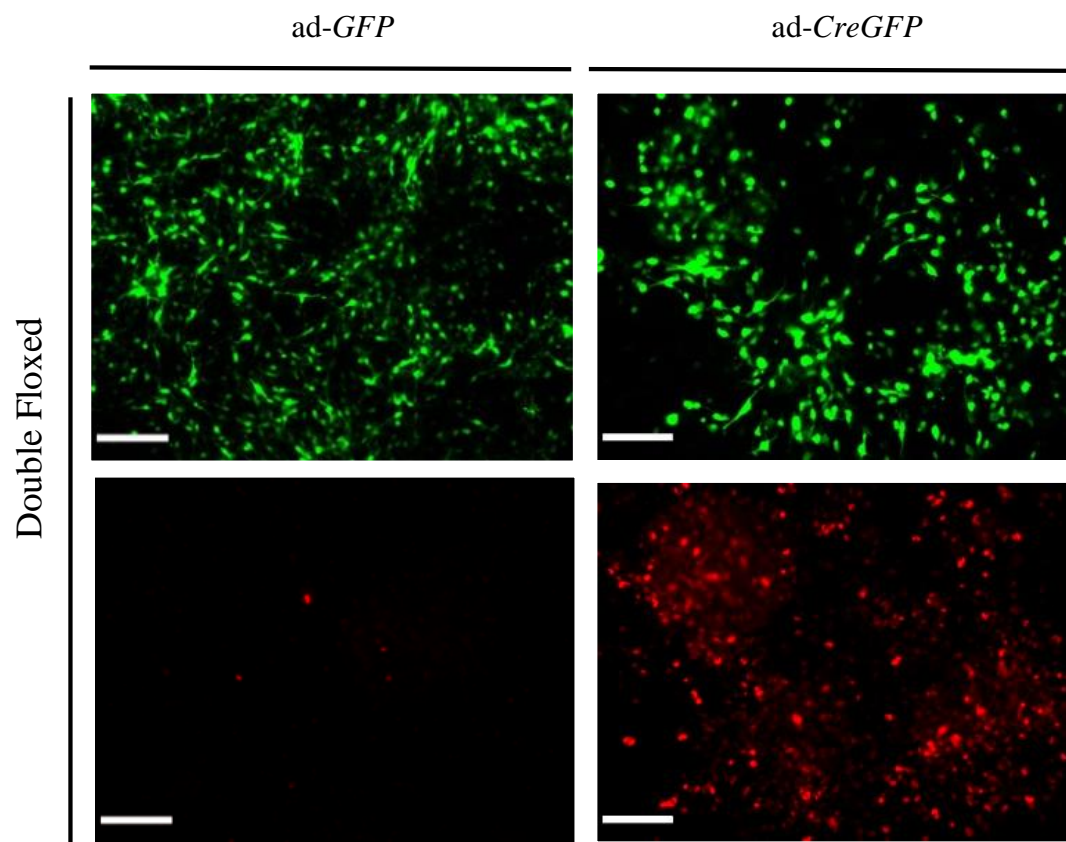
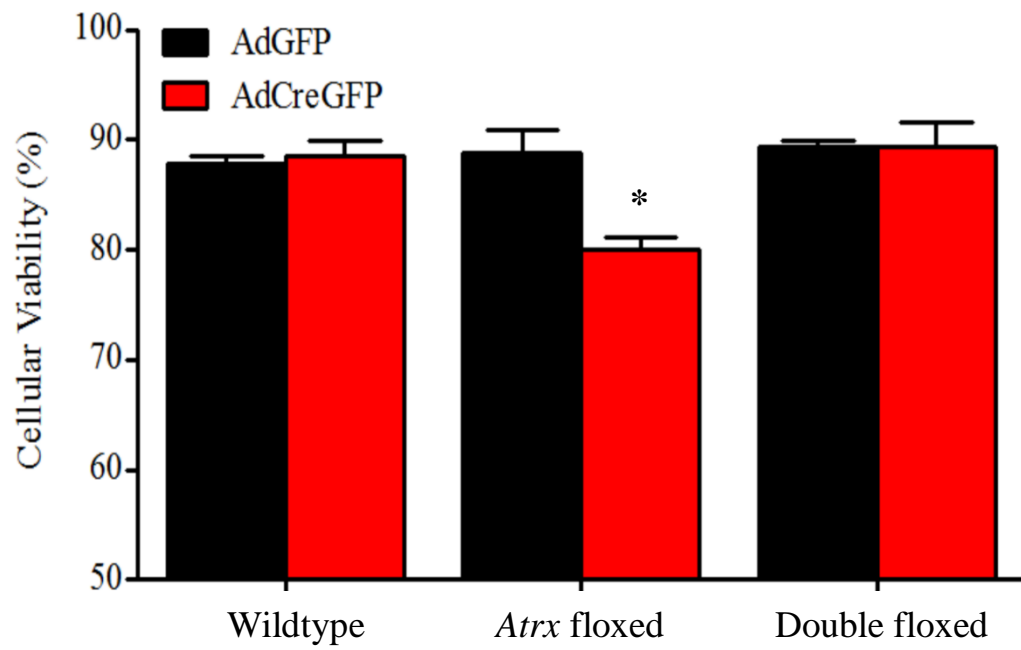


Figure 3.7. Cellular viability of ad-GFP and ad-CreGFP infected neuroprogenitor cells *in vitro*. Wildtype ($Atrx^{wt/y} Tp53^{wt/wt}$), *Atrx*-floxed ($Atrx^{f/y} Tp53^{wt/wt}$), and double floxed ($Atrx^{f/y} Tp53^{f/f}$) cells were grown in culture for two days and subsequently differentiated and infected with either ad-GFP or ad-CreGFP. After six DIV, cellular viability was assessed using a trypan blue dye exclusion assay. n=3, *p<0.05.



carcinogenesis; in fact, ATRX loss is associated with the stabilization of TP53 and activation of its downstream apoptotic pathways (Seah 2008; Watson 2013). Examination of *Atrx* and *Tp53* inactivation in cultured NPCs, both sequentially and simultaneously, identified increased genomic insult and restored cellular viability in both systems. These phenotypes are common characteristics of tumorigenic cells and may provide a model of early events in gliomagenesis. Furthermore, these results may afford insight into the molecular mechanisms of subpopulations of glioma that carry a loss of both ATRX and TP53 expression *in vivo*.

CHAPTER 4 – *In Vivo* Modelling of Gliomagenesis

4.1 Database Mining to Investigate Known *ATRX* Loss-of-Function Mutations

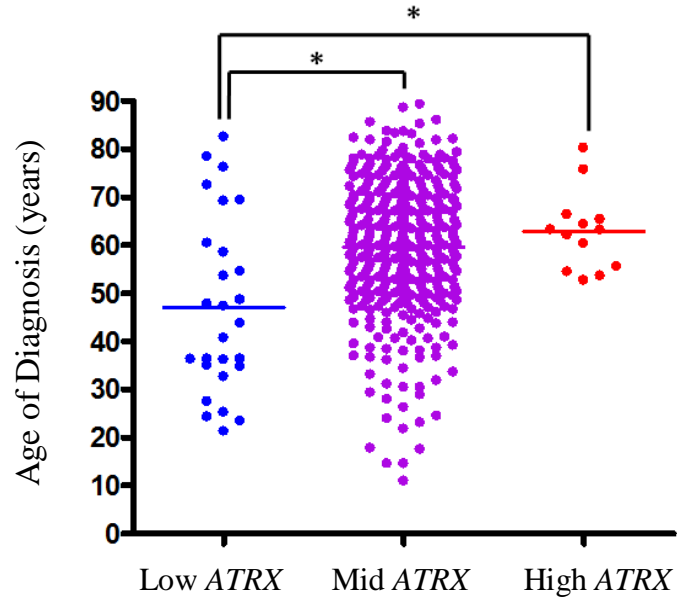
ATRX mutations have been identified in different types of cancers, and several web databases have begun cataloguing *ATRX* mutations, expression levels, and copy number variation across the cancer spectrum. The Cancer Genome Atlas (TCGA), curated by the National Institutes of Health (NIH) and the National Institute of Cancer (NIC) run by the U.S. Department of Health and Human Services, has catalogued relative expression levels for a wide array of genes across several hundred glioblastoma multiforme tissue samples. Using these data, expression levels for the *ATRX* gene was compared between all of the GBM patient samples, and tumours harbouring overexpression, normal, or underexpression of *ATRX* were catalogued.

Of the 483 total GBM patient samples available on TCGA, the majority of these tumours harboured wildtype expression levels for *ATRX*, according to log₂ expression cutoff values generated from past literature that used expression level data from TCGA (Cancer Genome Atlas Research Network, 2008). There were, however, several patient samples that did harbour either low (n=27) or high (n=13) expression of *ATRX*, and when correlated with patient survival, tumours harbouring lower expression of *ATRX* demonstrate better overall survival (p=0.065; Fig. 4.1a). As well, patient tumour samples with low *ATRX* expression demonstrated a significantly earlier age of diagnosis compared to tumour samples with normal or high expression of *ATRX* (Fig. 4.1b). These results are consistent with a previous report that identified an earlier age of diagnosis as well as better overall patient survival for patient with *ATRX*-null pancreatic neuroendocrine tumours (Jiao 2011). Thus, although detrimental to genome stability and normal mitosis, *ATRX* mutations may represent a subset of GBM tumours that demonstrates an earlier age of diagnosis as well as a better overall patient survival compared to tumours with normal or high expression of *ATRX*.

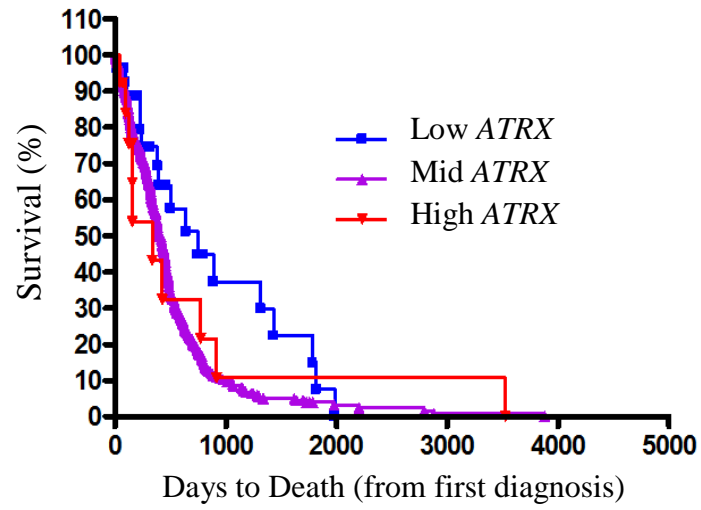
Data from the Catalogue of Somatic Mutations in Cancer (COSMIC) database include copy number variation status and mutation analysis for *ATRX* for established glioma cell lines. Several mutations in *ATRX* were identified, spanning across the entire *ATRX* gene,

Figure 4.1. Mining of The Cancer Genome Atlas database for glioblastoma multiforme tumour patients. (A) *ATRX* expression correlated with patient age of diagnosis. * $p < 0.05$, $n = 483$ tumour samples. (B) Expression of *ATRX* in GBM patients was correlated with patient time to death. $p = 0.065$, $n = 483$ tumour samples.

A



B



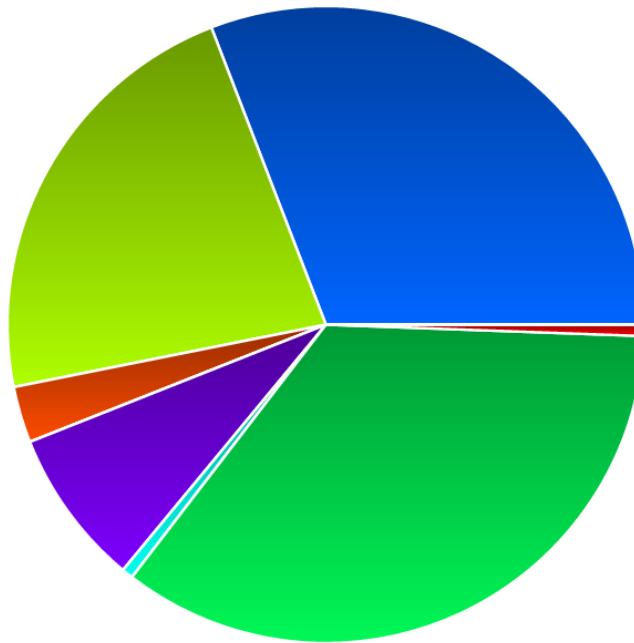
demonstrating the non-specificity and wide variety of *ATRX* mutations that are relevant to glioma development (Fig. 4.2). Additionally, the number of segments as well as abnormal segments throughout the genome of each glioma cell line could be counted from the copy number variation data on the COSMIC database (Fig. 4.3a,b), which can be used as a marker for genomic instability in these tumours. Cell lines created from female patients were not used in the analysis because of the lack of expression data for *ATRX*. Since female cells undergo random X-chromosome inactivation, there would be no way to know whether these cells had gained or lost the active or inactive copy of the *ATRX* locus. Given that only male samples were used, the total number of tumour samples included in the analysis was low (n=24).

Interestingly, none of the included male glioma cell lines harboured a loss of the *ATRX* gene locus; however, there were a number of samples that carried a gain (2 or 3+ copies; n=15 and 4, respectively) of the *ATRX* locus. *ATRX* copy number was correlated with the total number of segments across the genome, the number of abnormal segments, as well as the number of whole chromosome gain/loss events (Fig. 4.3), and even the gain of *ATRX* genomic loci may be detrimental to both genomic stability and normal chromosome segregation. Samples with added copies of the *ATRX* locus showed significant increases in the number of segments as well as the number of abnormal segments, indicative of enhanced genomic instability. As well, additional *ATRX* copies also correlated with an increase in whole chromosome gain or loss events (Fig. 4.3c), indicative of chromosome missegregation events during mitosis. These results indicate a dose-dependence for *ATRX*, demonstrating that both loss of *ATRX* expression or gain of the *ATRX* locus is associated with genomic instability and chromosome missegregation.

4.2 Using *In Vivo* Model Systems to Gain Insights into Gliomagenesis

The findings outlined in Chapter 3 of this thesis suggest that the combined inactivation of *ATRX* and *TP53* promotes NPC survival in the presence of genomic instability, which is a hallmark of cancer. In this chapter, we explored the possibility that loss of *ATRX* alone, or in combination with *TP53* loss, could be conducive to gliomagenesis.

Figure 4.2 Mutation distribution for *ATRX* within catalogued glioma samples. Data from the Catalogue of Somatic Mutation in Cancer (COSMIC; <http://cancer.sanger.ac.uk/>) database was analyzed and *ATRX* mutation distribution within glioma samples was organized. Colours within the pie chart correspond to the colours described in the table below, and mutation types are listed in order of frequency.










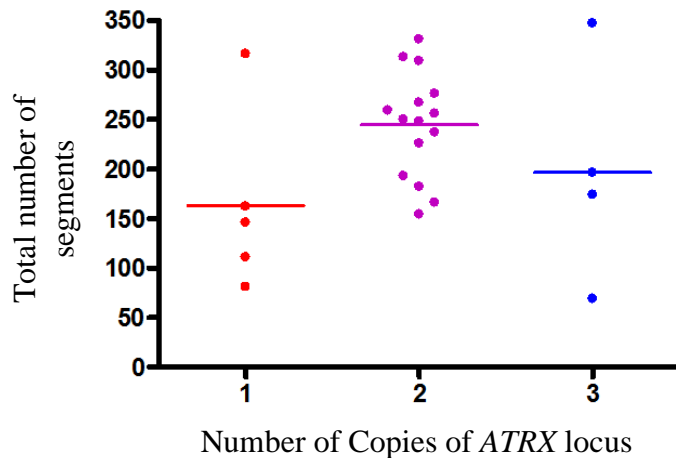
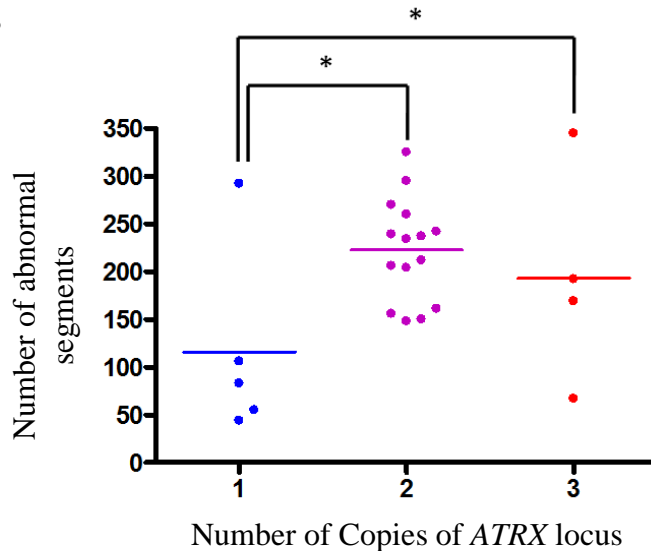
Colour	Mutation Type	Percentage
	Deletion Frameshift	32.62
	Substitution Nonsense	28.88
	Substitution Missense	20.86
	Insertion Frameshift	7.49
	Substitution Synonymous	2.67
	Deletion In-frame	0.53
	Complex	0.53

Figure 4.3. Mining of the Catalogue of Somatic Mutations in Cancer (COSMIC) database examining established glioma cell lines. The total number of segments within the genome (A), the number of abnormal segments (B), and the number of whole chromosome gains/losses (C) were counted in glioma cell lines originating from male tumour patients. Glioma cell lines with normal *ATRX* copy number (one copy, red) were compared with those cell lines harbouring two copies (purple) or three copies (blue) of the *ATRX* gene locus. n=24, *p<0.05

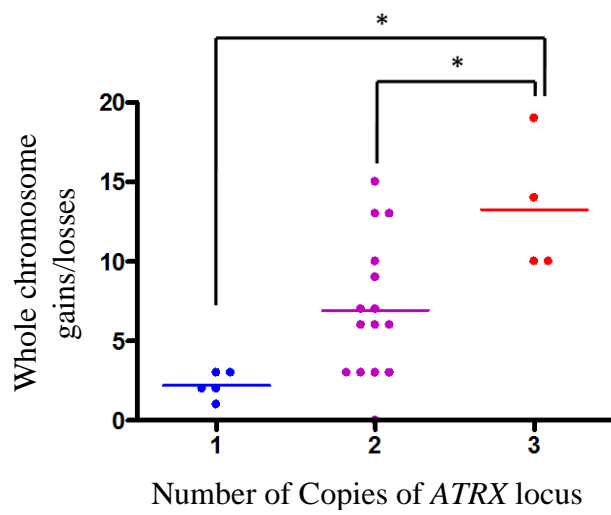
A



B



C



4.2.1 Transcriptional Profiling of the *Atrx*-null Neonatal Mouse Forebrain

To determine the transcriptional effects of *Atrx* loss alone in the mouse forebrain, a microarray was performed on control and *Atrx*-null mouse forebrains at birth (P0.5) (Levy 2008). Mice carrying the *Atrx* gene harbouring *loxP* sites surrounding exon 18 were mated to mice carrying the *Cre recombinase* gene under the control of the *FoxG1* promoter to inactivate the *Atrx* gene specifically in the mouse forebrain beginning at embryonic day 8.5 (E8.5) (Bérubé 2005). *FoxG1-Cre⁺ Atrx^{wt/y}* control mice were used to compare expression levels of genes across the genome upon the loss of ATRX in the neonatal mouse forebrain. In total, 861 genes were significantly upregulated on the microarray by 1.3-fold or more in the *Atrx*-null neonatal mouse forebrain, and many of these genes are involved in the development of glioma based on previous literature. Gene ontology (GO) term analysis of the top 100 increased targets in the *Atrx*-null neonatal mouse forebrain identified commonly upregulated pathways, a number of which are related to cancer development (Table 4.1). For example, genes involved in the WNT pathway were most significantly upregulated (including *Wnt7b*, *Wnt5a*, and *Fzd7*), while pathways involved in stem cell characteristics (*Role of NANOG in Embryonic Stem Cell Pluripotency* and *Human Embryonic Stem Cell Pluripotency*) and angiogenesis (*Factors Promoting Cardiogenesis in Vertebrates*) were also significantly upregulated. These results suggest that the loss of *Atrx* expression embryonically in the mouse forebrain is associated with the upregulation of a number of signaling pathways involved in cancer development in the differentiated and surviving cells of the neonatal mouse frontal cortex.

Further literature searches identified that several upregulated targets from the microarray are involved in the regulation of cellular processes important to gliomagenesis. For example, genes involved in migration/invasion (*Cxcl2*, *Mmp2*, *Mmp14*, *Igfbp2*, *Gsn*, *Lox*, *Mdk*, and *ErbB3*), epithelial-to-mesenchymal transition (EMT; *FoxC1*, *FoxC2*, *S100A11*, and *Ahnak*), and the WNT pathway (*Wnt5a*, *Wnt7b*, and *Fzd7*) were significantly upregulated on the microarray and have an established role in glioma development (Kamino 2011; Li 2013; Chen 2013A; Rahme 2014; Ulasov 2014; Han 2014A; Han 2014B; Luo 2014). These glioma-related genes were validated using quantitative real time

Table 4.1 GO term analysis of upregulated targets from the *Atrx*-null and control P0.5 microarray.

	Canonical Pathways	p-value	Molecules
1	Wnt/ β -catenin Signaling	4.72E+00	FZD8,SFRP2,CDH5,WNT7B,TGFBR3,TL E4,SFRP1,PPP2R1B,SOX5,FZD7,WNT5A
2	Basal Cell Carcinoma Signaling	4.34E+00	FZD8,WNT7B,BMP7,BMP6,BMP5,FZD7,WNT5A
3	Factors Promoting Cardiogenesis in Vertebrates	3.69E+00	FZD8,TGFBR3,BMP7,BMP6,BMP5,PRKD 1,FZD7
4	Role of NANOG in Mammalian Embryonic Stem Cell Pluripotency	3.11E+00	FZD8,WNT7B,BMP7,BMP6,BMP5,FZD7,WNT5A
5	Role of Osteoblasts, Osteoclasts and Chondrocytes in Rheumatoid Arthritis	3.08E+00	FZD8,SFRP2,MMP14,WNT7B,BMP7,SFR P1,BMP6,BMP5,FZD7,WNT5A
6	Human Embryonic Stem Cell Pluripotency	2.73E+00	FZD8,WNT7B,BMP7,BMP6,BMP5,FZD7,WNT5A
7	Aryl Hydrocarbon Receptor Signaling	2.62E+00	TGM2,GSTM1,GSTM2,NFIA,ALDH1 A2, CDKN1A,NFIB
8	Complement System	2.30E+00	SERPING1,C1QC,CFH
9	Role of Wnt/GSK-3 β Signaling in the Pathogenesis of Influenza	1.95E+00	FZD8,WNT7B,FZD7,WNT5A
10	Leukocyte Extravasation Signaling	1.95E+00	CDH5,CLDN1,CXCL12 (includes EG:20315), MMP14,MMP2,CLDN2,PRKD1

polymerase chain reaction (qRT-PCR) showing significantly increased mRNA expression levels in the *ATRX*-null mouse forebrain at birth (Fig. 4.4).

Due to the infiltrative and aggressive nature of gliomas, misregulation of cellular processes like migration/invasion and EMT could initiate the development and progression of glioma. *ErbB3* – a member of the epidermal growth factor receptor (EGFR) family – was the most upregulated target by qRT-PCR, and increased expression of this gene was validated further using both *in situ* hybridization (ISH) and immunoblotting of control and *Atrx*-null forebrain cryosections (Fig. 4.5). Qualitative analysis of *ErbB3* ISH performed on control and *Atrx*-null cryosections demonstrated a consistent upregulation of *ErbB3* mRNA (Fig. 4.5a). Western blots were then performed to examine whether ERBB3 and phosphorylated-ERBB3 protein levels were altered in the *Atrx*-null mouse forebrain at birth. Three out of four control and *Atrx*-null forebrain pairs demonstrated an increase in the protein expression of the 100kDa isoform of both ERBB3 and p-ERBB3 (Fig. 4.5b). The ERBB3 protein is known to lie at the top of a signalling cascade involved in promoting cell growth, migration, protein synthesis, and invasion (Kim 1998; Kamalati 2000; Jones 2006). Activated p-ERBB3 signals through the AKT pathway, and phosphorylated-AKT was also upregulated in the same three control/*Atrx*-null pairs. One pair that showed very low levels of ATRX protein, however, did not demonstrate increased expression of ERBB3, and thus downstream molecules like p-AKT also lacked increased expression in this pair. Therefore, ATRX loss is associated with the upregulation of several gene targets related to glioma development. We propose that *Atrx* loss may create a cellular environment conducive to tumorigenesis through the direct or indirect upregulation of gene targets known to be associated with cellular phenotypes common to glioma development, including the upregulation of ERBB3 and p-ERBB3 in some cases.

4.2.2 *In Vivo* Model of ATRX and TP53 Inactivation

As *Atrx*-null male mice have been shown in the literature to die postnatally around P17-21 or earlier (Bérubé 2005), using these mice for a long-term tumour study was not feasible. Therefore, female *Atrx* mosaic mice were used, as these mice do survive long-term and

Figure 4.4 Validation of P0.5 microarray target genes using quantitative real time PCR. RNA was extracted from neonatal mouse control (*Atrx^{wl/y} FoxG1-Cre⁺*) and *Atrx*-null (cKO; *Atrx^{f/y} FoxG1-Cre⁺*) forebrains, and qRT-PCR was performed to examine the expression status of target genes shown to be overexpressed on the P0.5 microarray. Target genes known to be involved in glioma development were examined, and these genes are involved in the regulation of such cellular processes as migration/invasion (A), epithelial-to-mesenchymal transition (B), and the WNT pathway (C). n=6-8, *p<0.05

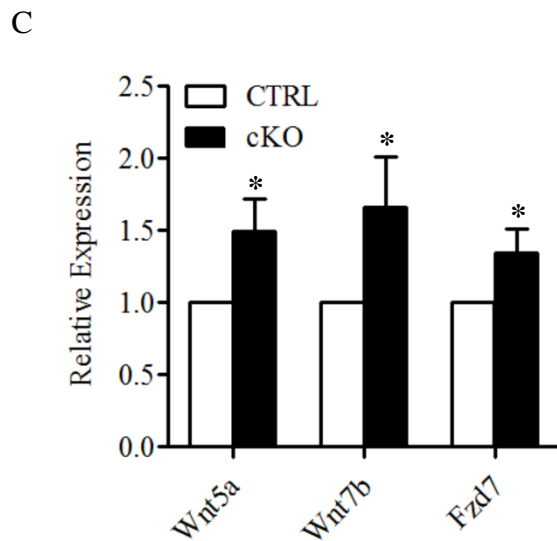
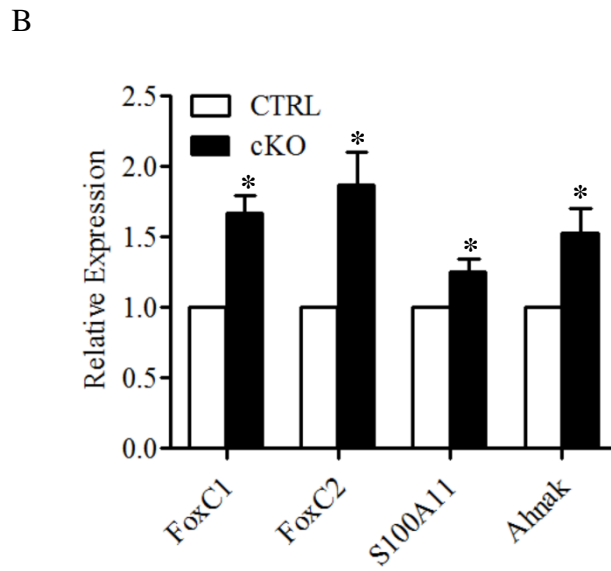
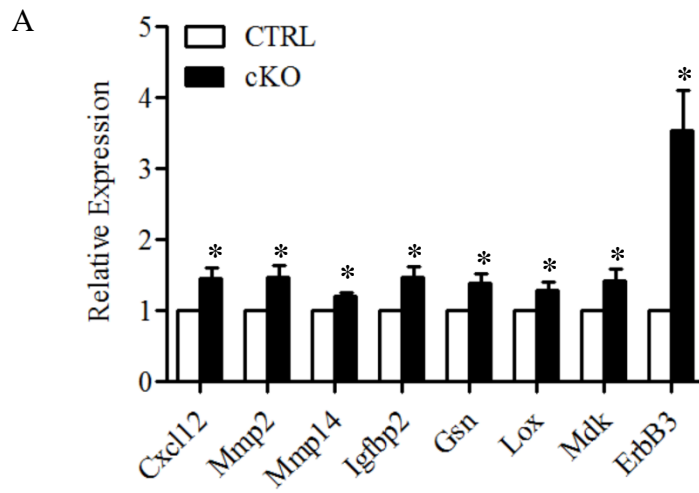
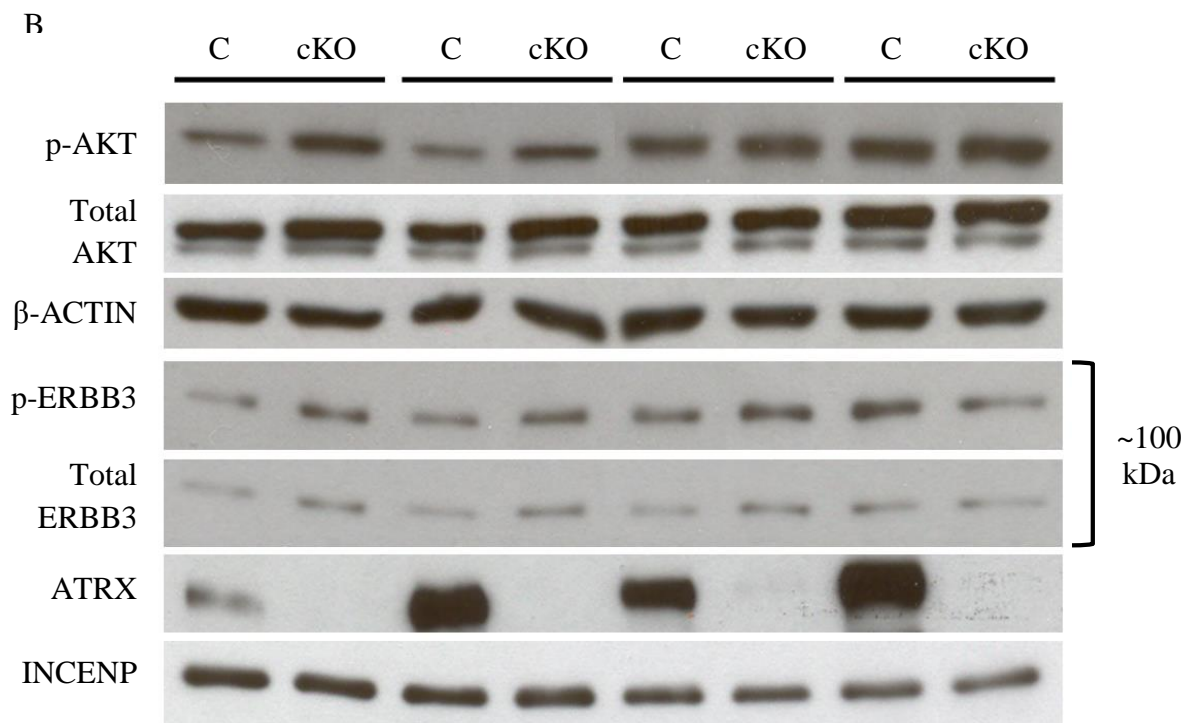
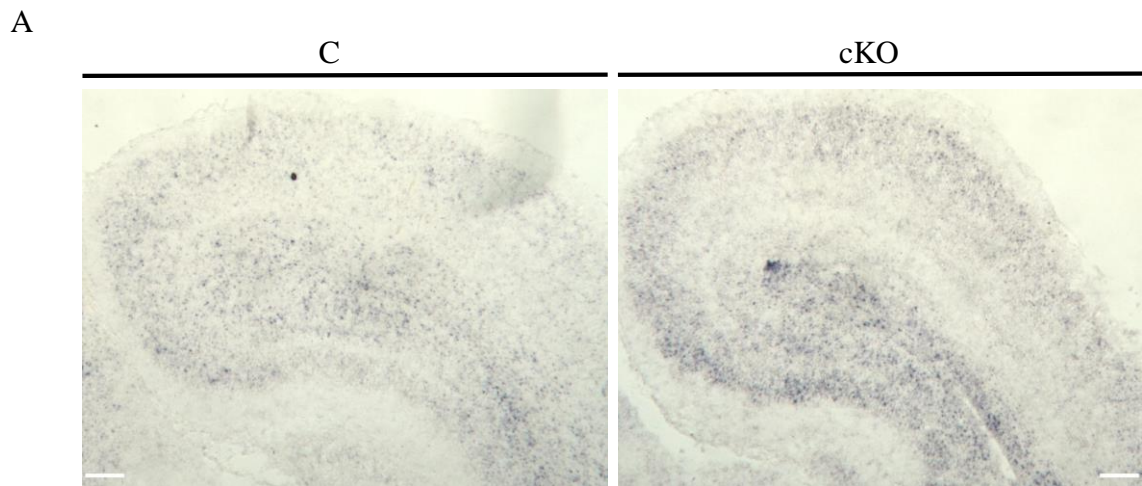


Figure 4.5 Validation of increased *ErbB3* mRNA and ERBB3 protein levels in the *Atrx*-null neonatal mouse forebrain. *In situ* hybridization (ISH; A) was performed on 8µm thick coronal cryosections from *Atrx*-null (cKO) and control neonatal mouse forebrains using a DIG-labeled *ErbB3* mRNA probe, Immunoblotting (B) was completed on protein extracts from the P0.5 forebrains of four control and *Atrx*-null pairs. Scale bars= 200µm.



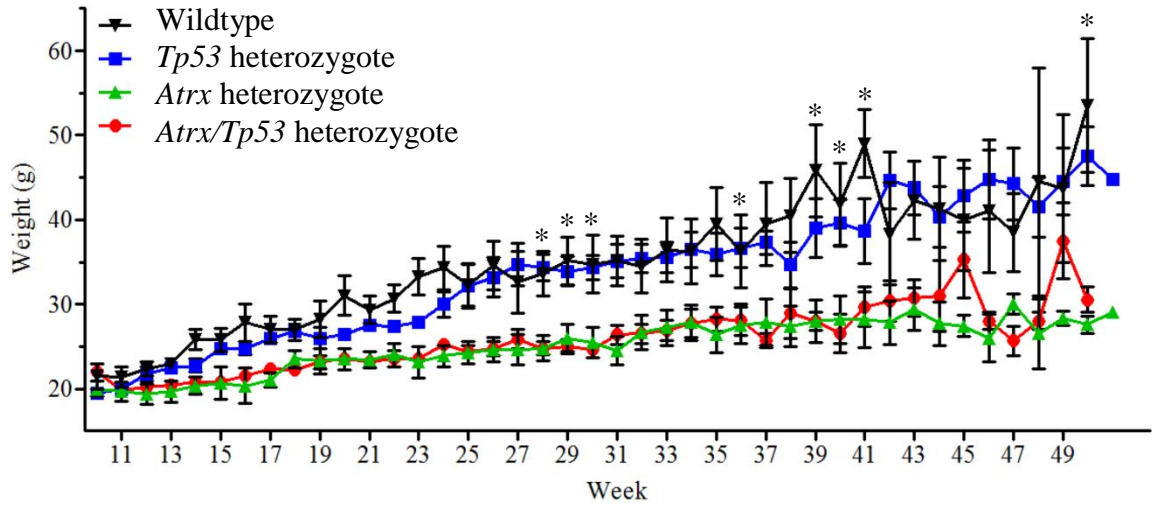
have a life expectancy similar to that of controls (Bérubé 2005). These female mice have one wildtype *Atrx* allele and one *Atrx*-floxed allele, and were mated with a mouse line harbouring the *Cre recombinase* gene under the control of the *Nestin* promoter (*Atrx^{f/wt} Nes-Cre⁺*). The *Nestin* promoter directs expression of *Cre recombinase* throughout the entire mouse CNS beginning at embryonic day 11.5 (Tronche 1999). However, because of random X-chromosome inactivation, female mice heterozygous for the floxed *Atrx* allele will show complete inactivation of *Atrx* in 50% of cells in the brain, while the other 50% will retain wildtype *Atrx* levels. This, therefore, creates a mosaic pattern of *Atrx*-expressing and *Atrx*-non-expressing cells in the CNS. Mice harbouring the floxed *Atrx* allele but negative for the *Nes-Cre recombinase* gene (*Atrx^{f/wt} Nes-Cre⁻*) were used as controls.

Mice with mosaic expression of ATRX in the brain (*Atrx^{f/wt} Nes-Cre⁺*) were then crossed to a mouse line heterozygous for the *Tp53* gene (Jacks 1994). Consequently, these mice harbour a complete loss of one *Tp53* allele in every cell of the body, and this expression is not affected by the presence of the *Cre recombinase* gene. Together, experimental (double heterozygous) mice contain one floxed *Atrx* allele along with the presence of the *Nes-Cre* gene, and they also harbour a deletion of one *Tp53* allele beginning from conception (*Atrx^{f/wt} Nes-Cre⁺ Tp53^{+/-}*). Mice heterozygous for *Atrx* or *Tp53* alone were used to control for the effects of each gene (*Atrx^{f/wt} Nes-Cre⁺ Tp53^{+/+}* or *Atrx^{f/wt} Nes-Cre⁻ Tp53^{+/-}*, respectively), along with fully wildtype mice as a negative control (*Atrx^{f/wt} Nes-Cre⁻ Tp53^{+/+}*).

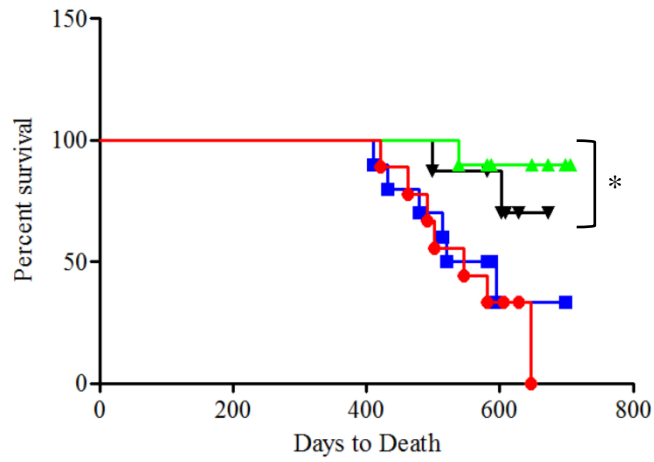
Weight measurements were taken weekly for each genotype and averaged between each cohort (Fig. 4.6a). Both wildtype and *Tp53* heterozygous mice demonstrated a typical growth pattern, and the weights of these two cohorts were not significantly different from one another. Additionally, both the double heterozygous and *Atrx* heterozygous mice shared a similar growth pattern, and the weights of these two cohorts were also not significantly different from one another. However, the double heterozygous and *Atrx* heterozygous mice demonstrated reduced average weights compared to the wildtype and *Tp53* heterozygous mice, and many of the timepoints showed a significant difference between these two groups of mice. This shows that mice lacking the *Atrx* gene in half of their brain cells starting from E11.5 exhibit reduced postnatal growth over time, while

Figure 4.6. Effect of *Atrx* and *Tp53* heterozygosity on mouse weight and survival over time. (A) Wildtype (black, n=8), *Tp53* heterozygous (blue, n=9), *Atrx* heterozygous (green, n=10), and double heterozygous (red, n=9) mice were weighed weekly from 10 weeks of age. Weights for each cohort were averaged and tracked over time. (B) Survival of wildtype (black, n=8), *Tp53* heterozygous (blue, n=9), *Atrx* heterozygous (green, n=10), and double heterozygous (red, n=9) mice was noted and cohort's survival was compared using a Mantel-Cox curve comparison test. *p<0.05

A



B



heterozygosity of *Tp53* does not affect overall growth. Combined heterozygosity of the *Atrx* and *Tp53* genes does not appear to affect the growth of these mice in a positive or negative way compared to the *Atrx* heterozygous mice alone (Fig. 4.6a).

Mouse growth and behaviour was examined throughout their lifetime, and mice were euthanized at endpoints deemed suitable according to the Canadian Council for Animal Care. For example, excessive lesions affecting the comfort level of the mouse or changes in the mouse's gait affecting its ability to feed properly would be deemed as appropriate endpoints for the mouse. The overall survival curves on each cohort was tracked, and survival was compared between genotypes (Fig. 4.6b). With the exception of a few outliers, the wildtype and *Atrx* heterozygous mice survived at a similar rate, with the majority surviving past 600 days. Additionally, the double heterozygous and *Tp53* heterozygous mice showed similar survival curves, with the majority or entirety of the cohort dying by around 600 days and a mean survival for both cohorts of around 500 days. Taken together the results show that heterozygosity of the *Tp53* gene (but not *Atrx*) leads to reduced lifespan in these mice. Combined *Atrx* and *Tp53* heterozygosity did not influence the survival of these mice in a positive or negative way compared to the *Tp53* heterozygous mice alone (Fig. 4.6b).

Prior to euthanasia, mice were perfused with 4% paraformaldehyde (PFA) and images were taken of the internal organs of each mouse to determine whether the onset of death was due to the presence of internal tumours or lesions, which are known to develop in *Tp53* heterozygous mice (Table 4.2). As expected, the majority of wildtype and *Atrx* heterozygous mice showed few or no internal lesions, lacked enlarged organs like the spleen and liver, and maintained normal internal organ function throughout their lifetime. However, both the *Tp53* heterozygous and *Atrx/Tp53* double heterozygous cohorts showed a large amount of internal dysfunction, including one or more of the following: intestinal, renal, thymic and hepatic lesions, enlarged spleens and livers, distended abdomens, and odd gaits (Table 4.2).

These results validate the likelihood that the internal lesions and abnormalities in the *Tp53* heterozygous and *Atrx/Tp53* double heterozygous mice were the cause of death, rather than any severe neurological phenotypes. However, there is a possibility of the combined

Table 4.2 Outline of internal abnormalities in *Atrx* and *Tp53* heterozygous mice.

Genotype	DOB (m/d/y)	Internal Lesions/Abnormalities						
		Liver	Kidneys	Intestines	Spleen	Thymus	Limbs	Other
Double Het	08/28/12	None	None	None	None	Yes	Yes	None
Double Het	10/24/12	None	None	None	None	None	Yes	None
Double Het	10/24/12	None	None	None	None	Yes	None	None
Double Het	11/16/12	None	None	Yes	None	None	None	None
Double Het	12/06/12	None	Yes	Yes	None	None	None	None
Double Het	12/06/12	None	Yes	None	None	None	None	Growth on spine
Double Het	12/09/12	None	None	Yes	Enlarged	None	None	None
Double Het	12/09/12	None	None	None	None	Yes	None	None
Double Het	12/09/12	None	None	None	None	None	None	None
<i>Atrx</i> Het	08/28/12	Yes	Yes	None	Enlarged	None	None	None
<i>Atrx</i> Het	09/05/12	None	None	None	None	None	None	None
<i>Atrx</i> Het	10/01/12	None	None	None	None	None	None	None
<i>Atrx</i> Het	10/01/12	None	None	Yes	None	None	None	None
<i>Atrx</i> Het	10/01/12	None	None	Fluid-filled	None	None	None	None
<i>Atrx</i> Het	12/27/12	None	None	None	None	None	None	None
<i>Atrx</i> Het	12/27/12	None	None	None	None	None	None	None
<i>Atrx</i> Het	01/01/13	None	None	None	None	None	None	None
<i>Atrx</i> Het	01/01/13	None	None	None	None	None	None	None
<i>Tp53</i> Het	08/28/12	None	None	None	None	None	Yes	None
<i>Tp53</i> Het	08/28/12	Yes	Yes	Yes	None	None	None	None
<i>Tp53</i> Het	09/05/12	None	Yes	Yes	None	None	None	None
<i>Tp53</i> Het	09/05/12	None	None	None	Enlarged	None	None	None
<i>Tp53</i> Het	11/16/12	None	Yes	Yes	Enlarged	None	None	None
<i>Tp53</i> Het	12/06/12	Yes	Yes	Yes	Enlarged	None	None	Distended abdomen
<i>Tp53</i> Het	12/27/12	None	None	None	None	None	None	None
<i>Tp53</i> Het	12/27/12	None	None	None	Enlarged	Yes	None	None
<i>Tp53</i> Het	01/01/13	None	None	Yes	Enlarged	None	None	None
Wildtype	08/28/12	None	None	None	None	None	None	None
Wildtype	09/12/12	None	None	None	None	None	None	None
Wildtype	10/01/12	None	None	None	None	None	None	None
Wildtype	11/16/12	None	None	None	None	None	None	None
Wildtype	11/16/12	None	None	None	None	None	None	None
Wildtype	12/06/12	None	None	None	None	None	None	None
Wildtype	01/01/13	None	None	None	None	None	None	None
Wildtype	01/01/13	None	None	None	None	None	None	None

heterozygosity of *Atrx* and *Tp53* in the brain leading to abnormal proliferation, potentially due to enhanced genomic instability in these cells as was seen in the *in vitro* systems developed and discussed in chapter 3. Brain sagittal cryosectioning and H&E staining is underway in order to investigate the brain histology of these mice cohorts and determine whether combined ATRX and TP53 loss leads to dysplasia or tumours. This *in vivo* model represents a tool that can be used in future studies to determine the interplay between *Atrx* and *Tp53* mutations in the development of glioma.

CHAPTER 5 – Discussion and Conclusions

5.1 Summary of Thesis Findings

The main objective of the experiments conducted in this thesis was to establish whether the loss of *Atrx* in combination with the loss of TP53 function, both *in vitro* and *in vivo*, could lead to genetic and molecular changes capable of transforming normal neurons in the central nervous system (CNS) into tumorigenic cells. To test this *in vitro*, two model systems were set up using primary mouse neuroprogenitor cell (NPC) cultures. These NPCs lacked either *Atrx* alone or lacked both *Atrx* and TP53 function. The first *in vitro* system harboured the genetic loss of the floxed *Atrx* allele embryonically, followed by the inhibition of TP53 using a reversible inhibitor drug called cyclic Pifithrin- α (cPFT α) in culture. The findings from these experiments showed that the loss of *Atrx* alone in mouse NPCs reduced cellular viability significantly *in vitro* after six days of culturing, as described previously (Bérubé 2005). However, *Atrx*-null cells treated with 20 μ M cPFT α to inhibit TP53 function demonstrated restored cellular viability, similar to viability levels of control cells treated with either DMSO or cPFT α . Despite restored cellular viability, *Atrx*-null cells treated with cPFT α demonstrated increased DNA damage, as shown by increased γ H2A.X immunostaining. *Atrx*-null cells grown in culture treated with DMSO also showed increased genomic instability; however, this instability was trending towards a further increase when both ATRX and TP53 functions were ablated. Thus, despite further genomic insult upon the sequential loss of function of both ATRX and TP53 *in vitro*, these ATRX/TP53 double-null cells exhibited restored cellular survival – a phenotype commonly noted in tumorigenic cells.

A second *in vitro* system was created that examined a more robust and simultaneous genetic inactivation of both *Atrx* and *Tp53* in culture. This system used *Atrx* and *Tp53* double floxed mouse NPCs grown in culture, and infected with an adenovirus harbouring the *Cre recombinase* gene linked to the *Green fluorescence protein (Gfp)* gene, along with appropriate controls. Expression of *Cre recombinase* enabled the genetic silencing of either *Atrx* alone, *Tp53* alone, or both *Atrx* and *Tp53* simultaneously. NPCs lacking only ATRX

expression showed reduced cellular viability compared to control cells. However, NPCs lacking both ATRX and TP53 expression had cellular viability comparable with controls and excessive genomic instability. This second *in vitro* system reiterates the abnormal cellular phenotypes shown in the first system; however, it appears that this second system may be more robust and reproducible likely because of the specificity of the adenovirus *Cre recombinase* infection versus the addition of a reversible TP53 inhibitor drug.

Examination of available data from online databases allowed us to identify patient tumor samples that harboured low, normal, and high gene expression levels of ATRX, as well as to assess copy number variation (CNV) at the ATRX locus. Examination of ATRX gene expression indicated that glioblastoma multiforme tumours harbouring low ATRX expression had a significantly earlier age of diagnosis, along with a trend towards longer overall survival, compared to those patients that had tumours carrying normal or even high expression levels for ATRX. As well, CNV analysis at the ATRX locus indicated that glioma tumour cell lines carrying an excess number of copies of ATRX had a significant increase in genomic instability – as signified by an increase in the total number and the number of abnormal segments. In addition, glioma cell lines carrying higher copy numbers for the ATRX locus also showed a trend towards more whole chromosome gains or losses, indicative of chromosomal congression and separation defects during mitosis.

Experiments conducted *in vivo* examined the effects of *Atrx* loss, both alone and in combination with *Tp53*, in the mouse CNS. Analysis of a microarray performed at birth (P0.5) on control and *Atrx*-null mouse forebrains indicated a significant increase in the expression of a number of genes known to be associated with glioma development and progression in the *Atrx*-null neonatal mouse forebrain. A number of these genes were validated by qRT-PCR based on their relevance to glioma, and were shown to be significantly upregulated in the P0.5 *Atrx*-null mouse forebrain compared to *Cre*-positive controls. Increased expression of the *ErbB3* gene was further validated using *in situ* hybridization (ISH) and immunoblotting techniques, as it is a member of the epidermal growth factor receptor (EGFR) family of proteins and signals through the AKT and MAPK pathways. Western blots indicated an increase in ERBB3 and phospho-ERBB3 proteins, as

well as phospho-AKT – a signalling molecule downstream of ERBB3 – showed an increase in the majority of *Atrx* -null mouse forebrains at P0.5.

Examination of *Atrx* and *Tp53* loss *in vivo* showed that mosaic expression of *Atrx* in the mouse brain leads to reduced postnatal growth of the mice, while *Tp53* heterozygosity caused tumours and abnormalities of several organs and reduced survival.

5.2 *In vitro* NPC Culture Systems as a Model of Glioma Development

Tumours within the glioma spectrum are highly heterogeneous, and the cell of origin for gliomas is a greatly disputed topic among scientists (Furnari 2007). Additionally, the underlying genetic and molecular alterations leading to glioma formation are vast and not well understood (Furnari 2007). Because of this complexity, the creation of systems to model the development of glioma has been extremely difficult. The present study describes two *in vitro* NPC culture systems that may be useful in modelling the initial steps of gliomagenesis.

Several studies have identified a significant overlap between mutations in *ATRX*, or loss of *ATRX* protein expression, and mutations in *TP53* (Schwartzentruber 2012; Liu 2012; Kannan 2013; Wu 2014). However, whether mutations in *ATRX* occur first and act to drive tumorigenesis, or are a result of other prior mutations, is unknown. Thus, the development of *in vitro* model systems allowing for different temporal inactivation of both TP53 and *ATRX* function in mouse NPCs was important to identify whether sequential or simultaneous loss of *ATRX* and TP53 function would better drive tumorigenic characteristics.

Mouse NPCs were used for both *in vitro* culture systems described in the present study. While the cell of origin for gliomas is still hotly debated within this field, recent evidence is pointing towards NPCs, or neural stem cells (NSCs), as potential targets. Several studies have now identified glioblastoma stem cells, or initiating cells (GICs), as playing a major role in tumor development, tumour maintenance, and therapeutic resistance (Salmaggi 2006; Johannessen 2009; Kroonen 2011). Furthermore, these GICs demonstrate many

properties akin to NSCs (Stiles 2008), creating the link between NSCs and glioma tumour formation. Finally, the adult brain harbours several NSC niches that retain the ability to produce neurons and glia throughout life, thus providing a source of progenitor cells in adults that could become oncogenic following mutagenesis (Luskin 1993; Lois 1994). This evidence justifies the use of NPCs *in vitro* as a model system for glioma development, and was the reason behind using this cell type for both the sequential and simultaneous *in vitro* systems described in the present study.

5.2.1 Sequential Loss of ATRX and TP53 Function in Mouse NPCs

The first *in vitro* model system took advantage of the *FoxG1-Cre⁺ Atrx^{f/y}* mouse NPC culturing system set up on our lab. *Atrx*-null NPCs in culture undergo massive TP53-mediated cell death at 6-7DIV (Bérubé 2005; Seah 2008; Watson 2013). To combat cell death *in vitro*, the reversible inhibitor of TP53 called cyclic Pifithrin- α (cPFT α) was added to the culture media after two days *in vitro*. Therefore, following genetic loss of *Atrx* at E8.5, TP53 protein function was ablated using cPFT α approximately 7 days later in culture. Trypan blue viability assays indicated that cellular survival in these *Atrx*-null/cPFT α -treated NPCs was restored to control levels.

Previous studies have shown that *Atrx* loss in cortical neurons during embryogenesis leads to an increase in replication-associated DNA damage foci, and this genomic instability is further enhanced upon the combined loss of ATRX and TP53 embryonically *in vivo* (Watson 2013). In the present study, genomic instability is shown to be significantly increased upon the loss of *Atrx* in NPCs, and this DNA damage is increased further upon the treatment of *Atrx*-null cells with cPFT α . Qualitatively, this enhancement of genomic instability can be easily seen; however, quantifying immunofluorescence signals in growing NPCs is a difficult task. This is because NPCs tend to grow in clumps and in small colonies, rather than creating a confluent cell monolayer across the culture plate (Leach 2011). Therefore, performing cell counts is challenging, and so the mean gray value of the DAPI stain (which stains the nuclei of all cells) was compared to the mean gray value of the γ H2A.X immunostain (which marks sites of double-stranded DNA breaks). This

quantification methodology is not as robust and reproducible as performing cell counts would be, and this may explain why the quantification for DNA damage foci in *Atrx*-null cells treated with cPFT α is not significantly higher than DNA damage foci in *Atrx*-null cells treated with only DMSO. However, this result does indicate that the loss of *Atrx* alone is associated with the induction of genomic instability, and this instability is maintained or even increased upon the loss of TP53 function. Furthermore, despite the maintenance of DNA damage in these double null cells, their ability to survive in culture is retained at levels comparable to controls – both of which are hallmarks of tumorigenic cells.

One advantage of this sequential *in vitro* system is that it models more realistically the series of early events that may unfold in a cell undergoing tumorigenic transformation. We know from previous literature that cells lacking *Atrx* expression alone do develop characteristics of tumorigenic cells – like mitotic defects, mis-segregated chromosomes, and DNA replication stress (Seah 2008; Ritchie 2008; Watson 2013). However, *Atrx*-null cells both *in vitro* and *in vivo* also activate the TP53 response pathway, leading to apoptosis (Seah 2008; Watson 2013). Thus, it is unlikely that a “single-hit” mutation in *ATR*X would lead to tumorigenic transformation in cells, supporting the requirement for a second mutation to promote carcinogenesis. Our *in vitro* system models the sequential loss of *Atrx* followed by TP53 inhibition, and we can see that this system does allow for increased cellular survival despite the accumulation of DNA damage foci. However, a disadvantage of this system is the use of a reversible drug to inhibit a specific protein’s function. Protein inhibitors are notorious for having off-target effects and for not always generating reproducible results. Cyclic Pifithrin- α is a more specific and less cytotoxic form of the original non-cyclic drug Pifithrin- α (Zuco 2008); however, it is still a reversible inhibitor of TP53 and may not produce as robust of a response as a more permanent and reproducible inactivation of TP53 function would. Thus, a more efficient and specific system to sequentially inactivate both *ATR*X and TP53 function would allow for a more robust and reproducible response *in vitro*.

5.2.2 Simultaneous Loss of ATRX and TP53 Function in Mouse NPCs

The second *in vitro* system allowed for the simultaneous genetic silencing of both the *Atrx* and *Tp53* genes using adenovirus-*CreGFP* infected NPCs. A reduction in cellular viability was identified, as expected, in *Atrx*-floxed ad-*CreGFP* infected NPCs in culture. Again, as was similarly seen in the first *in vitro* system, *Atrx/Tp53* double floxed cells infected with ad-*CreGFP* demonstrated restored cellular viability. This result demonstrates that *Atrx*-null NPCs are likely undergoing cell death via a TP53-dependent pathway, a result found previously in embryonic cortical neurons *in vivo* (Seah 2008). Loss of both TP53 and ATRX protein expression was therefore able to restore cellular survival, indicating TP53 activity as the main player in the reduction of *Atrx*-null cellular viability. Furthermore, the maintenance of high cellular viability in all NPC genotypes infected with ad-*GFP* alone indicates that neither adenoviral infection nor GFP expression affected cell survival on its own.

Atrx/Tp53 double floxed cells infected with only ad-*GFP* show basal levels of DNA damage foci, while infection of double floxed NPCs with ad-*CreGFP* leads to a qualitatively significant enhancement in γ H2A.X immunostaining throughout many cells in culture, indicative of an increase in genomic instability in these double-null cells in culture. Previous literature has identified that the loss of *Atrx* is associated with dysregulation in DNA damage repair and/or with proper DNA replication, thereby leading to the accumulation of DNA damage foci (Lovejoy 2012; Leung 2013; Watson 2013; Clynes 2014). Thus, cells that have lost both ATRX and TP53 protein expression no longer undergo apoptosis, but concomitantly acquire further genomic insult leading to massive chromosomal instability. Enhanced cellular survival and accumulation of DNA damage are two major hallmarks of cells undergoing tumorigenic transformation (Hanahan 2011), indicating that the combined loss of ATRX and TP53 simultaneously may be sufficient to drive NPCs into a tumorigenic state.

This second *in vitro* system is temporally different from the first system in that the expression of both *Atrx* and *Tp53* are lost simultaneously in cultured NPCs, rather than the stepwise loss of ATRX and TP53 function described in the first system. This simultaneous *in vitro* system may not as closely recapitulate genetic events that happen *in vivo*, as

typically patients will gain mutations in genes over time rather than acquire two “hits” at the exact same time. However, the use of an adenovirus carrying *Cre recombinase* is a much more robust and reproducible methodology in generating *Atrx/Tp53* double-null cells. Cells that fluoresce green are easily identified, and because the *Gfp* gene is tagged onto the end of the *Cre recombinase* gene, we know that all green cells will also be expressing *Cre*. The *Cre* gene is highly precise and efficient, thus enabling us to gain high specificity and efficacy in recombining and silencing both floxed genes in NPCs *in vitro*, as seen by the western blotting validation of ATRX and TP53 protein expression levels. Enhanced robustness resulted in a much more profound visual increase in γ H2A.X immunostaining, indicative of a more intense induction in genomic instability in this system.

Overall, both *in vitro* systems demonstrate two major phenotypic characteristics required in order to define a cell as cancerous (Hanahan 2011). Firstly, carcinogenic cells display changes, either genetic or epigenetic, to the so-called healthy genome (Hanahan 2011). This condition is met in both systems, whereby excess genomic instability is demonstrated upon the loss of both ATRX and TP53 function in cultured NPCs compared to controls. Secondly, cells must exhibit an atypical survival advantage despite the presence of excess DNA damage (Hanahan 2011). This condition is met in both systems whereby cells that have lost only *Atrx* expression show significantly reduced cellular survival, whereas cells that have lost both ATRX and TP53 function appear to have reduced apoptosis, and thus restored cellular survival, similar to levels of control cells along with enhanced genomic instability. Thus, these double-null NPCs in culture demonstrate abnormal survival in culture compared to their *Atrx*-null counterparts *in vitro*, indicating that these cells have acquired a survival advantage. I conclude that loss of ATRX and TP53 function *in vitro*, either sequentially or simultaneously, is capable of inducing characteristic phenotypes common to carcinogenic cells.

5.2.3 Future Directions for *In Vitro* Model Systems of Glioma

Although the previously described *in vitro* systems appear to have acquired important characteristics of tumorigenic cells upon the loss of both ATRX and TP53 function, there are many other characteristic phenotypes common to carcinogenesis that would be interesting to examine in these cells. Firstly, cellular viability and survival was measured in the present study, but proliferation was not. Examination of cell growth and proliferation over time, or monitoring for the presence of neurospheres, would indicate whether ATRX/TP53 double-null cells demonstrate enhanced proliferation *in vitro*. Additionally, cancerous cells will commonly demonstrate increased invasion or migration phenotypes, as tumorigenic cells typically migrate throughout and invade healthy tissues in order to spread and metastasize (Hanahan 2011). Placing *Atrx/Tp53* double-null NPCs in a Transwell migration and/or Matrigel invasion assay to determine whether these cells show higher levels of these phenotypes would be quite interesting, as gliomas in humans tend to have a highly invasive and infiltrative nature (Marumoto 2012). Additionally, tumorigenic cells *in vivo* are often capable of activating angiogenesis, in order to stimulate blood vessel growth to provide the growing tumour mass with a source of nutrients and oxygen as well as a source for depositing metabolic waste and carbon dioxide (Hanahan 2011). Injection of *Atrx/Tp53* double-null NPCs grown in culture back into nude, immuno-compromised mice would indicate whether these tumour-like NPCs are capable of attaching to tissue *in vivo* and continue growing, while at the same time promoting blood vessel growth towards the emerging tumour mass.

Finally, as was discussed in the introduction, glioma and PanNET patients with tumours carrying mutations in *ATR*X or harbouring a loss of ATRX staining via immunohistochemistry show a significant association with the activation of the alternative lengthening of telomeres (ALT) phenotype (Heaphy 2011; Jiao 2011; Schwartzentruber 2012; Abedalthagafi 2013). As well, loss of *Atrx* alone is associated with an increase in telomere dysfunction, DNA damage foci at the telomeres, and telomere fusions (Watson 2013), and *ATR*X loss of function in somatic cell hybrids also segregated with the activation of the ALT pathway (Bower 2012). These results are consistent with ATRX playing a role in telomere maintenance and acting as a repressor of ALT *in vivo*. It will be important in

the future to determine the presence of ALT in our culture systems using telomere-FISH to identify whether prolonged ATRX loss of function *in vitro* could promote excessive telomere recombination.

5.3 In Vivo Analysis of *Atrx* deletion in the mouse brain

Previous studies have characterized several phenotypes upon the loss of *Atrx* expression both *in vivo* and *in vitro* (reviewed in Bérubé 2011). Many characteristics of *Atrx*-null cells are shared by tumorigenic cells – like excessive DNA replication stress, mitotic defects, chromosomal fusions and missegregation (Seah 2008; Ritchie 2008; Watson 2013) – and thus it was not surprising that mutations in *ATRX* were found within a significant subset of gliomas (Jiao 2011; Schwartzenruber 2012; Liu 2012; Kannan 2013). Examination of glioma patient databases, as well as analysis of genetic and molecular changes *in vivo* upon the loss of *ATRX* expression, may provide evidence to decipher whether mutations in *ATRX* act as drivers or as passengers of tumorigenesis.

5.3.1 Dysfunction of *ATRX* in Glioma Patients

Analysis of *ATRX* expression in a large cohort of glioblastoma multiforme patient samples from The Cancer Genome Atlas database indicated that patients harbouring low expression levels of *ATRX* demonstrated a significantly earlier age of diagnosis as well as a trend towards better overall survival compared to tumours with normal or high levels of *ATRX*. These results have been both supported and opposed in the literature. For example, mutations in *ATRX* were associated with similar findings (earlier age of diagnosis and better overall patient survival) in patients with pancreatic neuroendocrine tumours (PanNETs; Jiao 2011). As well, *ATRX* loss defined a sub-population of astrocytic tumours with a more favourable prognosis demonstrating a time to treatment failure of 55.6 months versus 31.8 months in *ATRX* wildtype tumours (Weistler 2013). Other studies found no correlation between *ATRX* status and age of diagnosis or patient prognosis, but this may be due to small sample sizes or the specific tumour populations studied (Abedalthagafi 2013). Oppositely,

further studies of *ATRX* loss in panNETs have demonstrated a correlation with reduced time of relapse-free survival and decreased time of tumour-associated survival (Marinoni 2014). While it is still unclear how *ATRX* mutations influence patient progression, it is likely that *ATRX* mutation or expression status may be beneficial in defining discrete subsets of gliomas associated with treatment response and patient survival.

Furthermore, examination of copy number variation data for glioma cell lines on the Catalogue of Somatic Mutations in Cancer (COSMIC) database identified an association between amplification of the *ATRX* locus and increased genomic instability and whole chromosome gains/losses genome-wide. Unfortunately, as there was no mRNA expression data to correlate with the CNV data, we had to rule out cell lines originating from female patients as we would not be able to tell if the *ATRX* locus from the active or inactive chromosome was amplified. Additionally, even in males harbouring amplification of the *ATRX* locus on the X chromosome, without expression analysis we are unable to know whether these cells are gaining functional or non-functional copies of the *ATRX* gene. Nevertheless, glioma cell lines harbouring excessive copies of the *ATRX* locus demonstrated significantly more genomic instability, as quantified by increased numbers of abnormal genomic segments, as well as a trend towards increased whole chromosome events. We know from previous literature that not only does *ATRX* loss lead to cellular dysfunction, but overexpression of *ATRX* is also associated with severe developmental and cellular deficits (Bérubé 2002). Increased *ATRX* expression in transgenic mice led to abnormal growth and organization of the ventricular zone in E10.5 embryos, as well as growth retardation, neural tube defects, and a high incidence of embryonic death (Bérubé 2002). Therefore, *ATRX* dosage is likely crucial for proper neuronal development, and thus overexpression of *ATRX* may also be associated with phenotypes relative to cancer development, like enhanced genomic instability.

5.3.2 *Atrx* Loss in the Brain is Associated with Alterations in Cancer-Related Signalling Pathways

ATRX is a known chromatin-associated protein, using its N-terminal ADD domain to direct binding to sites of heterochromatin (Bérubé 2011; Dhayalan 2011; Argentaro 2007). *ATRX*

can be directed to specific sequences within the genome via histone modifications or protein recruitment (Dhayalan 2011; Nan 2007), and these sites are typically GC-rich and repetitive regions, like telomeres and G-quadruplexes (Law 2010). Given the roles of ATRX at chromatin, it comes as no surprise that ATRX loss leads to alterations in gene transcript levels both in cells undergoing mitosis and in non-dividing cells (Levy 2008). For example, analysis of the *Atrx*-null neonatal mouse forebrain identified consistent downregulation of ancestral pseudoautosomal region genes (Levy 2008; Levy 2014), as well as differential expression of many imprinted genes (Kernohan 2010; Kernohan 2014). Recent evidence indicates that at a subset of genes, ATRX is capable of binding G-rich secondary DNA structures called G-quadruplexes (G4) to enable bypass of transcriptional machinery and mRNA elongation (Levy 2014). As well, ATRX has been shown to be involved in chromatin looping, enabling the contact between distant enhancers and promoters in order to encourage gene expression (Kernohan 2014). Thus, although the full range of the ability of ATRX to affect gene expression changes has not yet been elucidated, it is clear that the loss of *Atrx* expression is associated with alterations in gene expression through both chromatin looping and through the resolution of secondary DNA structures.

Microarray analysis of control versus *Atrx*-null neonatal mouse forebrains identified numerous significant gene expression changes. GO term analysis for these genes indicated a large number as being involved in stem cell pluripotency, the WNT pathway, and cardiogenesis. Further literature searches identified several candidate genes within these GO pathways as known effectors of glioma initiation and progression. Real time PCR analysis validated the upregulation of many gene targets demonstrated in the literature to be associated with cellular characteristics common in glioma, like cellular migration and invasion (*Cxcl2*, *Mmp2*, *Mmp14*, *Igfbp2*, *Gsn*, *Lox*, *Mdk*, and *ErbB3*), epithelial-to-mesenchymal transition (EMT; *FoxC1*, *FoxC2*, *S100A11*, and *Ahnak*), and the WNT pathway (*Wnt5a*, *Wnt7b*, and *Fzd7*). Consistent upregulation of these targets indicates that *Atrx* loss in the surviving differentiated neurons of the neonatal mouse cortex may lead to the development of a cellular environment conducive of tumorigenesis.

One gene, *ErbB3*, was further validated by *in situ* hybridization and western blotting and was shown again to be upregulated in the *Atrx*-null neonatal mouse forebrain at both the

mRNA and protein levels. The ERBB3 protein is a member of the *epidermal growth factor receptor* (EGFR) family and lies upstream of a signalling cascade known to promote cellular migration, invasion, protein synthesis, and cell growth (Kim 1998; Kamalati 2000; Jones 2006). Dysregulation in ERBB3 protein has also been shown in gliomagenesis, as overexpression of ERBB3 is associated with pilocytic astrocytoma progression (Addo-Yobo 2006) and radiation-induced glioblastomas (Donson 2007), and prominent expression of ERBB3 was seen in CD-133 positive putative glioblastoma tumour stem cells (Duhem-Tonnelle 2010). Western blots for p-AKT also showed upregulation in the presence of upregulated p-ERBB3 indicating enhanced signalling through downstream oncogenic pathways. The consistent upregulation of *ErbB3* mRNA and p-ERBB3 protein in our system indicates that the loss of *Atrx* expression in cells of the neonatal mouse cortex induces the expression of genes known to promote glioma development and increase signalling through oncogenic pathways, therefore creating a cellular environment conducive to tumorigenesis.

5.4 *In Vivo* Modelling of Combined *Atrx* and *Tp53* Loss

Recent patient studies have indicated a common and consistent overlap between mutation of *ATRX* and *TP53* in a significant number of gliomas (Jiao 2011; Schwartzentruber 2012; Kannan 2013), indicating that the combined loss of *ATRX* and *TP53* function *in vivo* may enable cells to acquire tumorigenic characteristics while also avoiding cell death. This combinatorial genetic mutation may thus be the driving force of tumorigenesis in a specific subset of glioma patients.

The *in vivo* model developed in the present study used mice heterozygous for *Tp53*, along with heterozygosity for *Atrx* in the brain. *Tp53* heterozygosity in mice is known to confer a low spontaneous tumour incidence up to approximately 12 months of age (Harvey 1993; Donehower 1996), with about half of the heterozygous mice developing tumours by 18 months of age (Donehower 1996). This is because the mice retain a single, functional copy of the *Tp53* allele and therefore a second mutagenic event must occur to remove the remaining *Tp53* allele in order for cancer to develop (Harvey 1993). *Tp53* heterozygous

mice preferentially develop osteosarcomas, lymphomas, and soft-tissue sarcomas, which affect the supporting tissue (fat, blood vessels, nerves and ligaments) surrounding the body organs (Donehower 1996). These mice are useful in carcinogenesis studies with chemicals or additional mutagenic hits to study whether additional mutations can drive tumorigenesis in these mice at an enhanced rate. In the present study, CNS-specific loss of one *Atrx* allele was performed to identify whether combined *Atrx/TP53* loss could drive tumorigenesis in the mouse CNS before developing tumours throughout the body.

Current work in our lab has identified that *Nes-Cre⁺ Atrx^{+/-}* mice display reduced growth and decreased overall weight compared to wildtype mice, associated with reduced levels of circulating IGF-1 (unpublished data). Thus, it was not surprising to find that both the *Atrx* heterozygous and double heterozygous mice showed these same characteristics in the present study. Additionally, as explained above, *TP53* heterozygous mice have been shown to succumb to their tumours around 12-18 months of age (Donehower 1996; Harvey 1993), and these results were reiterated in the present study in which the *TP53* heterozygous and double heterozygous mice demonstrated a similar mean survival of around 500 days, or 15 months. These results indicate that heterozygosity of *Atrx* in the mouse CNS beginning at E11.5, as driven by *Nes-Cre* expression, is likely driving the reduced weight in the double heterozygous mice, while heterozygosity of *TP53* is likely responsible for the reduced survival of these mice. Combined heterozygosity of *Atrx* and *TP53* does not appear to further affect overall weight or survival in these mice.

Both the *TP53* heterozygous and double heterozygous mice developed internal lesions consistent with previous reports. These mice harboured tumours in the soft tissue of one or more organs including the intestines, liver, kidneys, and thymus, with a few even developing tumours in the hind limbs. As the double heterozygous mice did not demonstrate reduced survival compared to the *TP53* heterozygous mice alone, it is likely that these internal lesions are the cause of the early death of these mice. Future examination of the brain tissue of these mice will reveal if abnormal proliferation, increased DNA damage and tumour formation occur.

My studies have shown that combined loss of ATRX and TP53 function, both sequentially and simultaneously, was capable of increasing cell survival and genomic instability in

cultured NPCs; however, the phenotypic effects were relatively slight. This evidence indicates that perhaps *ATRX* loss is capable of driving tumorigenic phenotypes, but this loss may require further time or additional mutational hits to fully drive cells into a tumorigenic state. For example, the large majority of glioma patient studies have indicated a link between *ATRX* mutation, or a loss of *ATRX* immunostaining, and the presence of the alternative lengthening of telomeres phenotype (Jiao 2011; Schwartzentruber 2012; Liu 2013). As mouse telomeres are significantly longer than human telomeres, perhaps the loss of *Atrx* in the mouse is not leading to ALT activation as it does in human cells. The use of a mouse line harbouring already shortened telomeres may help in discovering whether the *Atrx* loss drives gliomagenesis through telomere destabilization and ALT activation. Furthermore, a more specific loss of *Tp53* in the mouse would bypass any non-specific tumour development and allow for precise examination of combined *Atrx* and *Tp53* loss in the brain.

5.4.1 Future Directions for *In Vivo* Modelling of Combined *Atrx/Tp53* Loss

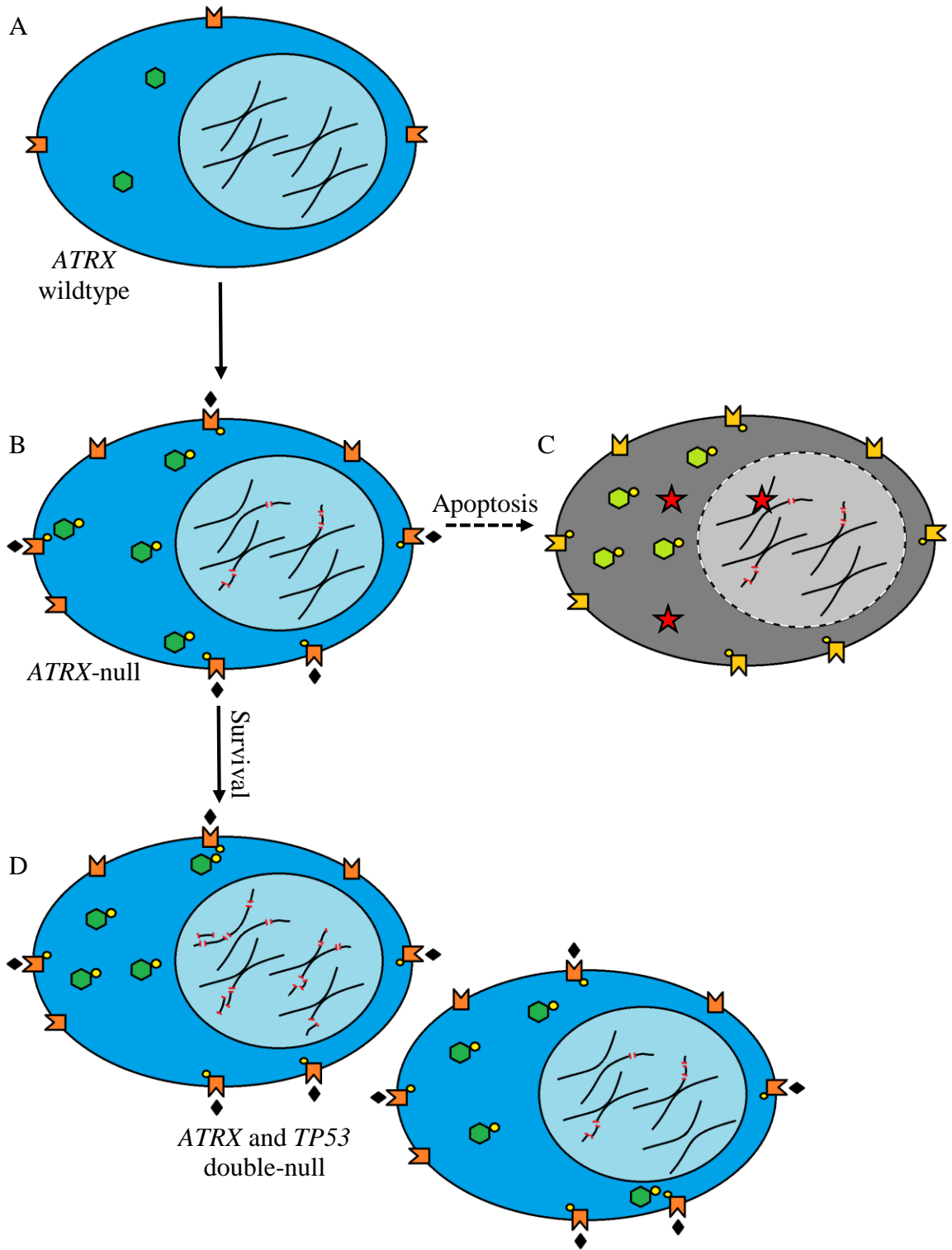
Further experiments looking for markers of overproliferation and stem-cell characteristics would indicate whether heterozygosity of *Atrx* and *Tp53* in the mouse brain could lead to tumorigenesis. For example, immunostaining for the presence of cell proliferation markers, like Ki67, or cell cycle analysis dyes, like propidium iodide (PI), would indicate regions of the mouse brain showing enhanced proliferation – a hallmark of tumorigenic cells. As well, immunostaining for γ H2A.X, a marker of double stranded DNA breaks, would identify areas of the mouse brain harbouring increased DNA damage, indicative of amplified genomic instability. Furthermore, as these heterozygous mice are mosaic for the loss of *Atrx* due to random X-chromosome inactivation, immunostaining for both *ATRX* and *TP53* would detect whether cells that harbour enhanced genomic instability and/or proliferative capacity are also negative for both *ATRX* and *TP53* proteins. This immunostaining would also further validate the mouse genotypes and indicate whether the double heterozygous mice show expansion of neurons harbouring a loss of both *ATRX* and *TP53*.

Other members of the lab are now developing a new mouse model of inducible *Atrx* and *Tp53* inactivation in neural stem cells and astrocytes. This mouse carries floxed alleles for both *Atrx* and *Tp53* and also includes the *Cre recombinase* gene under the control of the *Slc1a3* or *Glast3* promoter, which directs recombination of *Atrx* and *Tp53* specifically in the glial stem cells and radial glia of the mouse brain (Mich 2014). As well, this mouse model harbours a tamoxifen-inducible *Cre recombinase* gene under the control of the *Slc1a3* promoter, allowing for a more specific spatial and temporal deletion of *Atrx* and *Tp53* expression. This mouse model will drive *Atrx* and *Tp53* loss specifically in glial stem cells. The use of a more specific mouse model will allow for the direct and robust inactivation of both *Atrx* and *Tp53* in the glial stem cells of the brain, which are potential cells of origin for GBM, in order to determine whether these two mutagenic hits can lead to glioma development in the mouse brain.

5.5 Conclusions

In conclusion, combined loss of both ATRX and TP53 function *in vitro* leads to increased NPC survival and enhanced genomic instability (Fig. 5.1). Furthermore, *Atrx* loss in the neonatal mouse brain resulted in a consistent transcriptional upregulation of cancer-related genes involved in migration/invasion, EMT, and the WNT pathway – cellular pathways common in oncogenic cells (Fig. 5.1). Examination of available online data indicated that low expression of ATRX in GBM patients was associated with an earlier age of diagnosis and trended towards better overall survival compared to patients demonstrating normal or high expression of ATRX. Additionally, dosage of the ATRX locus appears to affect genomic instability, as glioma cell lines harbouring a gain of the ATRX locus demonstrated enhanced DNA damage and an increased number of whole chromosome gains and losses. Finally, an *in vivo* system was created that combined loss of *Atrx* and *Tp53* deficiency. Future studies will determine whether these mice develop cellular abnormalities or tumors in the brain. The use of mouse models with spatiotemporal control of *Atrx* and *Tp53* expression will provide a more robust and precise model in which to study glioma development *in vivo*.

Figure 5.1 Visual summary of the conclusions from this thesis. Cells harbouring intact *ATRX* and *TP53* expression (A) demonstrate undamaged double stranded DNA and correct chromosome architecture within the nucleus (light blue), along with basal levels of ERBB3 (orange shapes) and AKT (green hexagons) protein expression in the cytoplasm of the cell (dark blue). Upon mutation of *ATRX* or loss of *ATRX* expression (B), DNA acquires a significant amount of double stranded breaks, marked by the histone γ H2A.X (red lines). *ATRX* loss is also associated with an increase in both ERBB3 and phosphorylated (yellow circles) ERBB3 protein expression, along with a subsequent increase in phosphorylated AKT within the cytoplasm. The presence of significant genomic instability leads to the activation of TP53 (red stars) and the subsequent initiation of apoptosis (C). Cells double-null for *ATRX* and *TP53* survive, and thus cell progeny harbour excessive genomic instability and chromosomal abnormalities within the nucleus leading to proliferative advantage and gliomagenesis (D).



CHAPTER 6 – References

- Abedalthagafi M, Phillips JJ, Kim GE, Mueller S, Haas-Krogen DA, Marshall RE, Croul SE, Santi MR, Cheng J, Zhou S, Sullivan LM, Martinez-Lage M, Judkins AR, and Perry A. (2013) The alternative lengthening of telomere phenotype is significantly associated with loss of ATRX expression in high-grade pediatric and adult astrocytomas: a multi-institutional study of 214 astrocytomas. *Mod Pathol.* 26(11):1425-1432
- Addo-Yobo SO, Straessle J, Anwar A, Donson AM, Kleinschmidt-Demasters BK, and Foreman NK. (2006) Paired overexpression of ErbB3 and Sox10 in pilocytic astrocytoma. *J Neuropathol Exp Neurol.* 65(8):769-775
- Aihara K, Mukasa A, Gotoh K, Saito K, Nagae G, Tsuji S, Tatsuno K, Yamamoto S, Takayanagi S, Narita Y, Shibui S, Aburatani H, and Saito N. (2014) H3F3A K27M mutations in thalamic gliomas from young adult patients. *Neuro Oncol.* 16(1):140-146
- Argentaro A, Yang JC, Chapman L, Kowalczyk MS, Gibbons RJ, Higgs DR, Neuhaus D, and Rhodes D. (2007) Structural consequences of disease-causing mutations in the ATRX-DNMT3-DNMT3L (ADD) domain of the chromatin-associated protein ATRX. *Proc Natl Acad Sci USA.* 104(29):11939-11944
- Bechter OE, Shay JW, and Wright WE. (2004) The frequency of homologous recombination in human ALT cells. *Cell Cycle.* 3(5):547-549
- Bérubé NG, Smeenk CA, and Picketts DJ. (2000) Cell cycle-dependent phosphorylation of the ATRX protein correlates with changes in nuclear matrix and chromatin association. *Hum Mol Genet.* 9(4):539-547
- Bérubé NG, Jagla M, Smeenk C, De Repentigny Y, Kothary R, and Picketts DJ. (2002) Neurodevelopmental defects resulting from ATRX overexpression in transgenic mice. *Hum Mol Genet.* 11(3):253-261
- Bérubé NG, Mangelsdorf M, Jagla M, Vanderluit J, Garrick D, Gibbons RJ, Higgs DR, Slack RS, and Picketts DJ. (2005) The chromatin-remodeling protein ATRX is critical for neuronal survival during corticogenesis. *J Clin Invest.* 115(2):258-267

- Bérubé NG. (2011) ATRX in chromatin assembly and genome architecture during development and disease. *Biochem Cell Biol.* 89(5):435-444
- Bower K, Napier CE, Cole SL, Dagg RA, Lau LM, Duncan EL, Moy EL, and Reddel RR. (2012) Loss of wild-type ATRX expression in somatic cell hybrids segregates with activation of Alternative Lengthening of Telomeres. *PLoS One.* 7(11):e50062
- Bryan TM, Englezou A, Gupta J, Bacchetti S, and Reddel RR. (1995) Telomere elongation in immortal human cells without detectable telomerase activity. *EMBO J.* 14(17):4240-4248
- Cairncross JG, Ueki K, Zlatescu MC, Lisle DK, Finkelstein DM, Hammond RR, Silver JS, Stark PC, Macdonald DR, Ino Y, Ramsay DA, and Louis DN. (1998) Specific genetic predictors of chemotherapeutic response and survival in patients with anaplastic oligodendrogliomas. *J Natl Cancer Inst.* 90(19):1473-1479
- Cancer Genome Atlas Research Network. (2008) Comprehensive genomic characterization defines human glioblastoma genes and core pathways. *Nature.* 455(7216): 1061-1068
- Chen HL, Chew LJ, Packer RJ, and Gallo V. (2013A) Modulation of the Wnt/beta-catenin pathway in human oligodendroglioma cells by Sox17 regulates proliferation and differentiation. *Cancer Lett.* 335(2):361-371
- Chen SF, Kasajima A, Yazdani S, Chan MS, Wang L, He YY, Gao HW, and Sasano H. (2013B) Clinicopathologic significance of immunostaining of α -thalassaemia/mental retardation syndrome X-linked protein and death domain-associated protein in neuroendocrine tumors. *Hum Pathol.* 44(10):2199-2203
- Chen X, Bahrami A, Pappo A, Easton J, Dalton J, Hedlund E, Ellison D, Shurtleff S, Wu G, Wei L, Parker M, Rusch M, Nagahawatte P, Wu J, Mao S, Boggs K, Mulder H, Yergeau D, Lu C, Ding L, Edmonson M, Qu C, Wang J, Li Y, Navid F, Daw NC, Mardis ER, Wilson RK, Downing JR, Zhang J, Dyer MA, and the St. Jude's Children's Research Hospital-Washington University Pediatric Cancer Genome Project. (2014) Recurrent somatic structural variations contribute to tumorigenesis in pediatric osteosarcoma. *Cell Rep.* 7(1):104-112
- Cheung NK, Zhang J, Lu C, Parker M, Bahrami A, Tickoo SK, Heguy, Pappo AS, Federico S, Dalton J, Cheung IY, Ding L, Fulton R, Wang J, Chen X, Becksfort J, Wu J, Billups CA, Ellison D, Mardis ER, Wilson RK, Downing JR, Dyer ME, and the St.

- Jude's Children's Research Hospital-Washington University Pediatric Cancer Genome Project. (2012) Association of age at diagnosis and genetic mutations in patients with neuroblastoma. *JAMA*. 307(10):1062-1071
- Chow LM, Endersby R, Zhu X, Rankin S, Qu C, Zhang J, Broniscer A, Ellison DW, and Baker SJ. (2011) Cooperativity within and among Pten, p53, and Rb pathways induces high-grade astrocytoma in adult brain. *Cancer Cell*. 19(3):305-316
- Clynes D, Jelinska C, Xella B, Ayyub H, Taylor S, Mitson M, Bachrati CZ, Higgs DR, and Gibbons RJ. (2014) ATRX dysfunction induces replication defects in primary mouse cells. *PLoS One*. 9(3):e92915
- Conomos D, Stutz MD, Hills M, Neumann AA, Bryan TM, Reddel RR, and Pickett HA. (2012) Variant repeats are interspersed throughout telomeres and recruit nuclear receptors in ALT cells. *J Cell Biol*. 199(6):893-906
- Conte D, Huh M, Goodall E, Delorme M, Parks RJ, and Picketts DJ. (2012) Loss of Atrx sensitizes cells to DNA damaging agents through p53-mediated death pathways. *PLoS One*. 7(12):e52167
- Cryan JB, Haidar S, Ramkissoon LA, Bi WL, Knoff DS, Schultz N, Abedthalgafi M, Brown L, Wen PY, Reardon DA, Dunn IF, Folkherth RD, Santagata S, Lindeman NI, Ligon AH, Beroukhim R, Hornick JL, Alexander BM, Ligon KL, and Ramkissoon SH. (2014) Clinical multiplexed exome sequencing distinguishes adult oligodendroglial neoplasms from astrocytic and mixed lineage gliomas. *Oncotarget*. 5(18):8083-8092
- Dang L, White DW, Gross S, Bennett BD, Bittinger MA, Driggers EM, Fantin VR, Jang HG, Jin S, Keenen MC, Marks KM, Prins RM, Ward PS, Yen KE, Liao LM, Rabinowitz JD, Cantley LC, Thompson CB, Vander Heiden MG, and Su SM. (2009) Cancer-associated IDH1 mutations produce 2-hydroxyglutarate. *Nature*. 462(7274):739-744
- De Le Fuente R, Viveiros MM, Wigglesworth, K, and Eppig JJ. (2004) ATRX, a member of the SNF2 family of helicase/ATPases, is required for chromosome alignment and meiotic spindle organization in metaphase II stage mouse oocytes. *Dev Biol*. 272(1):1-14

- Dhayalan A, Tamas R, Bock I, Tattermusch A, Dimitrova E, Kudithipudi S, Ragozin S, and Jeltsch A. (2011) The ATRX-ADD domain binds to H3 tail peptides and reads the combined methylation state of K4 and K9. *Hum Mol Genet.* 20(11):2195-2203
- Donehower LA, Harvey M, Slagle BL, McArthur MJ, Montgomery CA Jr., Butel JS, and Bradley A. (1992) Mice deficient for p53 are developmentally normal but susceptible to spontaneous tumours. *Nature.* 356(6366):215-221
- Donehower LA. (1996) The p53-deficient mouse: a model for basic and applied cancer studies. *Semin Cancer Biol.* 7(5):269-278
- Donson AM, Erwin NS, Kleinschmidt-Demasters BK, Madden JR, Addo-Yobo SO, and Foreman NK. (2007) Unique molecular characteristics of radiation-induced glioblastoma. *J Neuropathol Exp Neurol.* 66(8):740-749
- Drané P, Ouararhni K, Depaux A, Shuaib M, and Hamiche A. (2010) The death-associated protein DAXX is a novel chaperone involved in the replication-independent deposition of H3.3. *Genes Dev.* 24(12):1253-1265
- Ducray F, Marie Y, and Sanson M. (2009) IDH1 and IDH2 mutations in gliomas. *N Engl J Med.* 360(21):2248-2249
- Duhem-Tonnelle V, Bièche I, Vacher S, Loyens A, Murage CA, Collier F, Baroncini M, Blond S, Prevot V, and Sharif A. (2010) Differential distribution of erbB receptors in human glioblastoma multiforme: expression of erbB3 in CD133-positive putative cancer stem cells. *J Neuropathol Exp Neurol.* 69(6):606-622
- Eustermann S, Yang JC, Law MJ, Amos R, Chapman LM, Jelinska C, Garrick D, Clynes D, Gibbons RJ, Rhodes D, Higgs DR, and Neuhaus D. (2011) Combinatorial readout of histone H3 modifications specifies localization of ATRX to heterochromatin. *Nat Struct Mol Biol.* 18(7):777-782
- Fendrich V, Waldmann J, Bartsch DK, and Langer P. (2009) Surgical management of pancreatic endocrine tumors. *Nat Rev Clin Oncol.* 6(7):419-428
- Furnari FB, Fenton T, Bachoo RM, Mukasa A, Stommel JM, Stegh A, Hahn WC, Ligon KL, Louis DN, Brennan C, Chin L, DePinho RA, Cavenee WK. (2007) Malignant astrocytic glioma: genetics, biology, and paths to treatment. *Genes Dev.* 21(21):2638-2710

- Garrick D, Samara C, McDowell TL, Smith AJ, Dobbie L, Higgs DR, and Gibbons RJ. (2004) A conserved truncated isoform of the ATR-X syndrome protein lacking the SWI/SNF-homology domain. *Gene*. 326:23-34
- Garrick D, Sharpe JA, Arkell R, Dobbie L, Smith AJ, Wood WG, Higgs DR, and Gibbons RJ. (2006) Loss of Atrx affects trophoblast development and the pattern of X-inactivation in extraembryonic tissues. *PLoS Genet*. 2(4):e58
- Gez J, Pollard H, Consalez G, Villard L, Stayton C, Millasseau P, Khrestchatisky M, and Fontes M. (1994) Cloning and expression of the murine homologue of a putative human X-linked nuclear protein gene closely linked to PGK1 in Xq13.3. *Hum Mol Genet*. 3(1):39-44
- Gibbons RJ, Picketts DJ, Villard L, and Higgs DR. (1995) Mutations in a putative global transcriptional regulator cause X-linked mental retardation with alpha thalassaemia (ATR-X syndrome). *Cell*. 80(6):837-845
- Gibbons R. (2006) Alpha thalassaemia-mental retardation, X-linked. *Orphanet J Rare Dis*. 1:15
- Goldberg AD, Banaszyski LA, Noh KM, Lewis PW, Elsaesser SJ, Stadler S, Dewell S, Las M, Guo X, Li X, Wen D, Chapgier A, DeKever RC, Miller JC, Lee YL, Boydston E, Holmes MC, Gregory PD, Grealley JM, Rafii S, Yang C, Scrambler PJ, Garrick D, Gibbons RJ, Higgs DR, Cristea IM, Urnov FD, Zheng D, and Allis CD. (2010) Distinct factors control histone variant H3.3 localization at specific genomic regions. *Cell*. 140(5):678-691
- Green DR and Kroemer G. (2009) Cytoplasmic functions of the tumour suppressor p53. *Nature*. 458(7242):1127-1130
- Guimaraes DP and Hainaut P. (2002) TP53: a key gene in human cancer. *Biochimie*. 84(1):83-93
- Günes C and Rudolph KL. (2013) The role of telomeres in stem cells and cancer. *Cell*. 152(3):390-393
- Hake SB, Garcia BA, Kauer M, Baker SP, Shabanowitz J, Hunt DF, and Allis CD. (2005) Serine 31 phosphorylation of histone variant H3.3 is specific to regions bordering centromeres in metaphase chromosomes. *Proc Natl Acad Sci USA*. 102(18):6344-6349

- Han S, Feng S, Yuan G, Dong T, Gao D, Liang G, and Wei X. (2014A) Lysyl oxidase genetic variants and the prognosis of glioma. *APMIS*. 122(3):200-205
- Han S, Li Z, Master LM, Master ZW, and Wu A. (2014B) Exogenous IGFBP-2 promotes proliferation, invasion, and chemoresistance to temozolomide in glioma cells via the integrin β 1-ERK pathway. *Br J Cancer*. 111(7):1400-1409
- Hanahan D and Weinberg RA. (2011) Hallmarks of cancer: the next generation. *Cell*. 144(5):646-674
- Harley CB. (2008) Telomerase and cancer therapeutics. *Nat Rev Cancer*. 8(3):167-179
- Hartmann C, Meyer J, Balss J, Capper D, Mueller W, Christians A, Felsberg J, Wolter M, Mawrin C, Wick W, Weller M, Herold-Mende C, Unterberg A, Jeuken JW, Wesseling P, Reifenberger G, and von Deimling A. (2009) Type and frequency of IDH1 and IDH2 mutations are related to astrocytic and oligodendroglial differentiation and age: a study of 1,010 diffuse gliomas. *Acta Neuropathol*. 118(4):469-474
- Harvey M, McArthur MJ, Montgomery CA Jr., Bradley A, and Donehower LA. (1993) Spontaneous and carcinogen-induced tumorigenesis in p53-deficient mice. *Nat Genet*. 5(3):225-229
- Heaphy CM, de Wilde RF, Jiao Y, Klein AP, Edil BH, Shi C, Bettegowda C, Rodriguez FJ, Eberhart CG, Hebbar S, Offerhaus GJ, McLendon R, Rasheed BA, HE Y, Yan H, Bigner DD, Oba-Shinjo SM, Marie SK, Riggins GJ, Kinzler KW, Vogelstein B, Hruban RH, Maitra A, Papadopoulos N, and Meeker AK. (2011) Altered telomeres in tumors with ATRX and DAXX mutations. *Science*. 333(6041):425
- Hébert JM and McConnell SK. (2008) Targeting of cre to the FoxG1 (BF-1) locus mediates loxP recombination in the telencephalon and other developing head structures. *Dev Biol*. 222(2):296-306
- Heuther R, Dong J, Chen X, Wu G, Parker M, Wei L, Ma J, Edmonson MN, Hedlund EK, Rusch MC, Shurtleff SA, Mulder HL, Boggs K, Vadodaria B, Cheng J, Yergeau D, Song G, Becksfort J, Lemmon G, Weber C, Cai Z, Dang J, Walsh M, Gedman AL, Faber Z, Easton J, Gruber T, Kriwacki RW, Partridge JF, Ding L, Wilson RK, Mardis ER, Mullighan CG, Gilbertson RJ, Baker SJ, Zambetti G, Ellison DW, Zhang J, and

- Downing JR. (2014) The landscape of somatic mutations in epigenetic regulators across 1,000 paediatric cancer genomes. *Nat Commun.* 5:3630
- Houillier C, Lejeune J, Benouaich-Amiel A, Laigle-Donadey F, Criniere E, Mokhtari K, Thillet J, Delattre JY, Hoang-Xuan K, and Sanson M. (2006) Prognostic impact of molecular markers in a series of 220 primary glioblastomas. *Cancer.* 106(10):2218-2223
- Huh MS, Price O'Dea T, Ouazia D, McKay BC, Parise G, Parks RJ, Rudnicki MA, and Picketts DJ. (2012) Compromised genomic integrity impedes muscle growth after Atrx inactivation. *J Clin Invest.* 122(12):4412-4423
- Iwase S, Xiang B, Ghosh S, Ren T, Lewis PW, Cochrane JC, Allis CD, Picketts DJ, Li H, and Shi Y. (2011) ATRX ADD domain links an atypical histone methylation recognition mechanism to human mental-retardation syndrome. *Nat Struct Mol Biol.* 8(7):769-776
- Jacks T, Remington L, Williams BO, Schmitt EM, Halachmi S, Bronson RT, and Weinberg RA. (1994) Tumor spectrum analysis in p53-mutant mice. *Curr Biol.* 4(1):1-7
- Jiao Y, Shi C, Edil BH, de Wilde RF, Kilmstra DS, Maitra A, Schulick RD, Tang LH, Wolfgang CL, Choti MA, Velculescu VE, Diaz LA Jr., Vogelstein B, Kinzler KW, Hruban RH, and Papadopoulos N. (2011) DAXX/ATRX, MEN1, and mTOP pathway genes are frequently altered in pancreatic neuroendocrine tumors. *Science.* 331(6021):1199-1203
- Jiao Y, Killela PJ, Reitman ZI, Rasheed AB, Heaphy CM, de Wilde RF, Rodriguez FJ, Rosemberg S, Oba-Shinjo SM, Nagahashi Marie SK, Bettgowda C, Agrawal N, Lipp E, Pirozzi C, Lopez G, He Y, Friedman H, Friedman AH, Riggins GJ, Holdhoff M, Burger P, McLendon R, Bigner DD, Vogelstein B, Meeker AK, Kinzler KW, Papadopoulos N, Diaz LA, and Yan H. (2012) Frequent ATRX, CIC, FUBP1 and IDH1 mutations refine the classification of malignant gliomas. *Oncotarget.* 3(7):709-722
- Johannessen TC, Wang J, Skaftnesmo KO, Sakariassen PØ, Enger PØ, Øyan AM, Kalland KH, Bjerkvig R, and Tysnes BB. (2009) Highly infiltrative brain tumours show reduced chemosensitivity associated with stem cell-like phenotype. *Neuropathol Appl Neurobiol.* 35(4):380-393

- Jones RB, Gordus A, Krall JA, and MacBeath G. (2006) A quantitative protein interaction network for the ErbB receptors using protein microarrays. *Nature*. 439(7073):168-174
- Kamalati T, Jolin HE, Fry MJ, and Crompton MR. (2000) Expression of the BRK tyrosine kinase in mammary epithelial cells enhances the coupling of EGF signalling to PI 3-kinase and Akt, via ErbB3 phosphorylation. *Oncogene*. 19(48):5471-5476
- Kamino M, Kishida M, Kibe T, Ikoma K, Iijima M, Hirano H, Tokudome M, Chen L, Koriyama C, Yamada K, Arita K, and Kishida S. (2011) Wnt-5a signalling is correlated with infiltrative activity in human glioma by inducing cellular migration and MMP-2. *Cancer Sci*. 102(3):540-548
- Kanamori M, Kumabe T, Shibahara I, Saito R, Yamashita Y, Sonoda Y, Suzuki H, Watanabe M, and Tominaga T. (2013) Clinical and histopathological characteristics of recurrent oligodendroglial tumors: comparison between primary and recurrent tumors in 18 cases. *Brain Tumor Pathol*. 30(3):151-159
- Kannan K, Inagaki A, Silber J, Gorovets D, Zhang J, Kasthuber ER, Heguy A, Petrini JH, Chan TA, and Huse JT. (2012) Whole-exome sequencing identifies ATRX mutation as a key molecular determinant in lower-grade glioma. *Oncotarget*. 3(10):1194-1203
- Kernohan KD, Jiang Y, Trembly DC, Bonvissuto AC, Eubanks JH, Mann MR, and Bérubé NG. (2010) ATRX partners with cohesion and MeCP2 and contributes to developmental silencing of imprinted genes in the brain. *Dev Cell*. 18(2):191-202
- Kernohan KD, Vernimmen D, Gloor GB, and Bérubé NG. (2014) Analysis of neonatal brain lacking ATRX or MeCP2 reveals changes in nucleosome density, CTCF binding and chromatin looping. *Nucleic Acids Res*. 42(13):8356-8368
- Killela PJ, Reitman ZJ, Jiao Y, Bettegowda C, Agrawal N, Diaz LA Jr., Friedman AH, Friedman H, Gallia GL, Giovanella BC, Grollman AP, He TC, He Y, Hruban RH, Jallo GI, Mandahl N, Meeker AK, Mertens F, Netto GJ, Rasheed BA, Riggins GJ, Rosenquist TA, Schiffman M, Shih leM, Theodorescu D, Torbenson MA, Valculescu VE, Wang TL, Wentzensen N, Wood LD, Zhang M, McLendon RE, Bigner DD, Kinzler KW, Vogelstein B, Papadopoulos N, and Yan H. (2013) TERT promoter

- mutations occur frequently in gliomas and a subset of tumors derived from cells with low rates of self-renewal. *Proc Natl Acad Sci USA*. 110(15):6021-6026
- Kim HH, Vijapurkar U, Hellyer NJ, Bravo D, and Koland JG. (1998) Signal transduction by epidermal growth factor and heregulin via the kinase deficient ErbB3 protein. *Biochem J*. 334(Pt 1):189-195
- Koivunen P, Lee S, Duncan CG, Lopez G, Lu G, Ramkissoon S, Losman JA, Joensuu P, Bergmann U, Gross S, Travins J, Weiss S, Looper R, Ligon KL, Verhaak RG, Yan H, and Kaelin WG Jr. (2012) Transformation by the (R)-enantiomer of 2-hydroxyglutarate linked to EGLN activation. *Nature*. 483(7390):484-488
- Komarov PG, Komarova EA, Kondratov RV, Christov-Tselkov K, Coon JS, Chernov MV, and Gudkov AV. (1999) A chemical inhibitor of p53 that protects mice from the side effects of cancer therapy. *Science*. 285(5434):1733-1737
- Krizhanovsky V and Lowe SW. (2009) Stem cells: The promises and perils of p53. *Nature*. 460(7259):1085-1086
- Kroonen J, Nassen J, Boulanger YG, Provenzano F, Capraro V, Bours V, Martin D, Deprez M, Robe P, and Rogister B. (2011) Human glioblastoma-initiating cells invade specifically the subventricular zones and olfactory bulbs of mice after striatal injection. *Int J Cancer*. 129(3):574-585
- Lacayo NJ, Meshinchi S, Kinnunen P, Yu R, Wang Y, Stuber CM, Douglas L, Wahab R, Becton DL, Weinstein H, Chang MN, Willman CL, Radich JP, Tibshirani R, Ravindranath Y, Sikic BI, and Dahl GV. (2004) Gene expression profiles at diagnosis in de novo childhood AML patients identify FLT3 mutations with good clinical outcomes. *Blood*. 104(9):2646-2654
- Law MJ, Lower KM, Voon HP, Hughes JR, Garrick D, Viprakasit V, Mitson M, Do Gobbi M, Marra M, Morris A, Abbott A, Wilder SP, Taylor S, Santos GM, Cross J, Ayyub H, Jones S, Ragoussis J, Rhodes D, Dunham I, Higgs DR, and Gibbons RJ. (2010) ATR-X syndrome protein targets tandem repeats and influences allele-specific expression in a size-dependent manner. *Cell*. 143(3):367-378
- Leach MK, Naim YI, Feng ZQ, Gertz CC, and Corery JM. (2011) Stages of neuronal morphological development *in vitro*—an automated assay. *J Neurosci Methods*. 199(2):192-198

- Leung JW, Ghosal G, Wang W, Shen X, Wang J, Li L, and Chen J. (2013) Alpha thalassaemia/mental retardation syndrome X-linked gene product ATRX is required for proper replication restart and cellular resistance to replication stress. *J Biol Chem.* 288(9):6342-6350
- Levy MA, Fernandes AD, Trembly DC, Seah C, and Bérubé NG. (2008) The SWI/SNF protein ATRX co-regulates pseudoautosomal genes that have translocated to autosomes in the mouse genome. *BMC Genomics.* 9:468
- Levy MA, Kernohan KD, Jiang Y, and Bérubé NG. (2014) ATRX promotes gene expression by facilitating transcriptional elongation through guanine-rich coding regions. *Hum Mol Genet.* pii:ddu596 [Epub ahead of print]
- Lewis PW, Elsaesser SJ, Noh KM, Stadler SC, and Allis C. (2010) Daxx is an H3.3-specific histone chaperone and cooperates with ATRX in replication-independent chromatin assembly at telomeres. *Proc Natl Acad Sci USA.* 107(32):14075-14080
- Li W, Fu X, Liu R, Bai J, Xu Y, Zhao Y, and Xu Y. (2013) FOXC2 often overexpressed in glioblastoma enhances proliferation and invasion in glioblastoma cells. *Oncol Res.* 21(2):111-120
- Liu XY, Gerges N, Korshunov A, Sabha N, Khuong-Quang DA, Fontebasso AM, Fleming A, Hadjadj D, Schwartzentruber J, Majewski J, Dong Z, Siegel P, Albrecht S, Croul S, Jones DT, Kool M, Tönjes M, Reifenberger G, Faury D, Zadeh G, Pfister S, and Jabado N. (2012) Frequent ATRX mutations and loss of expression in adult diffuse astrocytic tumors carrying IDH1/IDH2 and TP53 mutations. *Acta Neuropathol.* 124(5):615-625
- Lois C and Alvarez-Buylla A. (1994) Long-distance neuronal migration in the adult mammalian brain. *Science.* 264(5162):1145-1148
- Lorenzo E, Ruiz-Ruiz C, Quesada AJ, Hernández G, Rodríguez A, López-Rivas A, and Redondo JM. (2002) Doxorubicin induces apoptosis and CD95 gene expression in human primary endothelial cells through a p53-dependent mechanism. *J Biol Chem.* 277(13):10883-10892
- Louis DN, Ohgaki H, Weistler OD, Cavenee WK, Burger PC, Jouvet A, Scheithauer BW, and Kleihues P. (2007) The 2007 WHO classification of tumours of the central nervous system. *Acta Neuropathol.* 114(5):547

- Lovejoy CA, Li W, Reisenweber S, Thongthip S, Bruno J, de Lange T, De S, Petrini JH, Sung PA, Jasin M, Rosenbluh J, Zwang Y, Weir BA, Hatton C, Ivanova E, Macconail L, Hanna M, Hahn WC, Lue NF, Reddel RR, Jiao Y, Kinzler K, Vogelstein B, Papadopoulos N, Meeker AK, and the ALT Starr Cancer Consortium. (2012) Loss of ATRX, genome instability, and an altered DNA damage response are hallmarks of the alternative lengthening of telomeres phenotype. *PLoS Genet.* 8(7):e1002772
- Loyola A, Bonaldi T, Rohe D, Imhof A, and Almouzni G. (2006) PTMs on H3 variants before chromatin assembly potentiate their final epigenetic state. *Mol Cell.* 24(2):309-314
- Luo J, wang X, Xia Z, Yang L, Ding Z, Chen S, Lai B, and Zhang N. (2014) Transcriptional factor specificity protein 1 (SP1) promotes the proliferation of glioma cells by upregulating midkine (MDK). *Mol Biol Cell.* [Epub ahead of print]
- Luskin MB. (1993) Restricted proliferation and migration of postnatally generated neurons derived from the forebrain subventricular zone. *Neuron.* 11(1):173-189
- Marino S, Voojls M, van Der Gulden H, Jonkers J, and Berns A. (2000) Induction of medulloblastomas in p53-null mutant mice by somatic inactivation of Rb in the external granular layer of cells of the cerebellum. *Genes Dev.* 14(8):994-1004
- Marinoni I, Kurrer AS, Vassella E, Dettmer M, Rudolph T, Banz V, Hunger F, Pasquinelli S, Speel EJ, and Perren A. (2014) Loss of DAXX and ATRX are associated with chromosome instability and reduced survival of patients with pancreatic neuroendocrine tumors. *Gastroenterology.* 146(2):453-460
- Marión RM, Strati K, Li H, Murga M, Blanco R, Ortega S, Fernandez-Capetillo O, Serrano M, and Blasco MA. (2009) A p53-mediated DNA damage response limits reprogramming to ensure iPS cell genomic integrity. *Nature.* 460(7259):1149-1153
- Marumoto T and Saya H. (2012) Molecular biology of glioma. *Adv Exp Med Biol.* 746:2-11
- McDowell TL, Gibbons RJ, Sutherland H, O'Rourke DM, Bickmore WA, Pombo A, Turley H, Gatter K, Picketts DJ, Buckle VJ, Chapman L, Rhodes D, and Higgs DR. (1999) Localization of a putative transcriptional regulator (ATRX) at pericentromeric

- heterochromatin and the short arms of acrocentric chromosomes. *Proc Natl Acad Sci USA*. 96(24):13983-13988
- Mich JK, Signer RA, Nakada D, Pineda A, Burgess RJ, Vue TY, Johnson JE, and Morrison SJ. (2014) Prospective identification of functionally distinct stem cells and neurosphere-initiating cells in adult mouse forebrain. *Elife*. 3:e02669
- Morin GB. (1989) The human telomere terminal transferase enzyme is a ribonucleoprotein that synthesizes TTAGGG repeats. *Cell*. 59(3):521-529
- Nan X, Hou J, Maclean A, Nasir J, Lafuente MJ, Shu X, Kriaocionis S, and Bird A. (2007) Interaction between chromatin proteins MECP2 and ATRX Is disrupted by mutations that cause inherited mental retardation. *Proc Natl Acad Sci USA*. 104(8):2709-2714
- Ogino H, Nakabayashi K, Suzuki M, Takahashi E, Fujii M, Suzuki T, and Ayusawa D. (1998) Release of telomeric DNA from chromosomes in immortal human cells lacking telomerase activity. *Biochem Biophys Res Commun*. 248(2):223-227
- Parsons DW, Jones S, Zhang X, Lin JC, Leary RJ, Angenendt P, Mankoo P, Carter H, Siu IM, Gallia GL, Olivi A, McLendon R, Rasheed BA, Keir S, Nikolskaya Y, Nikolsky Y, Busam DA, Tekleab H, Diaz LA Jr., Hartigan J, Smith DR, Strausberg RL, Marie SK, Shinjo SM, Yan H, Riggins GJ, Bigner DD, Karchin R, Papadopoulos N, Parmigiani G, Vogelstein B, Velculescu VE, and Kinzler KW. (2008) An integrated genomic analysis of human glioblastoma multiforme. *Science*. 321(5897):1807-1812
- Phillips HS, Kharbanda S, Chen R, Forrest WF, Soriano RH, Wu TD, Misra A, Nigro JM, Colman H, Soroceanu L, Williams PM, Modrusan Z, Feuerstein BG, and Aldape K. (2006) Molecular subclasses of high-grade glioma predict prognosis, delineate a pattern of disease progression, and resemble stages in neurogenesis. *Cancer Cell*. 9(3):157-173
- Picketts DJ, Higgs DR, Bachoo S, Blake DJ, Quarrell OW, and Gibbons RJ. (1996) ATRX encodes a novel member of the SNF2 family of proteins: mutations point to a common mechanism underlying the ATR-X syndrome. *Hum Mol Genet*. 5(12):1899-1907
- Pohl J, Goldfinger N, Radler-Pohl A, Rotter V, and Schirmacher V. (1988) p53 increases experimental metastatic capacity of murine carcinoma cells. *Mol Cell Biol*. 8(5):2078-2081

- Pugh TJ, Morozova O, Attiyeh EF, Asgharzadeh S, Wei JS, Auclair D, Carter SL, Cibulskis K, Hanna M, Kiezun A, Kim J, Lawrence MS, Lichtenstein L, McKenna A, Pedamallu CS, Ramos AH, Shefler A, Sivachenko A, Sougnez C, Stewart C, Ally A, Birol I, Chiu R, Corbett RD, Hirst M, Jackman SD, Kamoh B, Khodabakshi AH, Krzywinski M, Lo A, Moore RA, Mungall KL, Qian J, Tam A, Thiessen N, Zhao Y, Cole KA, Diamond M, Diskin SJ, Mosse YP, Wood AC, Ji L, Sposto R, Badgett T, London WB, Moyer Y, Gastier-Foster JM, Smith MA, Guidry Auvil JM, Gerhard DS, Hogarty MD, Jones SJ, Lander ES, Gabriel SB, Getz G, Seeger RC, Kahn J, Marra MA, Meyerson M, and Maris JM. (2013) The genetic landscape of neuroblastoma. *Nat Genet.* 45(3):279-284
- Qadeer ZA, Harcharik S, Valle-Garcia D, Chen C, Birge MB, Vardabasso C, Duarte LF, and Bernstein E. (2014) Decreased expression of the chromatin remodeler ATRX associates with melanoma progression. *J Invest Dermatol.* 134(6):1768-1772
- Rahme GJ and Israel MA. (2014) Id4 suppresses MMP2-mediated invasion of glioblastoma-derived cells by direct inactivation of Twist1 function. *Oncogene.* [Epub ahead of print]
- Ratnakumar K, Duarte LF, LeRoy G, Hasson D, Smeets D, Vardabasso C, Bönisch C, Zeng T, Xiang B, Zhang DY, Li H, Wang X, Hake SB, Schermelleh L, Garcia BA, and Bernstein E. (2012) ATRX-mediated chromatin association of histone variant macroH2A1 regulates α -globin expression. *Genes Dev.* 26(5):433-438
- Ritchie K, Seah C, Moulin J, Isaac C, Dick F, and Bérubé NG. (2008) Loss of ATRX leads to chromosome cohesion and congression defects. *J Cell Biol.* 180(2):351-324
- Ritchie K, Watson LA, Davidson B, Jiang Y, and Bérubé NG. (2014) ATRX is required for maintenance of the neuroprogenitor cell pool in the embryonic mouse brain. *Biol Open.* 3(12):1158-1163
- Salmaggi A, Boiardi A, Gelati M, Russo A, Caltozzolo C, Ciusani E, Sciacca FL, Ottolina A, Parati EA, La Porta C, Alessandri G, Marras C, Croci D, and De Rossi M. (2006) Glioblastoma-derived tumorspheres identify a population of tumor stem-like cells with angiogenic potential and enhanced multidrug resistance phenotype. *Glia.* 54(8):850-860

- Sampathi S and Chai W. (2011) Telomere replication: poised but puzzling. *J Cell Mol Biol.* 15(1):3-13
- Sanson M, Marie Y, Paris S, Idbaih A, Laffaire J, Ducray F, El Hallani S, Boisselier B, Mokhtari K, Hoang-Xuan K, and Delattre JY. (2009) Isocitrate dehydrogenase 1 codon 132 mutation is an important prognostic biomarker in gliomas. *J Clin Oncol.* 27(25):4150-4154
- Schwartzentruber J, Korshunov A, Liu XY, Jones DT, Pfaff E, Jacob K, Sturm D, Fontebasso AM, Quang DA, Tönjes M, Hovestadt V, Albrecht S, Kool M, Nantel A, Konermann C, Lindroth A, Jäger N, Rausch T, Ryzhova M, Korbel JO, Hielscher T, Hauser P, Garami M, Klekner A, Bogner L, Ebinger M, Schuhmann MU, Scheurlen W, Pekrun A, Frühwald MC, Roggendorf W, Kramm C, Dürken M, Atkinson J, Lepage P, Montpetit A, Zakrzewska M, Zakrzewski K, Liberski PP, Dong Z, Siegel P, Kulozik AE, Zapatka M, Guha A, Malkin D, Felsberg J, Reifenberger D, von Deinling A, Ichimura K, Collins VP, Witt H, Milde T, Witt O, Zhang C, Catelano P, Lichter P, Faury D, Tabori U, Plass, C, Majewski J, Pfister SM, and Jabado N. (2012) Driver mutations in histone H3.3 and chromatin remodelling genes in paediatric glioblastoma. *Nature.* 482(7384):226-231
- Seah C, Levy MA, Jiang Y, Mokhtarzada S, Higgs DR , Gibbons RJ, and Bérubé NG. (2008) Neuronal death resulting from targeted disruption of the Snf2 protein ATRX is mediated by p53. *J Neurosci.* 28(47):12570-12580
- Slack RS, El-Bizri H, Wong J, Belliveau DJ, and Miller FD. (1998) A critical temporal requirement for the retinoblastoma protein family during neuronal determination. *J Cell Biol.* 140(6):1497-1509
- Stayton CL, Dabovic B, Gulisano M, Gecz J, Broccoli V, Giovanazzi S, Bossolasco M, Monaco L, Rastan S, Boncinelli E, Bianchi ME, and Giacomo Consalez G. (1994) Cloning and characterization of a new human Xq13 gene, encoding a putative helicase. *Hum Mol Genet.* 3(11):1957-1964
- Stieber VW. (2001) Low-grade gliomas. *Curr Treat Options Oncol.* 2(6):495-506
- Stiles CD and Rowitch DH. (2008) Glioma stem cells: a midterm exam. *Neuron.* 58(6):832-846

- Tang J, Wu S, Liu H, Stratt R, Barak OG, Shiekhattar R, Picketts DJ, and Yang X. (2004) A novel transcription regulatory complex containing death domain-associated protein and the ATR-X syndrome protein. *J Biol Chem.* 279(19):20369-20377
- Thon N, Eigenbrod S, Kreth S, Lutz J, Tonn JC, Kretzschmar H, Peraud A, and Kreth FW. (2012). IDH1 mutation in grade II astrocytomas are associated with unfavourable progression-free survival and prolonged postrecurrence survival. *Cancer.* 118(2):452-460
- Tronche F, Kellendonk C, Kretz O, Gass P, Anlag K, Orban PC, Bock R, Klein R, and Schütz G. (1999) Disruption of the glucocorticoid receptor gene in the nervous system results in reduced anxiety. *Nat Genet.* 23(1):99-103
- Turcan S, Rohle D, Goenka A, Walsh LA, Fang F, Yilmaz E, Campos C, Fabius AW, Lu C, Ward PS, Thompson CB, Kaufman A, Guryanova O, Levine R, Heguy A, Viale A, Morris LG, Huse JT, Mellinghoff IK, and Chan TA. (2012) IDH1 mutation is sufficient to establish glioma hypermethylator phenotype. *Nature.* 483(7390):479-483
- Ulasov I, Yi R, Guo D, Sarvaiya P, and Cobbs C. (2014) The emerging role of MMP14 in brain tumorigenesis and future therapeutics. *Biochem Biophys Acta.* 1846(1):113-120
- Verhaak RG, Hoadley KA, Purdom E, Wang V, Qi Y, Wilkerson MD, Miller CR, Ding L, Golub T, Msirov JP, Alexe G, Lawrence M, O'Kelly M, Tamayo P, Weir BA, Gabriel S, Winckler W, Gupta S, Jakkula L, Feiler HS, Hodgson JG, James CD, Sarkaria JN, Brennan C, Kahn A, Spellman PT, Wilson RK, Speed TP, Gray JW, Meyerson M, Getz G, Perou CM, Hayes DN, and the Cancer Genome Atlas Research Network. (2010) Integrated genomic analysis identifies clinically relevant subtypes of glioblastoma characterized by abnormalities in *PGFRA*, *IDH1*, *EGFR*, and *NF1*. *Cancer Cell.* 17(1):98-110
- Vousden KH and Prives C. (2009) Blinded by the light: The growing complexity of p53. *Cell.* 137(3):413-431
- Watanabe T, Nobusawa S, Kleihues P, and Ohgaki H. (2009) IDH1 mutations are early events in the development of astrocytomas and oligodendrogliomas. *Am J Pathol.* 174(4):1149-1153

- Watson LA, Solomon LA, Li JR, Jiang Y, Edwards M, Shin-ya K, Beier F, and Bérubé NG. (2013) Atrx deficiency induces telomere dysfunction, endocrine defects, and reduced life span. *J Clin Invest.* 123(5):2049-2063
- Weatherall DJ, Higgs DR, Bunch C, Old JM, Hunt DM, Pressley L, and Clegg JB. (1981) Hemoglobin H disease and mental retardation: a new syndrome or a remarkable coincidence? *N Engl J Med.* 305(11):607-612
- Weller M, Felsberg J, Hartmann C, Berger H, Steinbach JP, Schramm J, Westphal M, Schackert G, Simon M, Tonn JC, Heese O, Krex D, Nikkah G, Pietsch T, Wiestler O, Reifenberger G, von Deimling A, and Loeffler M. (2009) Molecular predictors of progression-free and overall survival in patients with newly diagnosed glioblastoma: a prospective translational study of the German Glioma Network. *J Clin Oncol.* 27(34):5743-5750
- Wen PY and Kesari S. (2008) Malignant gliomas in adults. *N Engl J Med.* 359(5):492-507
- Wiestler B, Capper D, Holland-Letz T, Korshunov A, von Deimling A, Pfister SM, Platten M, Weller M, and Wick W. (2013) ATRX loss refines the classification of anaplastic gliomas and identifies a subgroup of IDH mutant astrocytic tumors with better prognosis. *Acta Neuropathol.* 126(3):443-451
- Wong LH, McGhie JD, Sim M, Anderson MA, Ahn S, Hannan RD, George AJ, Morgan KA, Mann JR, and Choo KH. (2010) ATRX interacts with H3.3 in maintaining telomere structural integrity in pluripotent embryonic stem cells. *Genome Res.* 20(3):351-360
- Wu G, Diaz AK, Paugh BS, Rankin SL, Ju B, Li Y, Zhu X, Qu C, Chen X, Zhang J, Easton J, Edmonson M, Ma X, Lu C, Nagahawatte P, Hedlund, E, Rusch M, Pounds S, Lin T, Onar-Rhomas A, Huether R, Kriwacki R, Parker M, Gupta P, Becksfort J, Wei L, Mulder HL, Boggs K, Vadodaria B, Yergeau D, Russell JC, Ochoa K, Fulton RS, Fulton LL, Jones C, Boop FA, Broniscer A, Wetmore C, Gajjar A, Ding L, Mardis ER, Wilson RK, Taylor MR, Downing JR, Ellison DW, Zhang J, Baker SJ, and the St. Jude's Children's Research Hospital-Washington University Pediatric Cancer Genome Project. (2014) The genomic landscape of diffuse intrinsic pontine glioma and pediatric non-brainstem high-grade glioma. *Nat Genet.* 46(5):444-450

- Wu Y and Brosh RM Jr. (2010) G-quadruplex nucleic acids and human disease. *FEBS J.* 277(17):3470-3488
- Xu X, Zhao J, Xu Z, Peng B, Huang Q, Arnold E, and Ding J. (2004) Structures of human cytosolic NADP-dependent isocitrate dehydrogenase reveal a novel self-regulatory mechanism of activity. *J Biol Chem.* 279(32):33946-33957
- Xue Y, Gibbons R, Yan Z, Yang D, McDowell TL, Sechi S, Qin J, Zhou S, Higgs D, and Wang W. (2003) The ATRX syndrome protein forms a chromatin-remodeling complex with Daxx and localizes in promyelocytic leukemia nuclear bodies. *Proc Natl Acad Sci USA.* 100(19):10635-10640
- Yachida S, Vakiani E, White CM, Zhong Y, Saunders T, Morgan R, de Wilde RF, Maitra A, Hicks J, Demarzo AM, Shi C, Sharma R, Laheru D, Edil BH, Wolfgang CL, Schulick RD, Hruban RH, Tang LH, Klimstra DS, and Iacobuzio-Donahue CA. (2012) Small cell and large cell neuroendocrine carcinomas of the pancreas are genetically similar and distinct from well-differentiated pancreatic neuroendocrine tumors. *Am J Surg Pathol.* 36(2):173-184
- Yan H, Parsons DW, Jin G, McLendon R, Rasheed BA, Yuan W, Kos I, Batonic-haberle I, Jones S, Riggins GJ, Friedman H, Friedman A, Reardon D, Herndon J, Kinzler KW, Velculescu VE, Vogelstein B, and Bigner DD. (2009) IDH1 and IDH2 mutations in gliomas. *N Engl J Med.* 360(8):765-773
- Yeager TR, Neumann AA, Englezou A, Huschtscha LI, Noble JR, and Reddel RR. (1999) Telomerase-negative immortalized cells contain a novel type of promyelocytic leukemia (PML) body. *Cancer Res.* 59(17):4175-4179
- Zhang R, Poustovoitov MV, Ye X, Santos HA, Chen W, Daganzo SM, Erzberger JP, Serebriiskii IG, Canutescu AA, Dunbrack RL, Pehrson JR, Berger JM, Kaufman PD, and Adams PD. (2005) Formation of MacroH2A-containing senescence-associated heterochromatin foci and senescence driven by ASF1a and HIRA. *Dev Cell.* 8(1):19-30
- Zhang J, Wu G, Miller CP, Tatevossian RG, Dalton JD, Tang B, Orisme W, Punchihewa C, Parker M, Qaddoumi I, Boop FA, Lu C, Kandath C, Ding L, Lee R, Huether R, Chen X, Hedlund E, Nagahawatte P, Rusch M, Boggs K, Cheng J, Becksfort J, Ma J, Song G, Li Y, Wei L, Wang J, Shurtleff S, Easton J, Zhao D, Fulton RS, Fulton

- LL, Dooling DJ, Vadodaria B, Mulder HL, Tang C, ochoa K, Mullighan CG, Gajjar A, Kriwacki R, Sheer D, Gilbertson RJ, Mardis ER, Wilson RK, Downing JR, Baker SJ, Ellison DW, and the St. Jude's Children's Hospital-Washington University Pediatric Cancer Genome Project. (2013) Whole-genome sequencing identifies genetic alterations in pediatric low-grade gliomas. *Nat Genet.* 45(6):602-612
- Zuco V and Zunino F. (2008) Cyclic pifithrin-alpha sensitizes wild type p53 tumor cells to antimicrotubule agent-induced apoptosis. *Neoplasia.* 10(6):587-596

APPENDIX A – Ethics Approval

Submit - Animal Use Protocol - AUP Form

1. Investigator Contact Information

PI_FULL_NAME	Berube, Nathalie
AUP NUMBER	2008-041-02
AUP TYPE	
Primary Role	Principal Investigator
1. PI Full Name	Berube, Nathalie
2. Primary Institution & Department	Schulich School Of Medicine & Dentistry / Paediatrics
3. Office Location - Building & Room #	VRL A4-138
4. Weekday Phone #	55066
5. PI After-Hours Emergency Contact #	474-6577
6. Pager - Phone & Pager #	
7. Primary Email	nberube@uwo.ca
8. Other Email	
9. Lab Campus Location, if different from Q.3	Victoria Research Laboratory
10. Lab Phone #, if different from Q.4	55092

2. Protocol Title & Project Type

1. <i>Animal Use Protocol</i> Title
Investigating the role of chromatin proteins in brain development
2. Application Type, <i>Pick One</i>
Full Renewal
3. If 'Full Renewal' or 'Post-Pilot Full Protocol' provide Associated Previous Protocol Number
2008-041-01
4. If Post-Pilot Full Protocol or Full Renewal , Provide a 3 R'S PROGRESS REPORT SUMMARY that outlines progress relating to the REPLACEMENT of animals, REDUCTION of animal use numbers AND REFINEMENT of experimental technique. E.g. What did you previously learn that has resulted in a change in study design based upon application of the 3 R's. Link to CCAC's 3 R's Microsite for more information.
Replacement: For many of our experiments, we cannot use cell lines, as they do not completely replicate in vivo events. We can replace by establishing primary neuroprogenitor

Submit - Animal Use Protocol - AUP Form

<p>cultures, which mimic the neuronal differentiation process.</p> <p>Reduction: We are constantly striving to reduce our animal numbers by using each control/ ko pair for several different experiments. For example, we will use some pairs to investigate brain myelination or molecular events, but also keep the skeleton and other organs to investigate the systemic effects of ATRX loss of function.</p> <p>Refinement: For the CTCF project, we have now determined that inactivating CTCF with the Foxg1Cre driver line results in early complete loss of tissue. We are now concentrating our efforts on crossing with the NestinCre driver line, where we will investigate the histological and cellular outcomes of CTCF loss during embryogenesis. This refinement will translate into fewer mice used for this project.</p>
<p>5. If Post-Pilot Full Protocol or Full Renewal, provide previous Protocol Year's animal use number.</p>
<p>161</p>
<p>6. Proposed Start Date (<i>mm/dd/yy</i>)</p>
<p>03/01/2012</p>

Attachments List

File Spec	Description	Created
2008-041-02 7 0001 2008-041 <u>Berube REN 03.01.11.doc</u>	2011 Annual Renewal	08/13/2014

3. Lay Summary & Glossary

<p>1. Using non-scientific language, please describe the project's purpose, expected benefit, and a brief summary of your work with the animal model(s). <i>Please be aware that in the event of communications with Western Media Relations and the PI is not available, this summary will be sent to Western Media Relations.</i></p> <p>We are investigating the function of several proteins that regulate how DNA is structured and packaged in the nucleus. Mutations of several chromatin regulators cause developmental abnormalities, mental retardation syndromes, skeletal abnormalities, early aging phenotypes and cancer, emphasizing the importance of maintaining chromatin architecture in the developing brain. We are inactivating several proteins that cause cognitive deficits. ATRX, which is mutated in ATR-X</p>

Submit - Animal Use Protocol - AUP Form

mental retardation syndrome, MeCP2, which is mutated in the majority of Rett syndrome cases, and CTCF, a chromatin factor associated with ATRX. The experiments proposed under this protocol will help us delineate the cellular and molecular underpinnings of cognitive deficits and skeletal defects of the associated syndromes: ATR-X, Rett and Cornelia de Lange syndromes.

2. GLOSSARY OF TERMS - Identify each individual scientific term and abbreviation using *CAPITAL LETTERS*, and then briefly define each term to be referenced in any section of this protocol.

e.g. ALLELE - The genetic variant of a gene responsible for the different traits of certain characteristics and genetic diseases.

ATRX: Alpha Thalassemia mental Retardation syndrome, X-linked.

RTT: Rett syndrome

MeCP2: Methyl CpG binding protein 2

MUTATION; change in the nucleotide sequence

BrdU: Bromodeoxyuridine (BrdU) is a synthetic thymidine analog that gets incorporated into a cell's DNA when the cell is dividing (during the S-phase of the cell cycle).

Chromatin: the molecular structure comprised of DNA and its associated proteins

CTCF: CCCTC-binding factor, 11-zinc finger protein

4. CCAC Animal Procedural Outline

CCAC PROCEDURAL OVERVIEW - Use this field to convey in simple terms using approximately 40 words or less the nature of the procedures conducted on the animals.

Please use KEY WORDS provided through the above link.

The animals are used for fundamental and medical research purposes, and require the continuous maintenance of breeding colonies of genetically modified mice that model various human developmental syndromes. Mice are tagged, injected subcutaneously (BrdU or T4), or embryonic brain is used to establish primary cell cultures. In some cases, adult brain samples are taken for fixation and cryosectioning, or are frozen for subsequent isolation of RNA or protein. Sometimes the mice are euthanized to collect organs for DNA, RNA or protein extractions or are fixed and frozen for histological analyses. Blood samples will be taken for testing various metabolic parameters.

CURRICULUM VITAE

Name: Hannah Goldberg

**Post-Secondary
Education and
Degrees:** University of Western Ontario
London, Ontario, Canada
2008-2012 B.Sc.

University of Western Ontario
London, Ontario, Canada
2012-2015 M.Sc.

**Honours and
Awards:** Miller Thomson National Scholarship
2008-2009

Continuing Admission Scholarship, UWO
2008-2012

Dean's Honor Roll
2008-2012

Province of Ontario Graduate Scholarship
2012-2013

Western Graduate Research Scholarship
2012-2014

Publications:

Goldberg, Hannah. (Thursday Sept. 25th, 2014). Extending our knowledge into the DNA of brain tumours in children. *The Londoner*, page 6.